Evaluation of Phenol Formaldehyde Resin Cure Rate

By

Brian Cameron Scott

Masters Thesis submitted to the

Faculty of Virginia Polytechnic Institute and State University

in partial fulfillment of the requirements for the degree of:

Master of Science

In

Wood Science and Forest Products

Dr. Frederick A. Kamke, Chairman
Dr. Charles E. Frazier
Dr. Joseph R. Loferski

April, 2005

Blacksburg, Virginia

Keywords: dielectric analysis, parallel-plate rheometry, thermoset resin cure

Evaluation of Phenol Formaldehyde Resin Cure Rate

Brian Scott

(Abstract)

Cure time is often the bottleneck of composite manufacturing processes, therefore it is important to understand the cure of today's thermosetting adhesives. This research attempts to characterize the cure rate of two commercial phenol-formaldehyde adhesives. Two methods are used, parallel-plate rheometry and dielectric spectroscopy. Viscosity data from a parallel-plate rheometer may be used to track the advance of polymerization as a function of temperature. This data can then be used to optimize press conditions and reduce production times and costs.

The research will further examine resin cure through dielectric analysis; such a technique could monitor resin cure directly and in real-time press situations. Hot-pressing processes could conceivably no longer require a set press schedule; instead they would be individually set based on dielectric data for every press batch. Such a system may lead to a more efficient and uniform product because press times could be based on individual press cycles instead of entire product lines. A more likely scenario, however, is the use of *in situ* adhesive cure monitoring for troubleshooting or press schedule development.

This research characterized the cure of two phenol-formaldehyde resins using parallel-plate rheometry, fringe-field dielectric analysis, and parallel-plate dielectric analysis. The general shape of the storage modulus vs. time curve and the gel and vitrification points in a temperature ramp were found.

Both dielectric analysis techniques were able to characterize trends in the resin cure and detect points such as vitrification. The two techniques were also found to be comparable when the cure profiles of similar conditions were examined.

Acknowledgements

I would like to thank the people who helped me complete this project and my career at Virginia Tech. My committee members, Dr. Charles Frazier and Dr. Joseph Loferski helped instruct and guide me in my academic and career choices long before I began this project. Dr. Frazier, in particular helped me find the wood science major. Dr. Fredrick Kamke was instrumental in my graduate studies and provided guidance and direction when I got stuck.

I would also like to thank Linda Caudill for giving me my first opportunity in the wood-based composites field as a lab assistant for the Wood-Based Composites Center. Her advice on career advancement, academics, or even which movies to see helped me tremendously. Jim Fuller contributed greatly to my day-to-day experimentation and I would not have been able finish this research without his technical and help and instruction. Matt Reynolds, Paul Duvall, and Roncs Ese-Etame helped me pass my time at the Brooks Center and Blacksburg life when research was not going as planned. I couldn't have correctly filled out any of the university's paperwork without Angie Riegel's help.

Finally, I would like to thank the people who loved and supported me throughout my entire college life. My mother Jeanne Scott, who provided me with unquestioning support no matter what else was going on in my life. My father, Kevin Scott also supported me and helped me remain committed to my jogging and other nonacademic pursuits. Finally my sister, Katherine Scott was always there to offer her support and a sympathetic ear. There are too many others to mention individually, but I met a number of people during my time at Virginia Tech that I will cherish for the rest of my life.

Acknowledgements iv
1. Introduction and Objectives 1
2. Literature Review 2
2.1 Introduction 2
2.2 Rheometry 3
2.2.1 Cure Overview 3
2.2.2 Rheometry Theory 7
2.3 Dielectric Monitoring 8
2.3.1 Overview of Dielectric Spectroscopy 8
2.3.2 Complex Permittivity Theory 9
2.3.3 Methods of Dielectric Measurement 11
3. Materials and Methods 13
3.1 Resin Description 13
3.2 Sample Preparation 14
3.2.1 Rheometer Sample Preparation 14
3.2.2 DEA Sample Preparation 14
3.3 Experimental Design 18
3.3.1 Rheometer Experimental Design 18
3.3.2 DEA Experimental Design 19
3.4 Data Analysis 19
4. Results and Discussion 20
4.1 Rheometry Results 20
4.1.1 Face Resin 20
4.1.2 Core Resin 22
4.2 Dielectric Analysis Results 23
4.2.1 Influence of Moisture Content 24
4.2.2 Influence of Resin Formulation 31
4.2.3 Position 1 vs. Position 2 36
4.2.4 Parallel-Plate vs. Fringe-Field DEA Techniques 37
4.3 Summary of Results 45
5. Conclusions and Recommendations 47
5.1 Conclusions 47
5.2 Recommendations 47
6. References 49
7. Appendix 51

Figure 1 Generic TTT Diagram (1) 4
Figure 2 Generic CHT Diagram where the bottom, black line represents initial vitrification, the middle, red line represents gelation, the lower intersections on the blue curve represent vitrification, and the upper intersections on the blue line represent devitrification. 6
Figure 3 IDEX Sensor..... 15
Figure 4 Placement of fringe-field and parallel-plate sensors in a 2 ply sample. 16
Figure 5 Position locations for the fringe-field DEA in the plywood samples..... 17
Figure 6 Average parallel-plate rheometry results for the face resin, n=3. 21
Figure 7 Average degree of cure results for face and core resins. 22
Figure 8 Average parallel-plate rheometry results for the core resin, n=5 23
Figure 9 Loss factor vs. time of 2 ply samples grouped by MC at 200Hz using the fringe-field DEA. These are the average of the two samples run under the same conditions. 25
Figure 10 Loss factor vs. time of 3 ply samples grouped by MC at 200Hz using the fringe-field DEA. The two resins are averaged together. 26
Figure 11 Loss factor of 5 ply, position 1 samples grouped by MC at 200Hz using the fringe-field DEA. 27
Figure 12 Loss factor of 5 ply, position 2 samples grouped by MC at 200Hz using the fringe-field DEA. 28
Figure 13 Dielectric loss factor of individual 5 ply samples at 200Hz using the fringe-field DEA. 29
Figure 14 Dielectric loss factor of average 5 ply samples by moisture content at 200Hz using the fringe-field DEA..... 30
Figure 15 Dielectric loss factor of 2 ply samples grouped by resin and measured by the fringe-field DEA. 32
Figure 16 Dielectric loss factor of 3 ply samples grouped by resin type at 200Hz as measured by the fringe-field DEA. 33
Figure 17 Dielectric loss factor vs. time of 5 ply samples at 200 Hz by resin type and position..... 34
Figure 18 Dielectric loss factor vs. time for 5 ply samples at 200 Hz by fringe-field sensor location (see Figure 3.2.3). 36
Figure 19 Loss factor vs. time of sample 4MC2PCORE at 200 Hz using parallel-plate and fringe-field DEA. 37
Figure 20 Normalized time derivative of the loss factor vs. time of sample 4MC2P1FACE at 200 Hz using parallel-plate and fringe-field DEA.10 38
Figure 21 Normalized time derivative of the loss factor vs. time of sample 4MC2P1CORE at 200 Hz using parallel-plate DEA, fringe-field DEA and the moving average of the parallel-plate curve..... 39
Figure 22 Normalized time derivative of the loss factor at 200 Hz..... 40
Figure 23 Normalized time derivative of the loss factor of sample 4MC2PCORE at 200 with Hz of parallel-plate and fringe-factor DEA. 41
Figure 24 Normalized loss factor of sample 4MC2P1FACE at 200 with Hz of parallel-plate and fringe-factor DEA..... 41
Figure 25 Normalized loss factor of sample 8MC2P1CORE at 200 Hz of parallel-plate and fringe-field DEA. 42

Figure 26 Normalized loss factor at 200 Hz using parallel-plate and fringe-field DEA. . 43
Figure 27 Normalized loss factor at 200 Hz using parallel-plate and fringe-field DEA .. 44
Figure 28 Normalized loss factor at 200 Hz using parallel-plate and fringe-field DEA. . 45

Table 1 Properties of the face and core resins 14
Table 2 Types of samples used in DEA experiments. 16
Table 3 Degree of cure for the rheometer data at 2oC per minute temperature ramp. 22
Table 4 Final cure time and degree of cure at final cure times for 2 ply samples by differing MC, n= 4. 26
Table 5 Final cure time and degree of cure at final cure times for 3ply samples by differing MC, n=4. 27
Table 6 Final cure time and degree of cure at final cure times for 5P1 samples by differing MC, n=4. 29
Table 7 Time to reach 75% obtained cure for 5P2 samples by differing MC, n=4. 29
Table 8 Time to reach 85% obtained cure for 5P2 samples by differing MC, n=4. 31
Table 9 Values of final cure times and degree of cure at final cure times for 2ply samples by different resins. 33
Table 10 Final cure time and degree of cure at final cure times for 3ply samples by different resins, n=4. 34
Table 11 Final cure time and degree of cure at final cure times for 5 ply samples at position 1 by different resins, n=4. 35
Table 12 Slope of the loss factor with respect to time for the 5 ply samples at position 2 by different resins, n=4. 35

1. Introduction and Objectives

The purpose of this project was to study the validity and merit of large field dielectric analysis (DEA) of wood composites versus fringe-field DEA in bond-lines. Large field DEA has several advantages, including ease of setup and the ability to reuse the sensors in a number of trials. Because the sensor is not placed in the bond-line, the panel also is unaffected by both the test and recovery of the sensor. This would allow for non-destructive testing in an industry setting without affecting the final product.

Hot-pressing of wood composites is the most expensive and time consuming process involved in wood-based composite manufacture; it is also the most critical process regarding the final characteristics of the panel. Understanding the cure kinetics of the resins used in the manufacture of wood-based composites is critical to the efficient production of these products.

Dielectric analysis predominantly uses two types of sensors that are appropriate for different DEA situations. This research attempts to compare the data gathered from fringe-field and parallel-plate sensors. By determining the validity of the parallel-plate DEA, a new tool that can fulfill an industrial application could be obtained.

Objectives:

1. To characterize the curing rate of two phenol-formaldehyde resins using a parallel-plate rheometer.

2. Characterize the curing rate of two phenol-formaldehyde resins using fringe-field dielectric spectroscopy.
3. Characterize the curing rate of two phenol-formaldehyde resins using parallel-plate dielectric spectroscopy.
4. To assess if the cure monitoring techniques provide similar results.

2. Literature Review

2.1 Introduction

In large scale wood-composites manufacturing, companies strive to produce as much product as possible in the shortest amount of time for the lowest possible cost. Because the hot-press step is the most time consuming and the most expensive, manufacturers cure only to the minimum time and temperature levels needed to stop panel blows or delamination. To achieve this manufacturers rely on press schedules determined by trial and error that regulate temperature ramps, press closing and time in press. These schedules are based on past experience using specific resins and wood moisture content (MC) with little regard for actual cure progression. A system that could monitor or control the press schedule using dielectric cure information would be a valuable tool that could reduce product variability and increase product yield and manufacturing efficiency. A more likely scenario is the use of dielectric data as a quality control (QC) tool. Cure abnormalities could be identified and investigated before product shipment.

This thesis will attempt to use both chemorheology data from PF resin analyzed in a parallel-plate rheometer and dielectric data from *in situ* monitoring during panel

formation. A better understanding of actual cure progression is vital to the improvement of press schedules and product conformity in the wood-based composites industry. Finally, this work is part of a larger project investigating methods of degree of cure of thermosetting resins in cooperation with Washington State University (Pullman, WA) and The University of Ljubljana (Ljubljana, Slovenia).

2.2 Rheometry

2.2.1 Cure Overview

Resin cure is a critical factor in wood-based composite manufacture. Understanding cure behavior is vital to predicting panel properties (1).

When a thermosetting adhesive, such as phenol-formaldehyde (PF), cures it undergoes two main transition points, gelation and vitrification. As the thermoset forms cross-links the viscosity approaches infinity, this indicates gelation has occurred. Vitrification is the change from network gel to glassy solid. This occurs when the glass transition temperature (T_g) equals the cure temperature (1).

Gillham (2) developed the time-temperature-transformation (TTT) isothermal cure diagram and the continuous heating time-temperature-transformation (CHT) cure diagram that shows that resin cure is dependant on both time and temperature. The rate of temperature increase can greatly influence how a thermoset will cure. It is possible to

cure a resin to a solid without ever reaching vitrification if the heating rate is too high, or char a resin if the rate is slow enough and the temperature high enough (2).

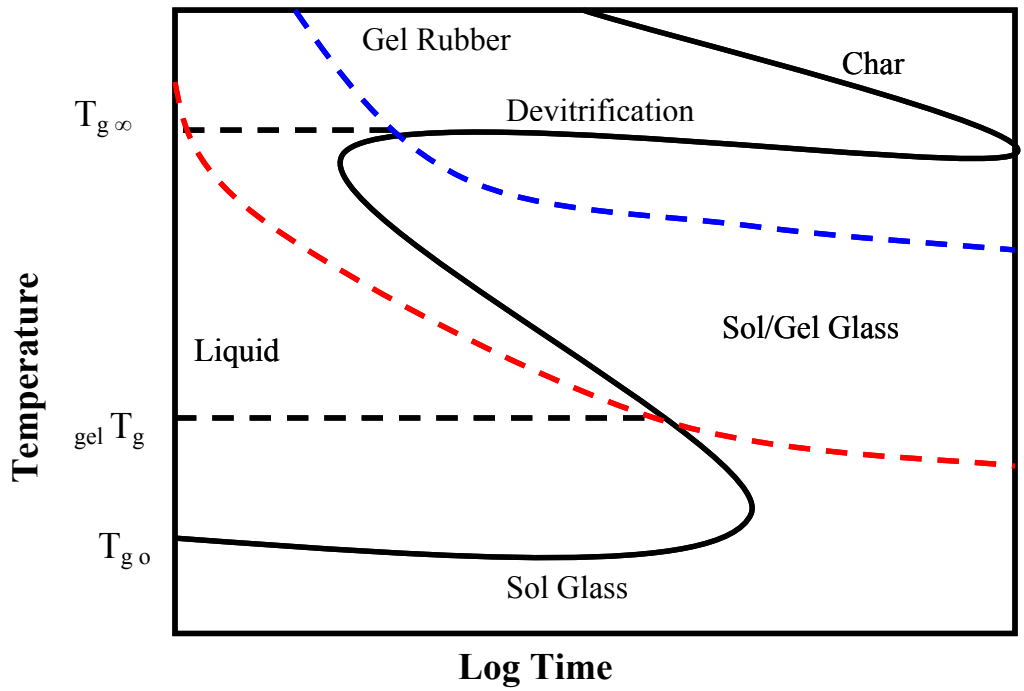

Figure 1 Generic TTT Diagram

This diagram is very important in understanding isothermal polymer thermoset cure. It maps out the various stages in the cure profile and shows how the time temperature relationship will affect the condition of the resulting polymer.

Each line that intersects the Y-axis represents a T_g. The red dashed line represents the T_g where gelation occurs, and therefore represents the temperature at which T_g equals the gel point. The blue dashed line represents the T_g at full cure or the $T_{g\infty}$. This is the final T_g, and no matter how much higher the temperature is raised there is not another T_g. The

center black curve represents the vitrification point or the transition from a gel to a solid, either a cross-linked rubber or an uncross-linked glass.

Each time a polymer crosses a line in isothermal cure it enters a new category that describes the state it is now in. For example, a polymer undergoing isothermal cure between the $T_{g\,o}$ and the ${}_{gel}T_g$ will never form any cross links. Depending how long it is left at that temperature, it will form a solid, but it will be a glass. A polymer held at a temperature above the ${}_{gel}T_g$, but below the $T_{g\,\infty}$, will go from a liquid to a gel to a solid that is a mixture of a glass and a rubber, some cross-linking has occurred but there are amorphous regions as well. Finally if a polymer is cured at a temperature above its $T_{g\,\infty}$, it will undergo full cure and form a gel rubber. However, if left too long at this temperature, the polymer will char and degrade.

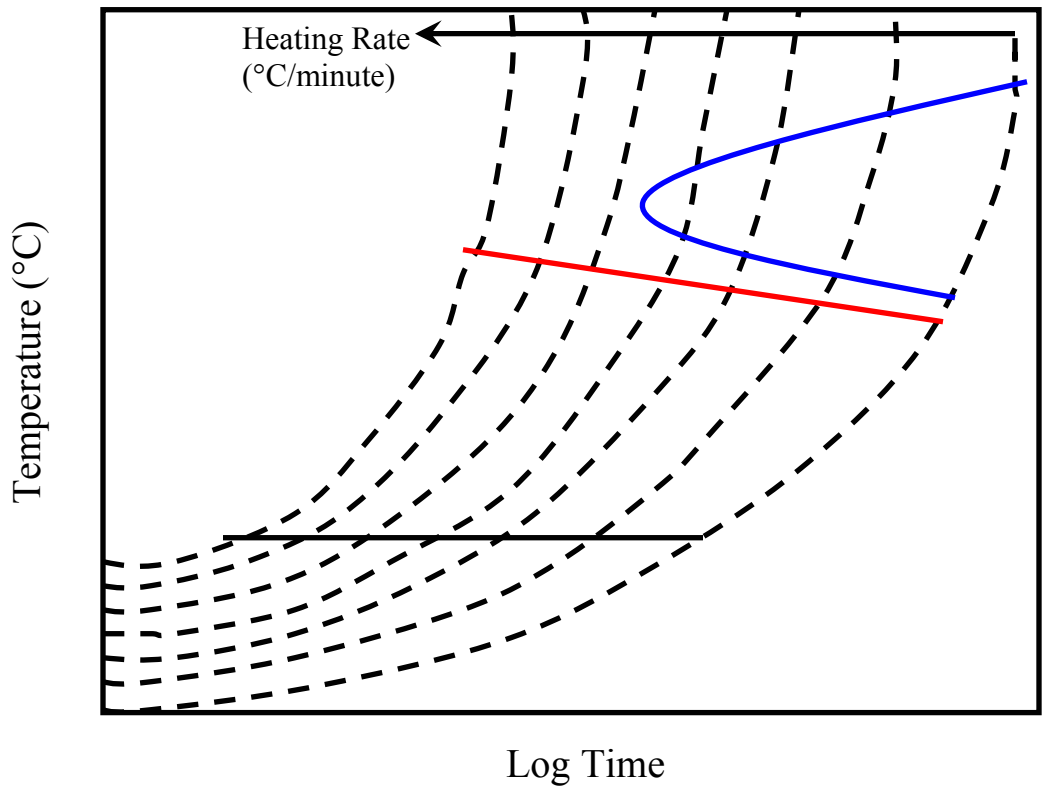

Figure 2 Generic CHT Diagram where the bottom, black line represents initial vitrification, the middle, red line represents gelation, the lower intersections on the blue curve represent vitrification, and the upper intersections on the blue line represent devitrification.

The CHT diagram is used to describe non-isothermal thermoset cure. It has the same divisions as the TTT diagram, but describes the process for thermoset cure using heat ramps. The dotted lines represent generic heating ramps, as they move left the heating rate increases. Using different heating ramps will dramatically affect how a thermoset would cure; for example a fast heating ramp, such as the third dotted line from the left, would cause the thermoset to devitrify, or pass from a glassy solid into a liquid, then gel, but never achieve vitrification. A slower heating ramp, such as the line second from the right, would devitrify, go through its gel point, vitrify as it forms a true solid, then devitrify again as it softens and forms more cross-links.

2.2.2 Rheometry Theory

Oscillation tests are commonly used to test the cure behavior of thermosetting adhesives. The literature has shown that using a parallel-plate rheometer to measure storage modulus (G'), loss modulus (G'') and tan δ (G''/G') can provide valuable information about the cure behavior of a thermoset. Thermosets have a typical curve of G' and G'' when they are analyzed in a parallel-plate rheometer using either a temperature ramp or isothermal test. G'' typically starts out larger than G'. Both G' and G'' then decrease as the viscosity of the thermoset decreases because of the temperature increase. Eventually the influence of polymerization overtakes the influence of temperature, and as the thermoset starts to cure, both G' and G'' increase. However the rate of increase of G' is greater than G''. Because of this, a crossover of G' and G'' will occur and may indicate a gel point. Finally, G' will plateau, and G'' will experience a peak and approach zero. Both the peak of G'' and the plateau of G' indicate vitrification (3, 4).

Because not all thermosets behave in this way, other methods to determine gelation have been devised. A peak in the tan δ curve has been used to indicate gelation (5). Additionally, gelation can be classified by a sharp rise in G' as a gel network is formed; these two methods are the most clear in a wide variety of thermosetting systems (6). Winter and Chambon suggest that gelation is better identified by frequency independence of tan δ between 0 and 1 using an isothermal multi-wave Fourier transformation response. This simple measurement can easily find the gel point in a wide variety of thermoset systems provided the equipment used can perform the necessary frequency sweeps (4, 7, 8).

Rheometry can be useful for determining the degree of cure of a resin during a temperature ramp experiment. Because a linear temperature ramp can approximate resin cure in a wood-based composite, it approximates the cure response during industrial use. This experiment must use a temperature ramp that allows for temperature equilibration of the sample. Additionally, cure kinetics expressed during a temperature ramp experiment has been illustrated. Gelation has been shown to coincide with a maximum of G″ and vitrification occurs at the plateau of G′ (4).

2.3 Dielectric Monitoring

2.3.1 Overview of Dielectric Spectroscopy

Dielectric cure monitoring is valuable because of its ability to non-destructively monitor polymer cure *in situ.* DEA monitors the changes in the mobility of ions and the rotational mobility of dipoles in response to an electric field. These responses can vary based on interference from water content, impurities, or dipoles or ions from outside materials, such as wood in wood-based composites. Fortunately, dielectric response is highly frequency dependent. Varying the frequency of the current can improve the resolution of the response (9).

Changes in the molecular mobility of a curing polymer are at the heart of the mechanical changes occurring such as gelation or vitrification. Because dipoles and ions will lose their mobility as a polymer cures, DEA is essentially a direct measurement of degree of

cure (9). This fact is what makes DEA such an attractive tool in wood-based composites analysis.

Dipole rotational mobility, or dipole polarization, occurs because of permanent charge distribution differences found in many molecules. As an electric field is applied to the material, the permanent dipoles found in the polymer will align in the direction of that applied field. This alignment forces polymer chains to move and will cause a delay in reorientation if the field is removed or reversed. This delay is a major component of dielectric response. The second major component of dielectric response is free charge or ion migration; these ions are present in almost all dielectric materials, either naturally or as impurities (10).

2.3.2 Complex Permittivity Theory

The dielectric response is expressed by its complex permittivity, ε*, defined as (9, 11, 12):

$$\varepsilon^* = \varepsilon' - i\varepsilon'' \qquad \textbf{Equation 1}$$

Where ε', or the dielectric constant, is calculated from the capacitance, C, of the polymer; ε", loss factor, is calculated from the conductance, G, and i is the imaginary number. They can be calculated individually from the following equations, where C_0 is the air replacement capacitance of the sensor.

$$\varepsilon'(\omega) = \frac{C(\omega)material}{C_0}$$

$$\varepsilon''(\omega) = \frac{G(\omega)material}{\omega C_0}$$ **Equation 2**

$\omega = 2\pi f$, where f is the frequency of the electric field.

Both the dielectric constant and loss factor contain dipolar and ionic contributions that are expressed in the following equations:

$$\varepsilon' = \varepsilon'_d - i\varepsilon'_i$$

$$\varepsilon'' = \varepsilon''_d - i\varepsilon''_i$$ **Equation 3**

In the lower frequency range, ionic mobility tends to dominate the loss factor signal (13). Preliminary tests run to determine which frequencies best isolated the PF resin response found these lower frequencies to produce the most dramatic response. Using the loss factor and normalized curve of the derivative of the loss factor $(d\varepsilon''/dt)/(\varepsilon''_{max} - \varepsilon''_{min})$ in these lower frequencies should provide enough of a response to calculate degree of cure and *in situ* monitoring. Additionally, the loss factor is used to calculate degree of conversion (α), or cure; it is simply a ratio of the difference between the initial loss factor and the loss factor at the time of interest, and the difference between the initial and final loss factor.

$$\alpha = \frac{\varepsilon_i'' - \varepsilon_t''}{\varepsilon_i'' - \varepsilon_f''}$$ **Equation 4**

Where ε_i'' is the initial dielectric loss factor, ε_f'' is the final dielectric loss factor, and ε_t'' is the dielectric loss factor at the time of interest. Because the loss factor will rise as temperature increases the initial peak that indicates gelation is not due to resin cure. This will cause some negative calculated degree of cure values; any such negative values were set to zero (14, 15).

In the loss factor vs. time curve there are three points of interest when examining the cure process of various thermosetting polymers, two peaks occur. The first indicates a softening event in solid polymer films, which might not occur as a response to a lowered viscosity in a liquid adhesive. The second peak indicates cross-linking and a possible gel point of the polymer. Finally, an asymptote is approached indicating complete cure (15). This cure point is not necessarily an industrial or mechanical cure point, it is the point where the molecules can no longer rotate; the wood-based composites industry would consider sufficient cure for cessation of hot-pressing and mechanical integrity to occur much earlier.

2.3.3 Methods of Dielectric Measurement

The two most common methods of dielectric analysis use either fringe-field, also called micro-dielectric, or parallel-plate sensors. Each sensor has advantages and disadvantages

and is best suited for different situations. Fringe-field consists of a printed circuit with both electrodes on the same surface. This sensor will only gather dielectric data in the immediate area (a few microns deep); this means fringe-field sensors can be inserted into individual bond-lines or measure the dielectric response of specific areas of a composite (14). Fringe-field sensors tend not to be reusable, because they must be used inside the mat or inside a bond-line to gather meaningful data. However, the data gathered is much more specific and can be placed with greater precision into problem areas if used for quality control.

Parallel-plate sensors measure the dielectric response across a much broader region. The parallel-plate method places each electrode on opposite surfaces, with the dielectric material placed between them. Alternatively, one electrode may be used with a grounded metal plate acting as the opposing electrode. Because the dielectric material is between the two electrodes, an average of the dielectric response of the material between the electrodes is measured. This makes the parallel-plate sensor ideal for measuring an entire mat in wood-based composite manufacture, and makes it reusable since it does not come directly in contact with a bond-line. The large field of detection of parallel-plate sensors gives them potential for overall cure monitoring or control. However, this large field can introduce variability, since it is not measuring the bond-line, or a small region of the material being tested. It measures the dielectric response of the entire material and may not be able to isolate the area of interest.

3. Materials and Methods

This chapter illustrates the techniques used in the experimentation performed. Sample preparation, experimental design, and data analysis techniques are discussed. Two phenol formaldehyde resins were selected for this project. These were commercial formulations intended for the face and core layers of OSB. For the remainder of the paper, the face resin will be referred to as Face and the core resin will be referred to as Core.

3.1 Resin Description

The two resins used were donated by Georgia Pacific Resins in the summer of 2003, and were separated into single use batches and frozen within 24 hours of their arrival. The freezer in which they were kept is maintained at -23°C. Cure characterization was performed using the parallel-plate rheometer initially in February 2004 and again as late as October 2004 with no significant difference in the final cure temperature.

Initial characterization was performed at Washington State University (17); the results can be seen in Table 1.

Table 1 Properties of the face and core resins

	Core Resin	Face Resin
Non Volatile %	45	54.5
Specific Gravity	1.195-1.215	1.22
Viscosity at 25°C, cps	175-300	100-225
NaOH%	5.53-5.73	2.96-3.16
Free Phenol %	< 1.0	<0.2
Free Formaldehyde %	<0.2	<0.2
pH	11.0-11.5	9.8-10.2
M_n	3895	440
Mw	6580	620
M_w/M_n	1.72	1.41

As the table shows the two resins differ across most categories, particularly, the molecular weight and caustic levels. The higher molecular weight of the core resin shows it is more advanced leading to a faster cure and lower cure temperature.

3.2 Sample Preparation

3.2.1 Rheometer Sample Preparation

Rheometer samples were prepared using recently thawed samples of a face and core resin. Care was taken to apply similar volumes of resin in each sample using gap and temperature control. Resin was applied only when the rheometer plates were at 25°C and a gap of approximately 1 mm was used.

3.2.2 DEA Sample Preparation

For the DEA portion of this project small laminated veneer panels were produced. Each ply was cut from 1/8th inch rotary-peeled yellow-poplar (*Liriodendron tulipifera)* veneers

that were cut to a length of 8 inches and a width of 4 inches. The cut plys were oven-dried to 0% MC at 150° C in order to enable low panel moisture contents so the dielectric response of the curing resin could be better isolated.

Even resin distribution on the veneer was ensured by using a draw rod. An inter-digitated electrode (IDEX by Netzsch) fringe-field dielectric sensor was placed in the bond-line of interest and the parallel-plate dielectric sensor was placed on top of the panel and displaced laterally to eliminate any interference between the two sensors. The parallel-plate sensor had a 1-inch diameter sensing area and was supplied by Signature Control Systems (Denver, Colorado). The sensor comprises one side of what was essentially a capacitor. An electric current with controlled frequency is generated by the sensor, while a metal sheet on the other side of the sample completed the circuit.

Panels with differing moisture contents, number of plys, and types of resin were measured, and the IDEX sensor was placed at different bond-line locations. The dimensions of the sensing area were 5 mm by 10 mm.

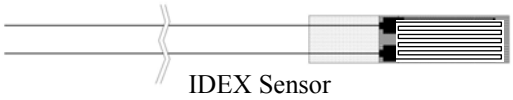

Figure 3 IDEX Sensor

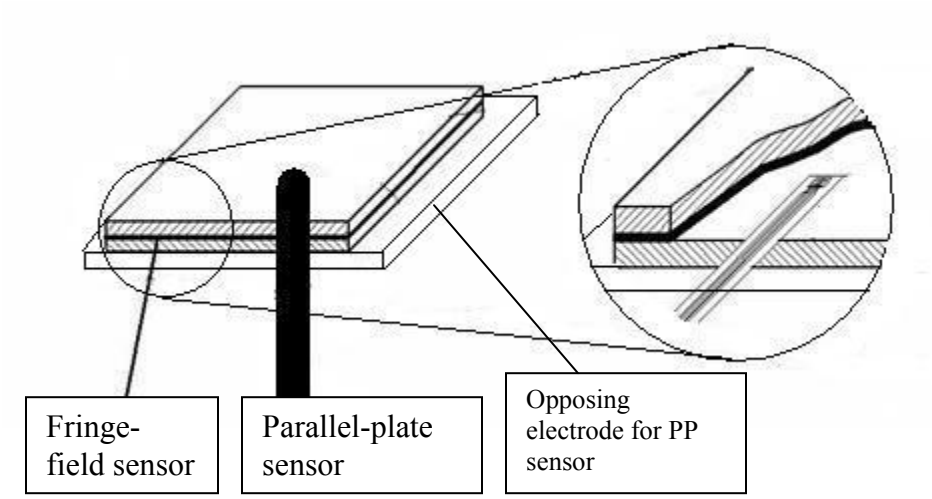

Figure 4 Placement of fringe-field and parallel-plate sensors in a 2 ply sample.

Table 2 Types of samples used in DEA experiments.

Moisture Content, %	Number of Plys	Fringe-field Sensor Position	Number of Samples/Resin Type		
			Core	Face	No Resin
4	2	1	2	2	2
4	3	1	2	2	
4	5	1	2	2	
4	5	2	2	2	
8	2	1	2	2	2
8	3	1	2	2	
8	5	1	2	2	
8	5	2	2	2	

Table 2 shows the experimental design for the dielectric analysis. The varying moisture contents were chosen to determine the effect, if any, water content had on DEA signals. Industry manufactured plywood commonly has an MC of approximately 5%. Four percent was chosen because it was the lowest MC achievable given the solids content of the resins chosen, and 8% was chosen to in order to ensure that the MC was at a level well beyond normal manufacturing conditions.

All samples contained the same amount of resin; 6% resin content by weight was used on every panel. Therefore there was some variance on resin content per bond-line. The spread had a range of 186 to 361 g/m^2 per bond-line, the actual resin spread will be reported in the appendix.

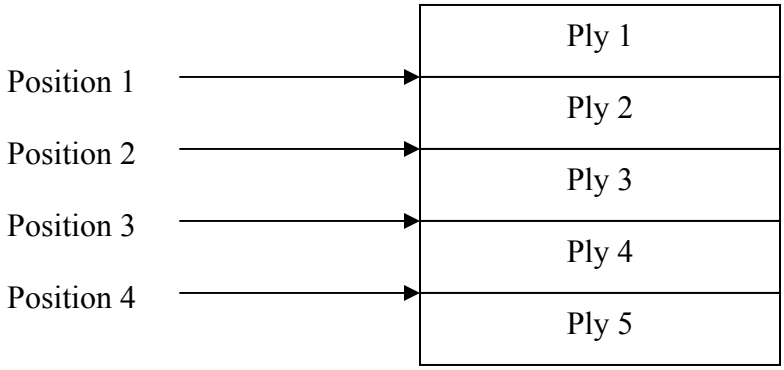

Figure 5 Position locations for the fringe-field DEA in the plywood samples.

Table 2 also shows the number of plys used in the sample and the position of the fringe-field dielectric sensor. Figure 5 is an illustration of the position labeling system used in the experiment. Labeling starts at the top and continues down; a 2 or 3 ply sample would be numbered in the same way with fewer available positions. Commercially produced plywood can have a number of plys, and because of this, samples of 3 and 5 plys were made. The addition of a five ply sample also allows for analysis of cure in bond-lines that are farther from the hot-press platens. The cure rate should slow down in bond-lines farther from the platens in the hot-press, and should differ from the response of the entire panel that is measured by the parallel-plate DEA. Finally, the resin type refers to the type of resin used. The two resins are nearly identical except for their solids content. The core resin has a higher molecular weight and is therefore more advanced in its cure when applied. It should cure faster than the face resin.

3.3 Experimental Design

3.3.1 Rheometer Experimental Design

In the rheometry experiments a TA Instruments AR 1000 model rheometer was used to characterize the cure of both resins. In order to decrease the variability of the resin cure, a temperature ramp of 2°C per minute was used. Previous runs found that controlling the rheometer by oscillation torque gave a smoother modulus response, and a strain of 0.03% was chosen to protect the rheometer from damage as the resin cured. Because it was necessary for the rheometer to use an iterative equation to determine the oscillation torque necessary to produce the chosen percent strain level; a higher temperature ramp caused too much variation in the percent strain as the software had difficulty determining the correct force. The 2°C per minute temperature ramp ensures that the resin reaches equilibrium before the next temperature rate increase occurs and allows for the rheometer to calculate the necessary oscillation torque.

The oscillation frequency was set at 1 Hz and controlled to 0.03% strain because 1 Hz is commonly used as a reference frequency, and 0.03% will not damage the resin structure in the early formation stage of cure, in addition to protecting the rheometer.

An initial gap of 1000 micrometers was used that allowed for enough sample to gather meaningful data, but not so much that it caused squeeze out.

Five repetitions were performed on both resins. Once G′ reached a plateau, indicating complete cure, the experiment was stopped.

3.3.2 DEA Experimental Design

The purpose of the DEA experiments was to compare the results of the fringe-field sensor to the parallel-plate sensor. Because both platens are heated to 200°C there is no need to perform a test with the fringe-field sensor in bond-line 1 and bond-line 2 in a 3 ply sample, or bond-line 1 and 4, or 2 and 3 in a 5 ply sample. Additionally, two different types of panels were tested without resin. It is assumed the moisture content influence is the same with different number of plys in a panel.

In order to minimize variability and moisture masking the dielectric response of the resin, the yellow-poplar plys were oven-dried and water was added to the resin in the 8% MC samples as necessary.

To ensure that both sensors were started simultaneously, the press was closed and each sensor was activated manually by the same individual. Though a few seconds of data are lost, the guaranteed synchronous measurement is vital to a valid comparison of the two systems.

3.4 Data Analysis

A graphical comparison of the degree of cure measurements was prepared. All statistical analysis was performed using JMPIN (18), a commercially available statistical analysis software program. Means were tested by analysis of variance with a significance level set

at α=0.05. The dielectric comparison was also performed graphically. Statistical differences were evaluated using a Tukey's HSD, with α=0.05.

4. Results and Discussion

This chapter will examine the result of the rheometry and dielectric experiments. The two resins will be compared, along with the different conditions of the dielectric experimental design.

4.1 Rheometry Results

The rheometry results were broken down by resin type. First, the core resin was examined, then the face resin, and finally the two were compared.

4.1.1 Face Resin

As can be seen from Figure 6 the face resin behaved exactly as predicted. A plateau in G′ was observed to start at 124.1 °C and the peak in G″ was observed at 121.7°C. Both phenomena are indicators of the onset of the vitrification on a thermosetting polymer in parallel-plate rheometry. Additionally, there was a peak in the tan δ that occurs very near to the onset of rapid gains in the storage and loss moduli of the resin, indicating a possible gel point occurring at this temperature.

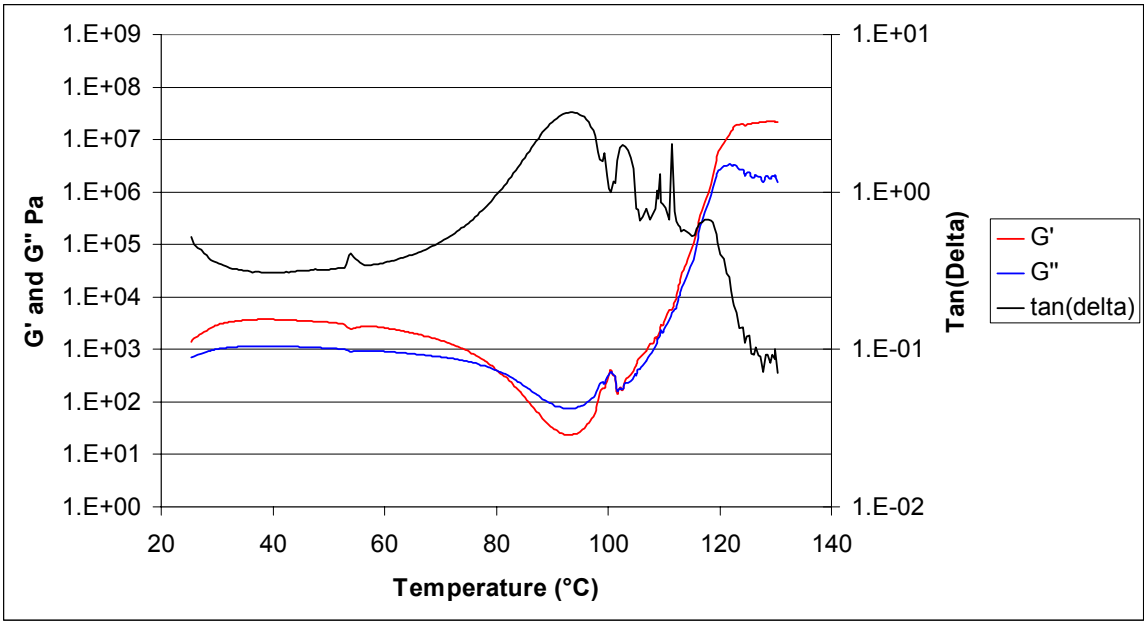

Figure 6 Average parallel-plate rheometry results for the face resin, n=3.

The degree of cure was computed from G" using Equation 4 and plotted in Figure 7 This resin exhibited an average cure point of 126°C, while the core resin had an average cure point of 130 °C. As would be expected, the core resin initially looses mobility faster than the face resin. However, the face resin reaches a plateau in G" prior to the core resin. This is most likely due to the polymerization pathways taken by the two resins. The face resin is such a lower molecular weight resin its chains are more mobile in the beginning of the cure pathway; this allows the resin to form cross-links more rapidly initially, Evidence of this exists in the G′ curve. The face resin exhibits a classic loss in viscosity before cure starts and the storage modulus starts increasing. The core resin does not go through this softening as dramatically. Though complete vitrification occurs more rapidly for the face resin, there still may be fewer cross-links in the face than the core resin.

When the degree of cure data is analyzed the two groups are found to be significantly different (p=0.0426).

Table 3 Degree of cure for the rheometer data at 2oC per minute temperature ramp.

	Time to Complete Cure by Rheometer measurements	
Resin Type	**Core, n=5**	**Face, n=3**
Mean	130.5	126.1
Std Dev	2.51	1.91
%COV	1.93	1.51

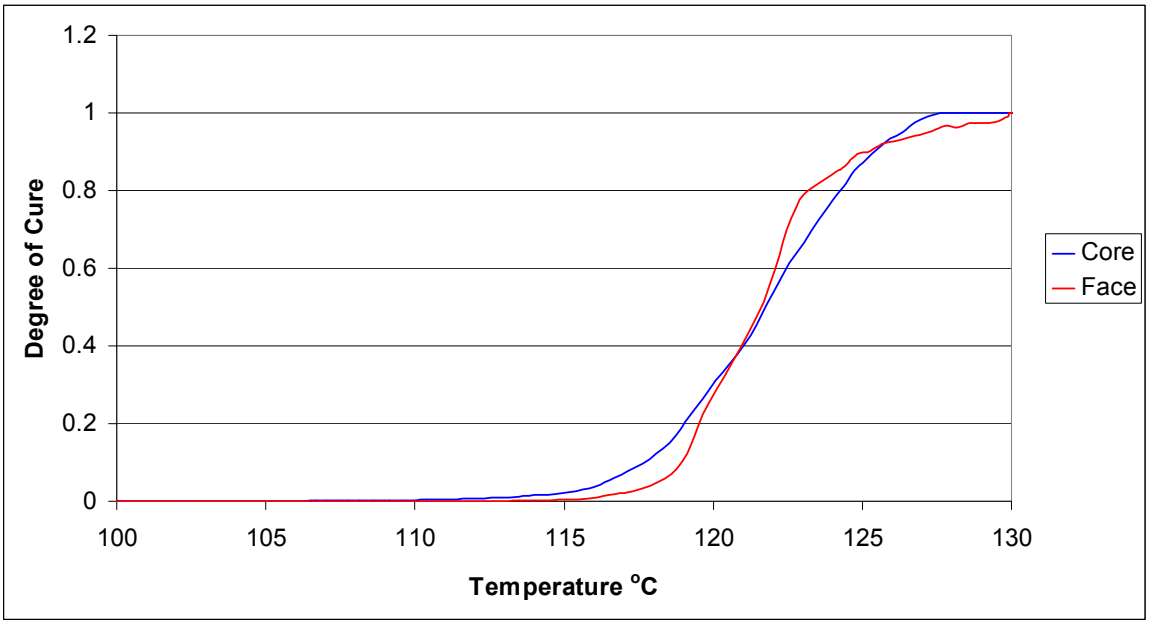

Figure 7 Average degree of cure results for face and core resins.

4.1.2 Core Resin

As can be seen from Figure 8 the core resin also behaved in a predictable manner; it also exhibits a loss in viscosity before the storage modulus begins to increase, though the loss is not as dramatic. The plateau in G′ started at 127.2 °C and the peak in G″ was observed

at 124.4 °C. Again, the peak in the tan δ curve occurs very near to the onset of the section of the profile with the first rapid gains in mechanical integrity are achieved.

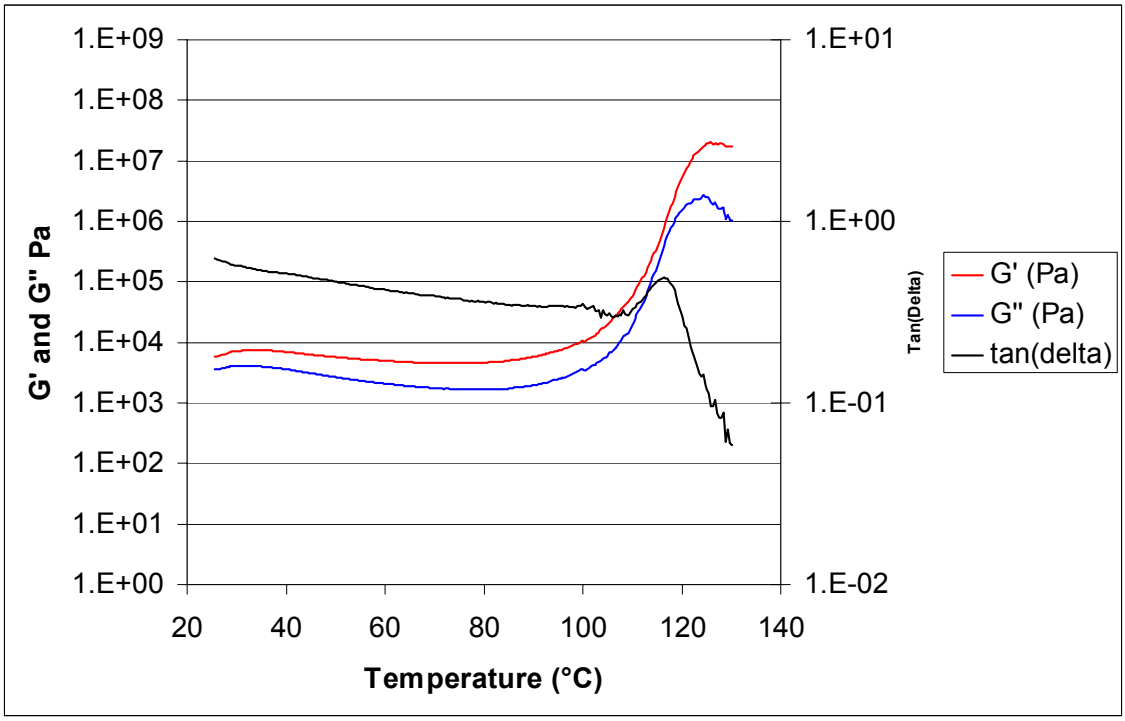

Figure 8 Average parallel-plate rheometry results for the core resin, n=5

4.2 Dielectric Analysis Results

The dielectric analysis was broken down into five sections according to the experimental design. The results of the fringe-field dielectric conditions were examined by comparing the results of the differing variables, including moisture content, resin type, and position of the fringe-field sensor. Finally, the fringe-field and parallel-plate dielectric analysis techniques were compared. Because two different instruments, with two different air replacement capacitance values were used the reported loss factor is not the same. Loss factor is an absolute measurement, and the fringe-field DEA accounted for the air replacement value of the sensor in its software; the parallel-plate DEA did not. However,

since the reported value is proportional to the loss factor of the system, and still detects the change in the degree of mobility of the resin, it can detect polymerization. In order to account for this a normalized loss factor was used when comparing the two systems, shown by equation 5.

$$\varepsilon''_n = \frac{\varepsilon''}{\varepsilon''_{MAX} - \varepsilon''_{MIN}} \qquad \textbf{Equation 5}$$

4.2.1 Influence of Moisture Content

Fringe-field DEA was performed on two different moisture contents, based on the total dry weight of the wood and resin system. The panels tested at 4% MC had a slightly higher MC due to the water contained in the resin; the plys were oven-dried and 6% resin solids was added by weight. Consequently, the actual MC ranges from 4-5%, depending on the specific sample, actual moisture contents can be found in the appendix. All 8% MC panels have an actual 8% MC.

Figures 9 to 11 illustrate the influence of moisture content. In the interest of statistically comparing a similar cure point of the panels, a slope of -500 s^{-1} was chosen to represent the point where the asymptote is approached and labeled final cure. This value does not necessarily represent complete chemical cross-linking, but will provide a point where the samples can be compared. When examining the time to final cure and the degree of cure at final cure there was no statistically significant effect detected.

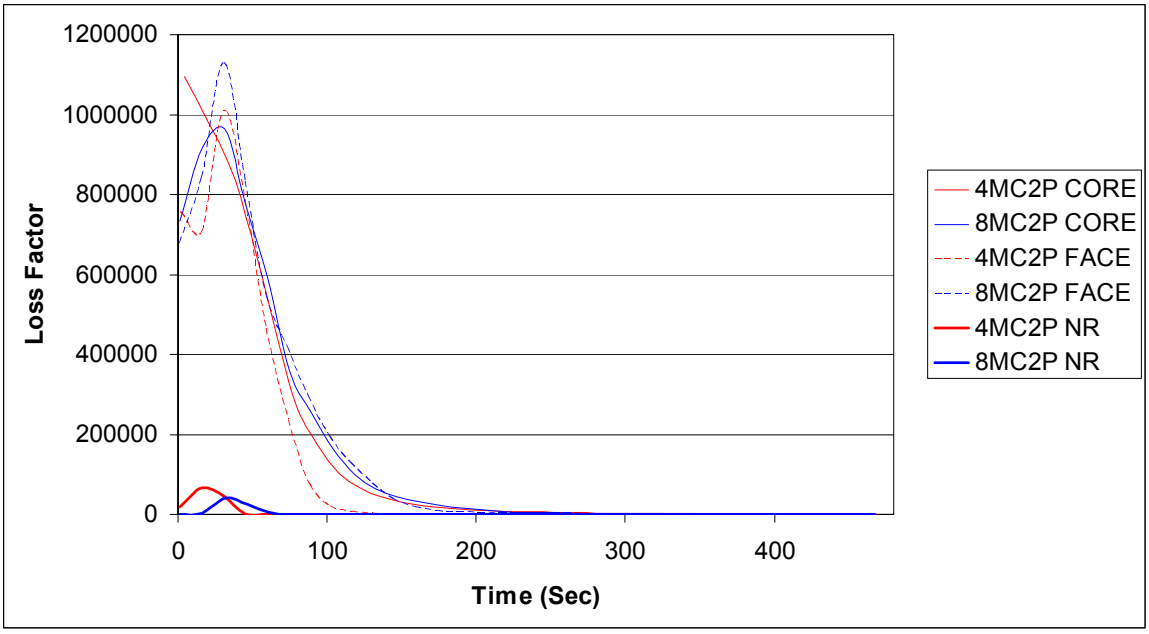

Figure 9 Loss factor vs. time of 2 ply samples grouped by MC at 200Hz using the fringe-field DEA. These are the average of the two samples run under the same conditions.

The 2 ply samples showed a clear trend as the cure progressed. However there was little difference between the panels based on moisture content. Because the response of the samples without resin is so small, regardless of moisture content, the measured dielectric loss factor must be a response due to the curing of the resin. Statistical analysis showed no significant difference between the mean final cure time based on the slope ($p=0.09$) and the degree of cure at the final cure time ($p=0.13$). A larger sample size may give greater significance to the two moisture contents, but this study was unable to detect a difference. There is also no difference between the samples with no resin added.

Table 4 Final cure time and degree of cure at final cure times for 2 ply samples by differing MC, n= 4.

	Time of Final Cure		Degree of Cure at Final Cure	
Moisture Content	4% MC	8% MC	4% MC	8% MC
Mean	143	183	0.993	0.983
Std Dev	38.6	12.1	0.006	0.011
%COV	27.1	6.60	0.577	1.08

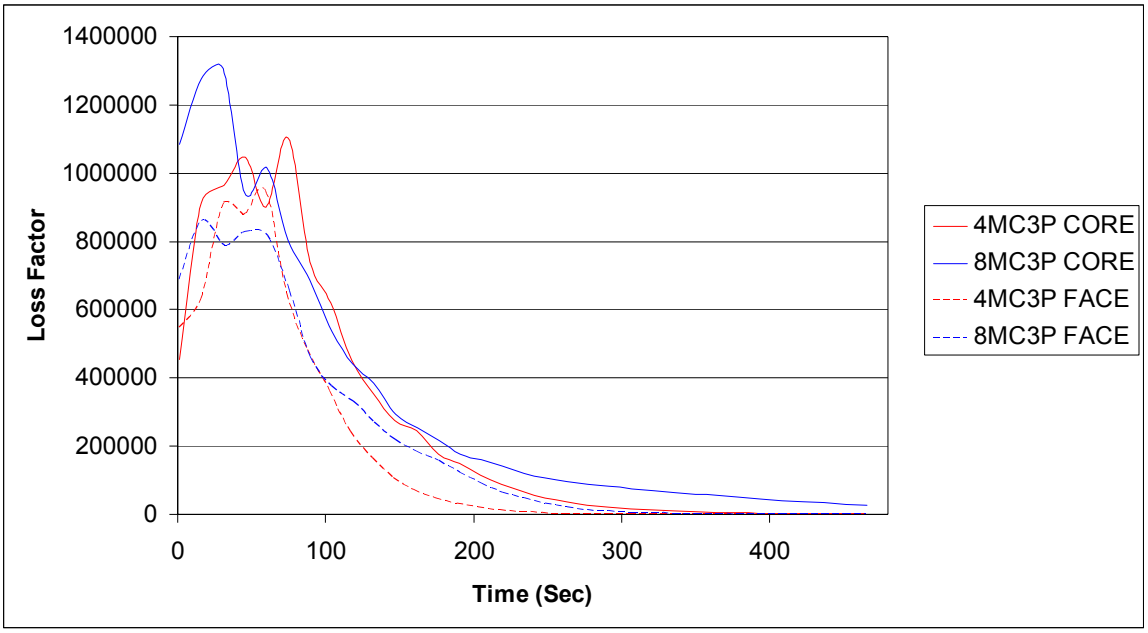

Figure 10 Loss factor vs. time of 3 ply samples grouped by MC at 200Hz using the fringe-field DEA.

When statistical comparisons were made on the mean final cure time and degree of cure at the final cure time, no significant difference was found ($p>0.5$).

Table 5 Final cure time and degree of cure at final cure times for 3ply samples by differing MC, n=4.

	Time of Final Cure		Degree of Cure at Final Cure	
Moisture Content	**4% MC**	**8% MC**	**4% MC**	**8% MC**
Mean	250	268	0.962	0.964
Std Dev	42.9	35.5	0.014	0.021
%COV	17.2	12.3	1.50	2.16

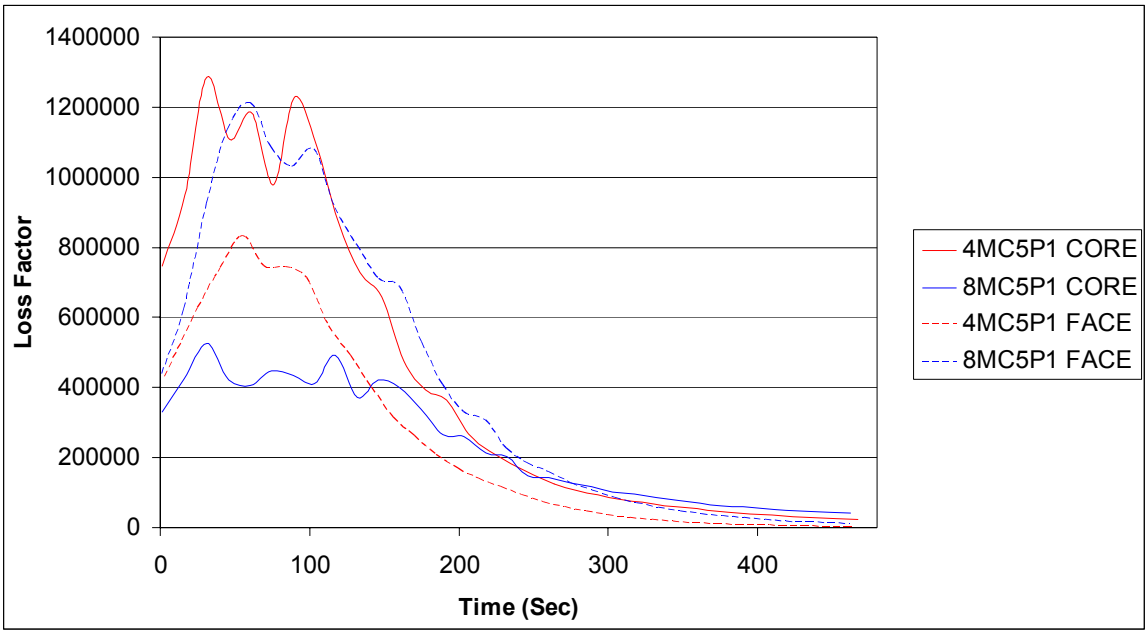

Figure 11 Loss factor of 5 ply, position 1 samples grouped by MC at 200Hz using the fringe-field DEA.

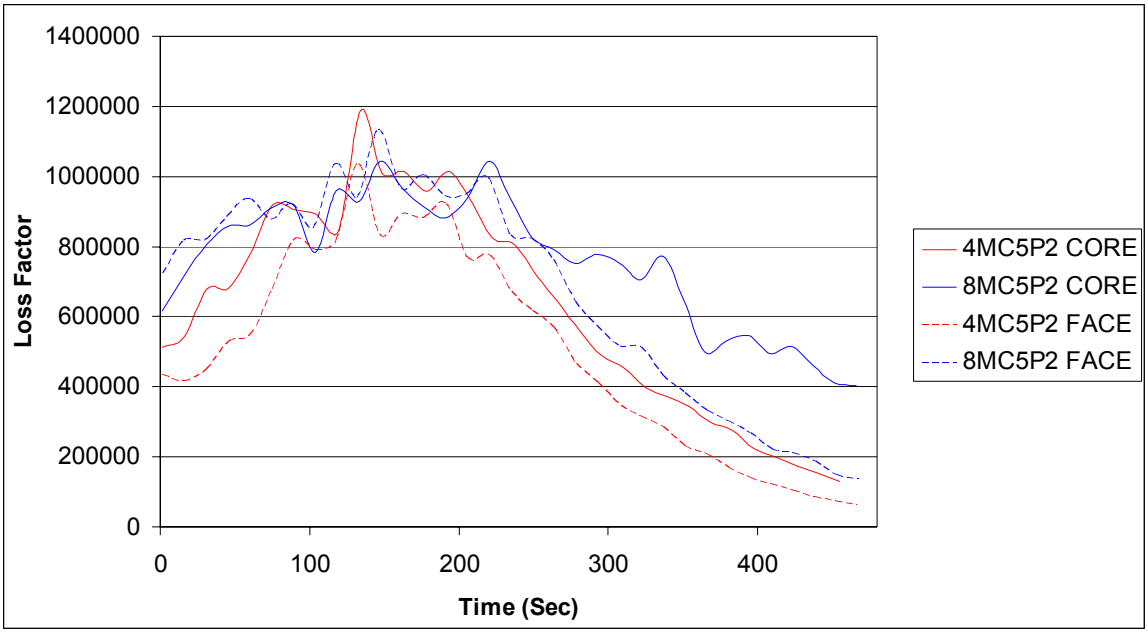

Figure 12 Loss factor of 5 ply, position 2 samples grouped by MC at 200Hz using the fringe-field DEA.

The data shown in Figures 11 and 12 show the loss factor of 5 ply samples separated by fringe-field sensor position. When position 1 is looked at individually, there is no significant difference between the two moisture contents in either the final cure time or the degree of cure at the final cure time. The data for position 2 indicates a final cure was not attained, though the veneers were bonded. It is clear, however, from Figure 13 that the position 2 results are not statistically different when the loss factor curves are displayed on the same graph. Though a true degree of cure as defined above cannot be calculated, a value defined as degree of cure of the cure obtained can be calculated and compared. It is calculated using the same equation as degree of cure, but the distinction must be made for samples where complete cure was not obtained. By calculating what percent of the total change of loss factor the sample undergoes, a value that is comparable between the different samples analyzing the cure at the 2nd position is obtained. However, it cannot be used to compare the 2nd to the 1st position panels. When the time to reach

75% of the cure obtained is calculated there is no statistical difference between the two moisture contents (p=0.21).

Table 6 Final cure time and degree of cure at final cure times for 5P1 samples by differing MC, n=4.

	Time of Final Cure		Degree of Cure at Final Cure	
Moisture Content	**4% MC**	**8% MC**	**4% MC**	**8% MC**
Mean	333	344	0.945	0.903
Std Dev	21.5	12.08	0.009	0.091
%COV	6.46	19.9	0.936	10.1

Table 7 Time to reach 75% obtained cure for 5P2 samples by differing MC, n=4.

	Time at 75% Obtained Cure	
Moisture Content	**4% MC**	**8% MC**
Mean	330	356
Std Dev	16.7	33.4
%COV	5.05	9.37

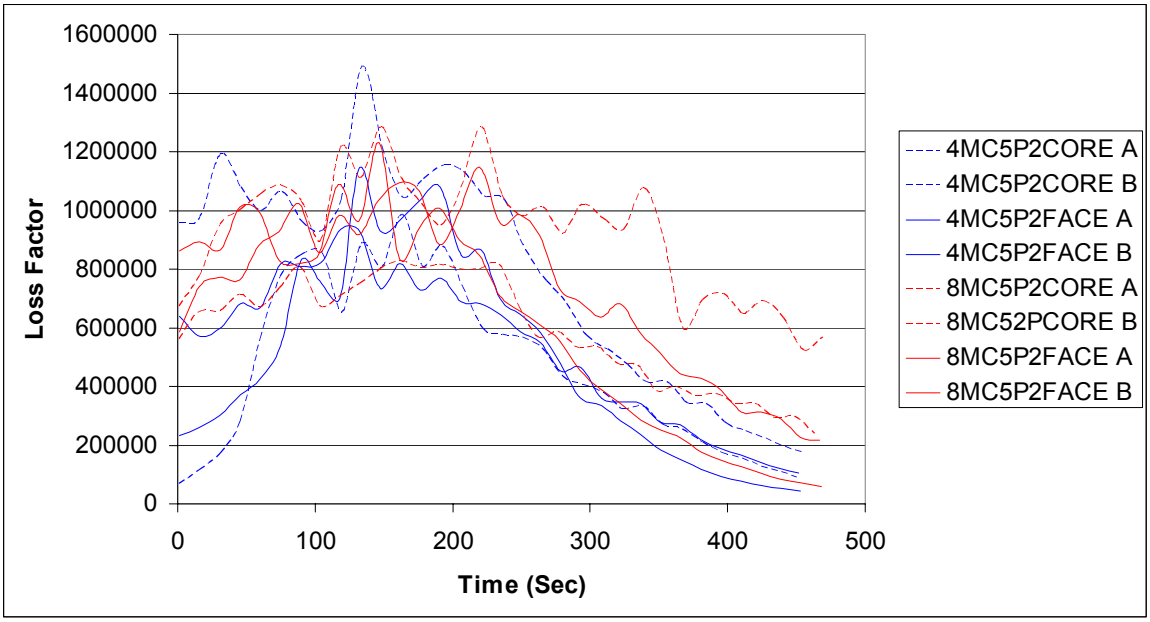

Figure 13 Dielectric loss factor of individual 5 ply samples at 200Hz using the fringe-field DEA.

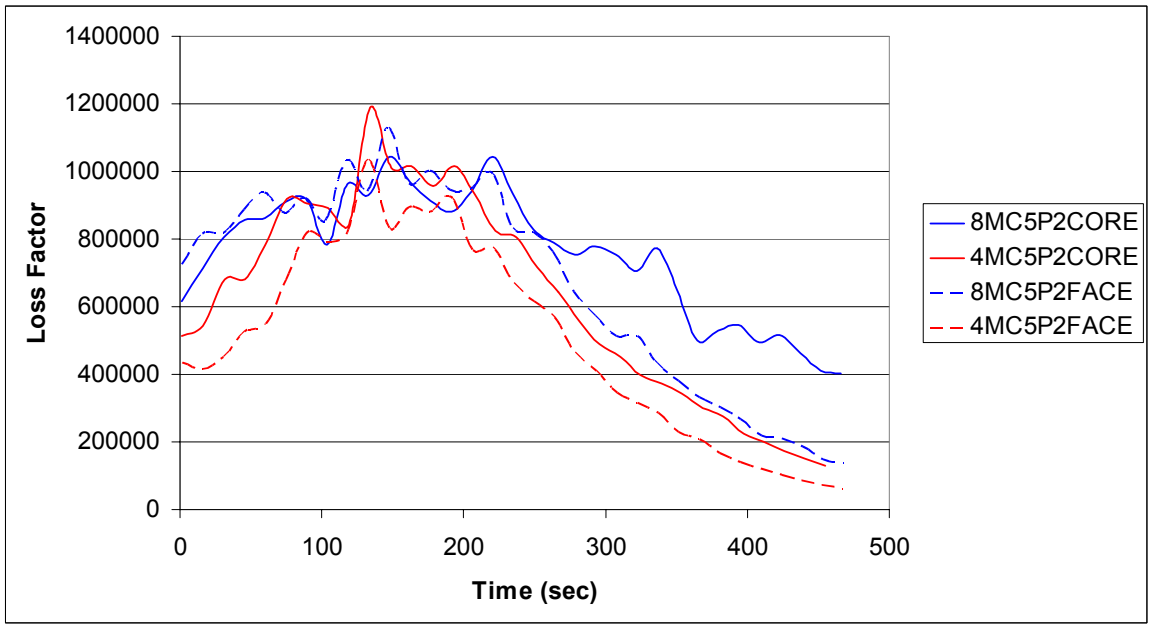

Figure 14 Dielectric loss factor of average 5 ply samples by moisture content at 200Hz using the fringe-field DEA.

As can be seen by Figure 14 the 8MC samples seem to cure at a slower rate than the 4MC samples after about 300 seconds. In order to test this, the time to reach a degree of obtained cure of 85% was compared ($p<0.001$). There is clearly a significant effect occurring with such a pronounced difference in the time it takes to reach certain cure points. This difference may be due to the effect of the extra water evaporating. The energy lost due to the heat of vaporization could slow down the heating rate substantially enough to cause such an effect. The reason this vaporization effect is more significant in the 2nd position is due to the insulating effect of the outer plys; this insulating effect would also cause the heating rate to slow. Such a lower heating rate would cause the vaporization of the water to last longer. Further research with a temperature profile would be valuable in exploring this effect.

Table 8 Time to reach 85% obtained cure for 5P2 samples by differing MC, n=4.

	Time at 85% Obtained Cure	
Moisture Content	**4% MC**	**8% MC**
Mean	374	432
Std Dev	11	9.04
%COV	2.95	2.09

Also noticeable is the extra noise that is inherent in the 2nd position when compared to the 1st position samples. This extra noise is also likely due to the insulating effect of the outer plys. Since the water takes more time to vaporize it may boil inside the bond-line: bubbles are apparent in the cured PF layers. The bubbles of trapped steam or water would introduce great variability until the steam could escape. Such a scenario would explain why the noise dissipates later in the profile. Again, a temperature profile of the bond-line as the cure progresses would be valuable in answering these questions.

4.2.2 Influence of Resin Formulation

Dielectric analysis was performed on two different resins, an OSB core resin and an OSB face resin. As can be seen by the analysis supplied by Washington State University, the two resins are similar. The difference most directly related to cure rate is the higher molecular weight of the core resin. The core resin is therefore more advanced in the cure process at application which should lead to a more rapid cure..

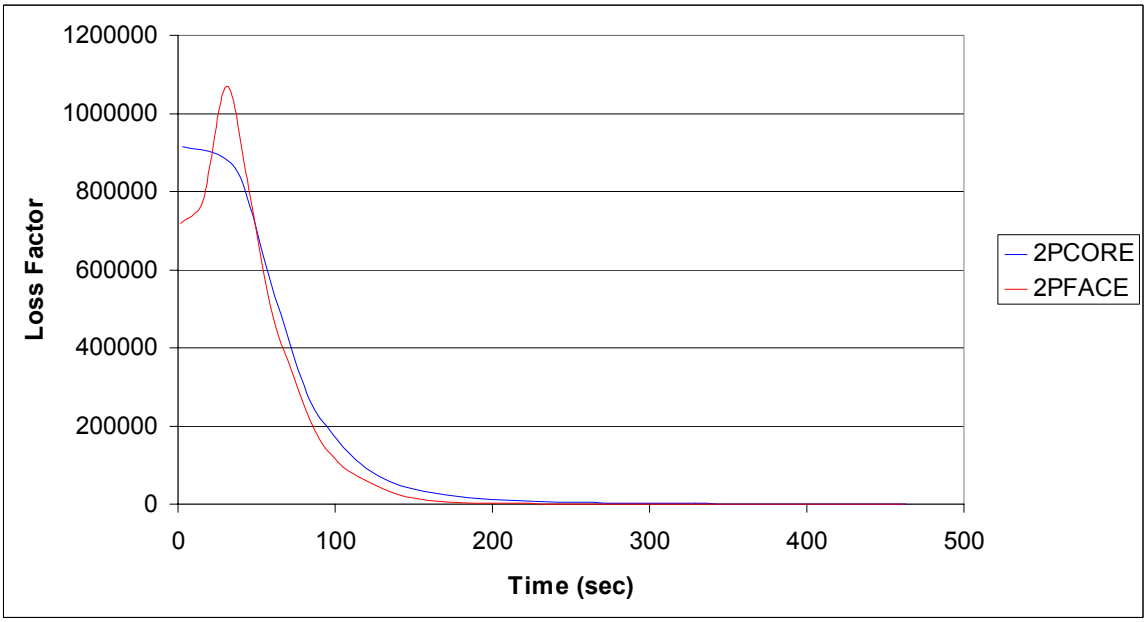

Figure 15 Dielectric loss factor of 2 ply samples grouped by resin and measured by the fringe-field DEA.

As Figure 15 shows, there is very little separation in the loss factor profiles between the two resins when the two ply samples are compared. It is possible that the temperature is rising too rapidly for the cure profiles of the two resins to differ greatly. The temperature necessary for the cure of the face resin was reached very soon after the cure temperature of the core resin because the 2 ply samples were thin and heat transfer rapid.

When the final cure temperature and the degree of cure are examined, there is no statistical significance between the two resins. Again there is simply too much variation between the samples for any statistically significant effect to be noticed. Table 9 shows the values for the time at the final cure slope and the degree of cure at the final cure slope.

Table 9 Values of final cure times and degree of cure at final cure times for 2ply samples by different resins.

	Time of Final Cure, sec		Degree of Cure at Final Cure	
Moisture Content	Core	Face	Core	Face
Mean	174.3	151.3	0.984	0.993
Std Dev	37.3	31.5	0.011	0.007
%COV	21.4	20.8	1.13	0.670

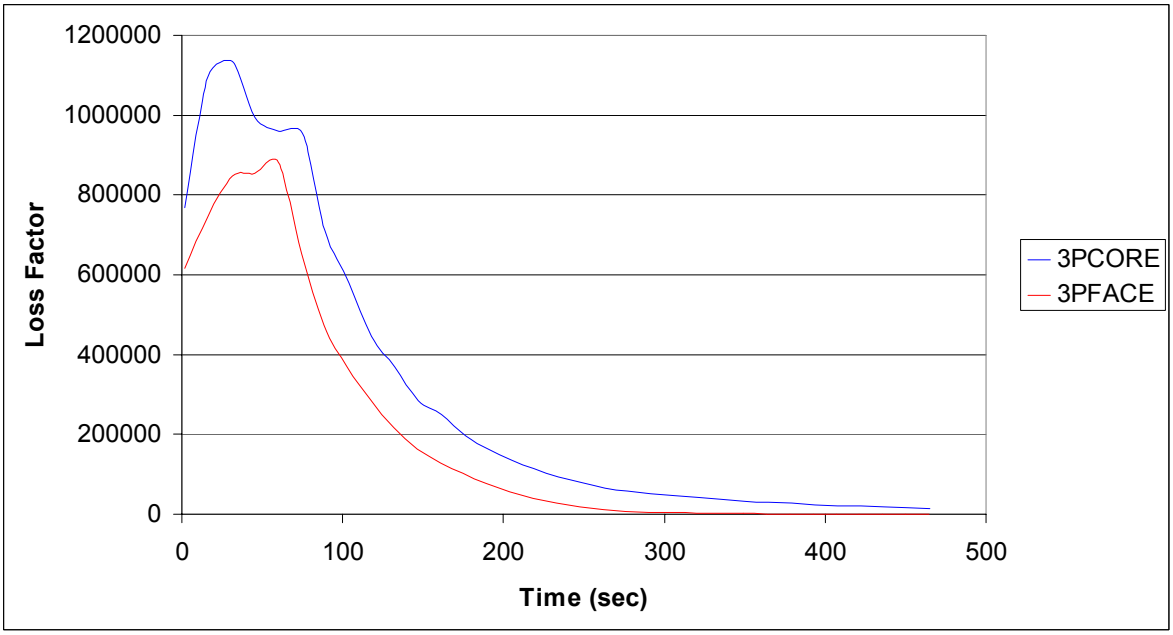

Figure 16 Dielectric loss factor of 3 ply samples grouped by resin type at 200Hz as measured by the fringe-field DEA.

Some separation between the resins is achieved in the three ply samples, though the variation in the individual samples is too great for the final cure time to be statistically significant (p=0.069). More samples should lower the P value and show some significant differences. However, the degree of cure at that time was found to be significantly different (p=0.0007). This difference further indicates that a larger sample size would help to differentiate between the two resins. This DEA analysis was able to detect some

large trends with a few samples, but the inherent variability between sample groups makes it impossible to differentiate between two similar cure profiles.

Table 10 Final cure time and degree of cure at final cure times for 3ply samples by different resins, n=4.

	Time of Final Cure, sec		Degree of Cure at Final Cure	
Moisture Content	**Core**	**Face**	**Core**	**Face**
Mean	282	236	0.948	0.977
Std Dev	6.55	42.4	0.007	0.006
%COV	2.32	18	0.738	0.605

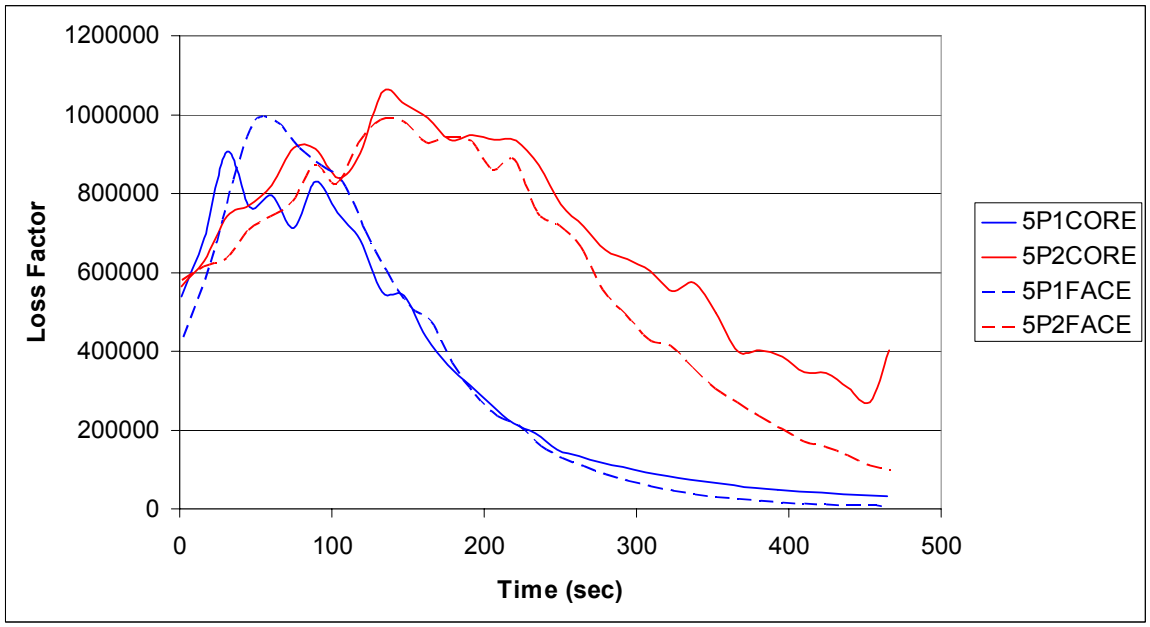

Figure 17 Dielectric loss factor vs. time of 5 ply samples at 200 Hz by resin type and position.

In regard to the 5 ply samples, again there is no significant separation between the two resins. When the 5ply samples from position 1 were compared the p value was calculated to be 0.11. While not within the α=0.05 confidence interval, additional samples may decrease the p value sufficiently to determine a statistically significant difference. In order to compare the two sample types statistically at position 2, the loss factor slope between times 395 and 450 seconds was examined. The time spread was chosen to help to lessen the effect of the greater noise in the position 2 samples, and provide a point at which to compare the two loss factor profiles. Unfortunately, the variance was still too great for the test to detect any differences in the degree of cure. Tables 11 and 12 show the variation inside the sample groups.

Table 11 Final cure time and degree of cure at final cure times for 5 ply samples at position 1 by different resins, n=4.

	Time of Final Cure, sec		Degree of Cure at Final Cure	
Moisture Content	Core	Face	Core	Face
Mean	174.3	151.3	0.984	0.993
Std Dev	37.3	31.5	0.011	0.007
%COV	21.4	20.8	1.13	0.670

Table 12 Slope of the loss factor with respect to time for the 5 ply samples at position 2 by different resins, n=4.

	Slope Between T395 and T450	
Resin Type	Core	Face
Mean	-1930	-1916
Std Dev	665	433
%COV	-34.4	-45.2

4.2.3 Position 1 vs. Position 2

The bond-line position comparison is the only situation where the DEA was sensitive enough to capture a clear difference between treatments. In the 5 ply samples, position 1 was much closer to the heated platens, and therefore, cured more rapidly. As can be seen from Figure 19, there is a clear difference in the loss factor profile of the two positions.

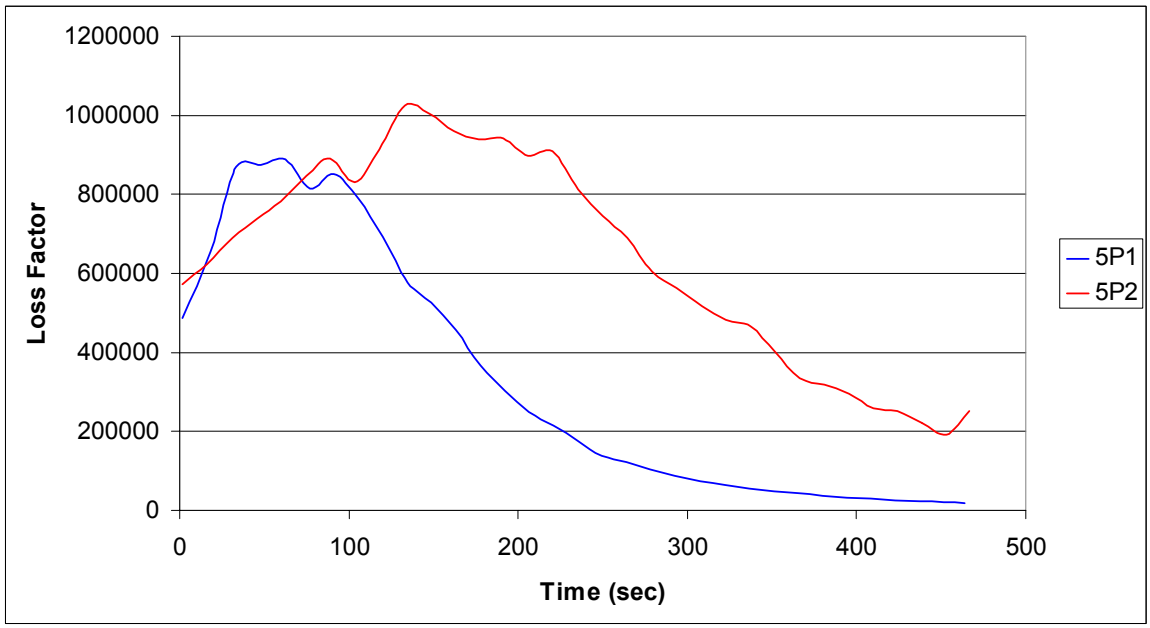

Figure 18 Dielectric loss factor vs. time for 5 ply samples at 200 Hz by fringe-field sensor location (see Figure 3.2.3).

Figure 19 clearly shows differences in the shape of the curves. The 5P1 samples have reached an inflection point at approximately 200 seconds, while the 5P2 samples are clearly still reacting when the cure process was stopped. The same method used to compare different resin types in the 5P2 samples was used to compare the two fringe-field positions. When the two positions are compared, there is a clear difference between the two cure profiles between 395 and 450 seconds into the cure ($p<0.0001$). The extra

plys between position 2 and the platens substantially slow down the heat flow to the bond line and consequently slow the cure of the resin.

4.2.4 Parallel-Plate vs. Fringe-Field DEA Techniques

Since fringe-field and parallel-plate dielectric analysis measure such different portions of the board and use dramatically different geometries, it is necessary to find a way to normalize the data for comparison. The differences are further compounded by the nature of the parallel-plate method of measuring the loss factor; it reports a value that is proportional to the loss factor. While the true loss factor can be calculated, it would not match the fringe-field loss factor because of the different geometries and areas of analysis. Figure 19 illustrates this. The normalized loss factor derivative can account for all of the above factors regardless of which value is used, as seen in Figure 20.

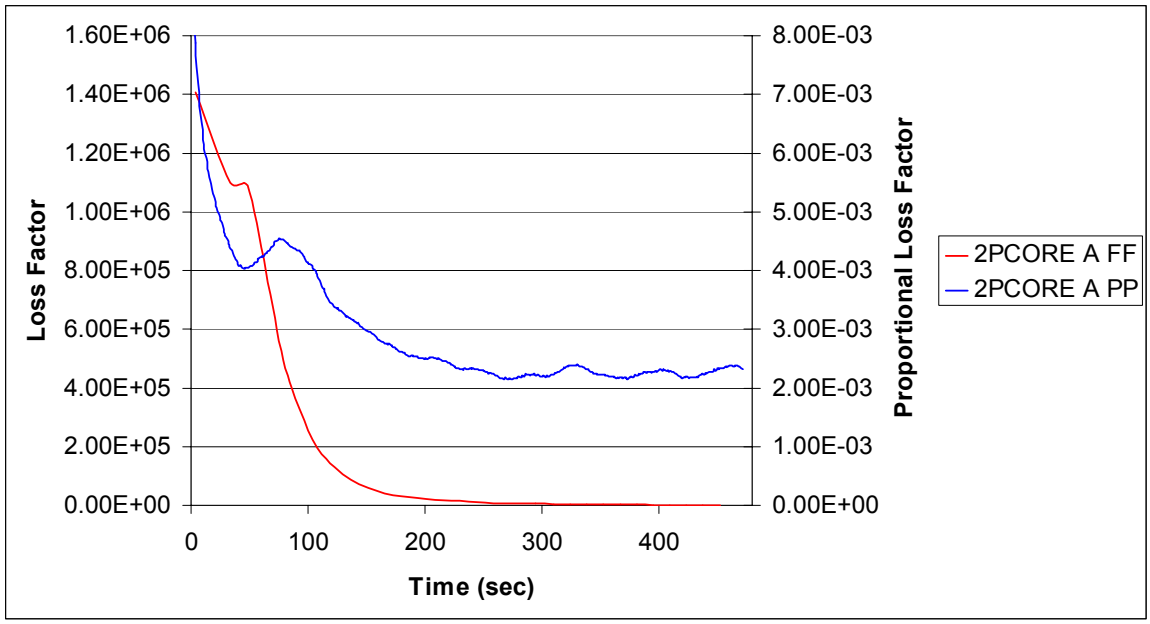

Figure 19 Loss factor vs. time of sample 4MC2PCORE at 200 Hz using parallel-plate and fringe-field DEA.

The two cure profiles differ greatly, not only do they have vastly different magnitudes and slopes, there appears to be relatively strong dielectric activity occurring until 200 seconds in the parallel-plate sample, where the activity stops soon after 100 seconds of press time in the fringe-field sample.

As can be seen from Figure 20, the normalized curve is essentially the slope of the original loss factor curve, but it has been normalized, using equation 5, in order for the two methods to be observed on the same scale. Since the shape remains the same, similar methods to the analysis used in previous sections can be performed in order to compare the two types of DEA.

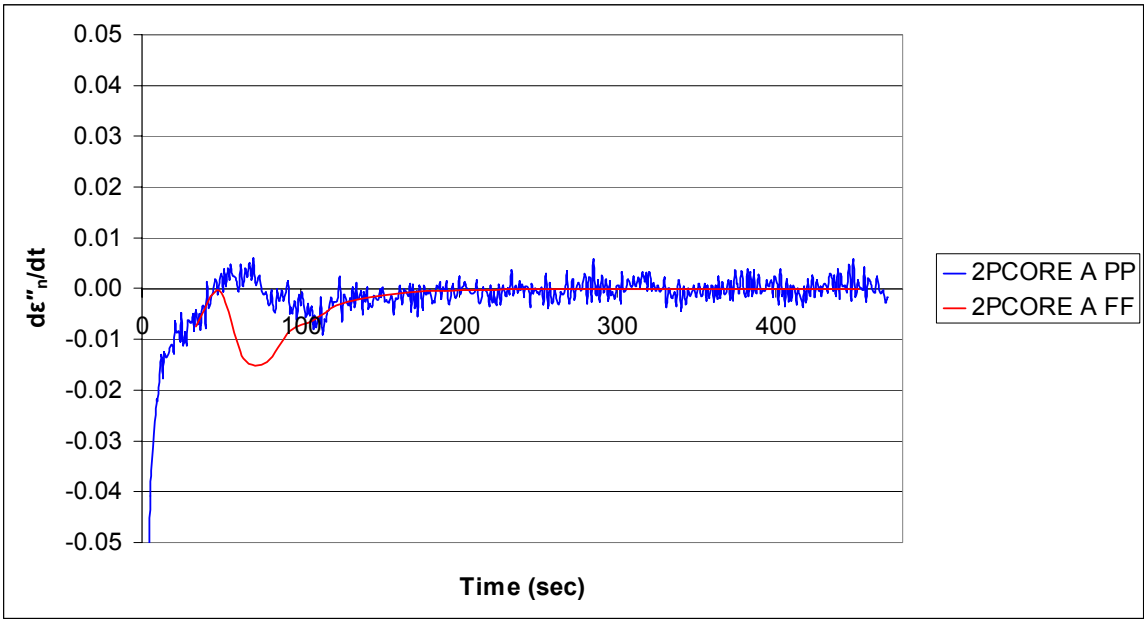

Figure 20 Normalized time derivative of the loss factor vs. time of sample 4MC2P1FACE at 200 Hz using parallel-plate and fringe-field DEA.10

The data was recorded every second for the parallel-plate method, as opposed to the fringe-field software, which took a measurement approximately every 14 seconds. This accounts for the appearance of a "noisy" signal in comparison to the fringe-field method. The parallel-plate response curve also tends to be flatter and have a smaller range in the slope values due to the measurement of the loss factor through the thickness of the panel rather than solely the bond-line. When a moving trendline is used to help smooth the parallel-plate's normalized time derivative, the correlation is more obvious.

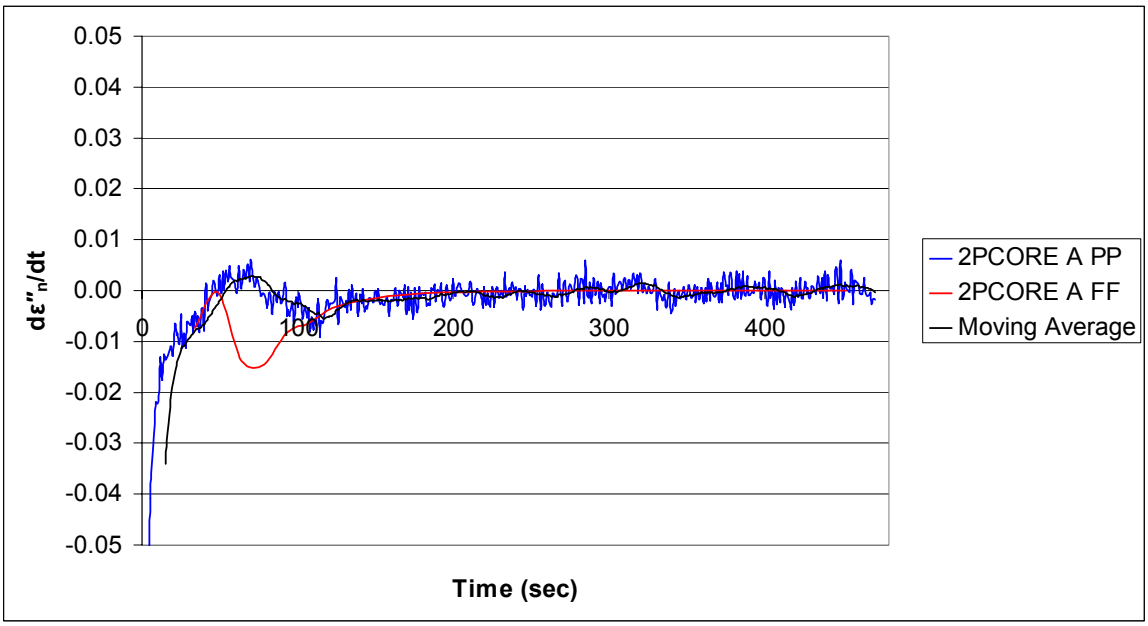

Figure 21 Normalized time derivative of the loss factor vs. time of sample 4MC2P1CORE at 200 Hz using parallel-plate DEA, fringe-field DEA and the moving 15-point average of the parallel-plate curve.

Figure 21 shows how a moving average could help to determine the point where the normalized time derivative approaches zero, signaling complete cure.

The cleanest and easiest data to examine should come from the 2ply samples at the 4% MC. Figure 22 will examine these samples.

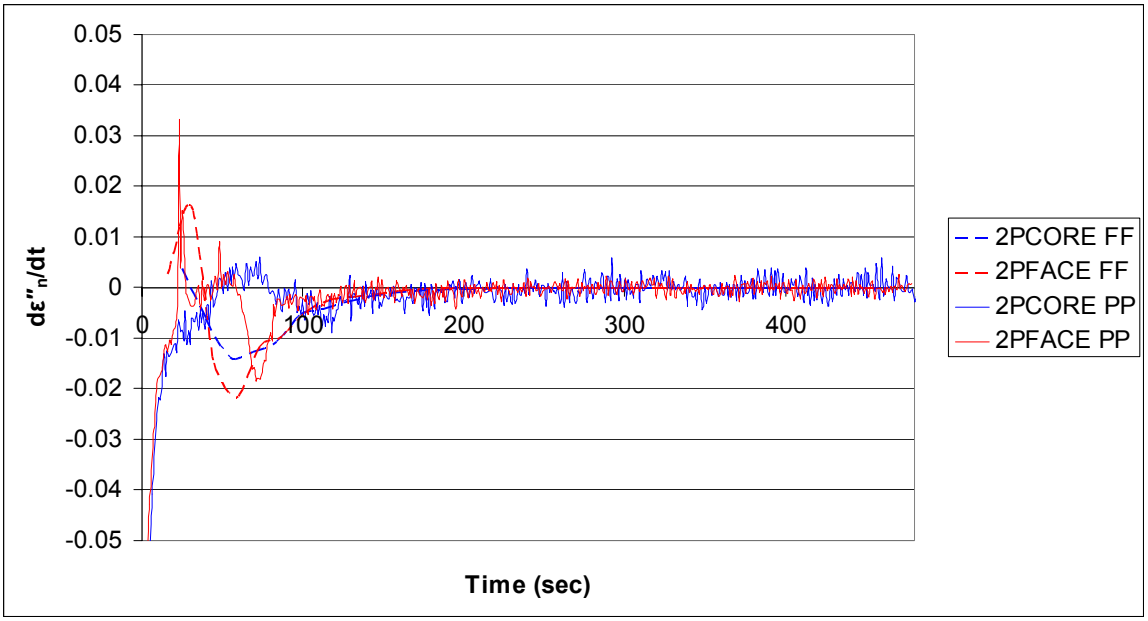

Figure 22 Normalized time derivative of the loss factor at 200 Hz for the 2ply samples using parallel-plate and fringe-field DEA.

The curves shown in Figure 22 appear to show agreement between the fringe-field and parallel-plate results. The normalized time derivative of the loss factor approaches zero at the same time for both techniques. Looking at Figure 23, which is a plot of an individual sample that was included in the averaged data in Figure 22, shows good agreement between the DEA methods.

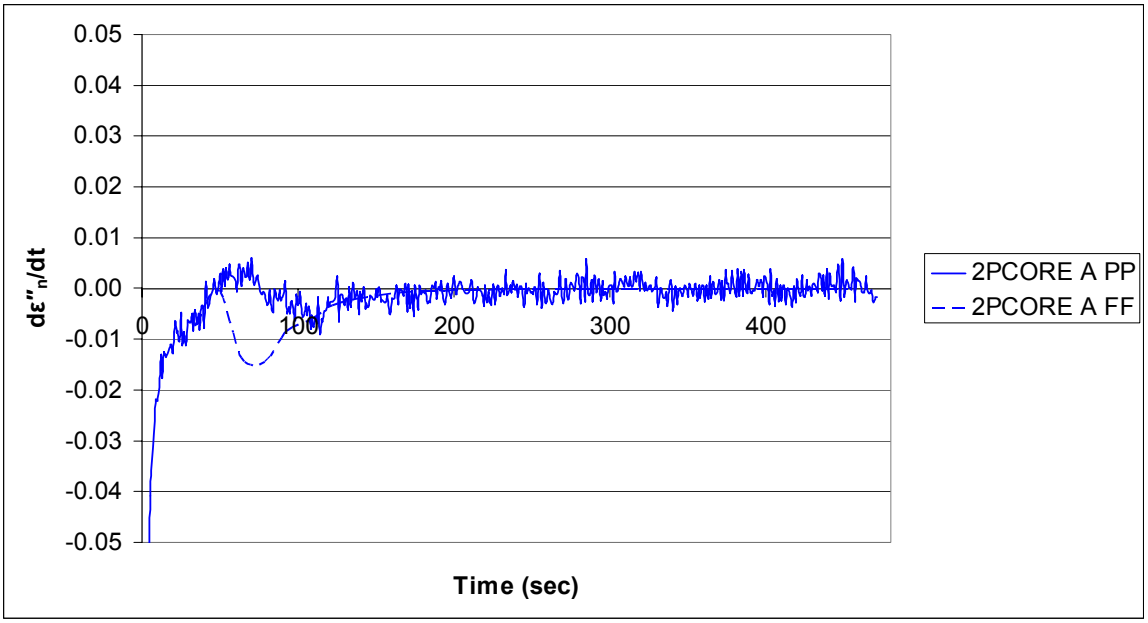

Figure 23 Normalized time derivative of the loss factor of sample 4MC2PCORE at 200 with Hz of parallel-plate and fringe-factor DEA.

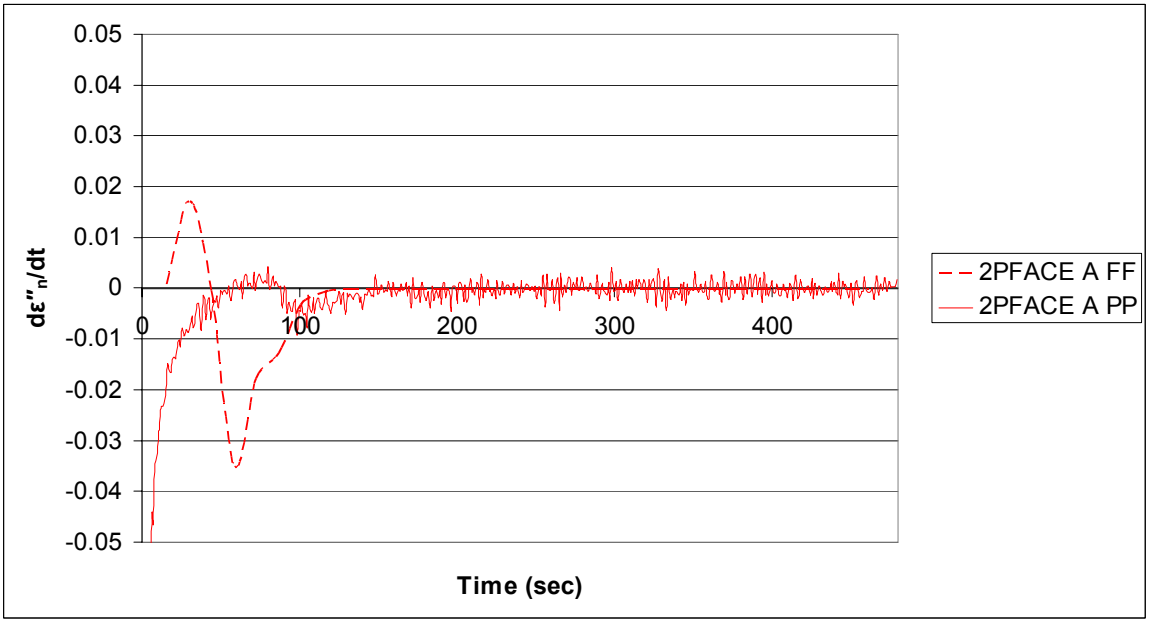

Figure 24 Normalized time derivative of the loss factor of sample 4MC2P1FACE at 200 Hz with parallel-plate and fringe-factor DEA.

Figures 23 and 24 show individual samples. There is a high correlation between the corresponding samples once the curves start to approach zero.

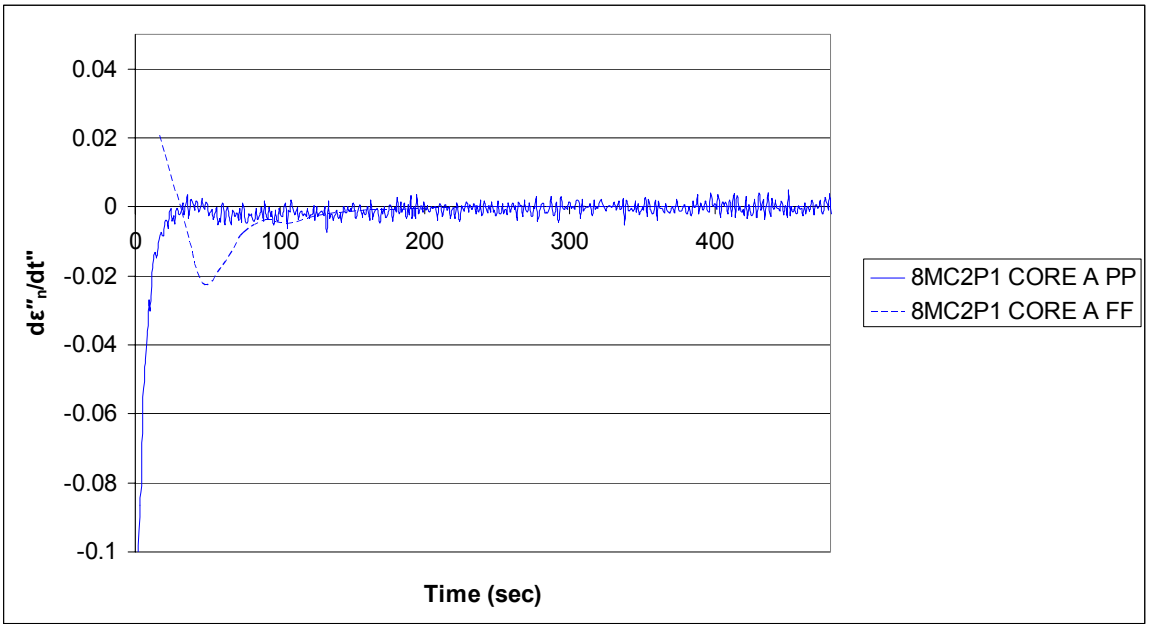

Figure 25 Normalized time derivative of the loss factor of sample 8MC2P1CORE at 200 Hz of parallel-plate and fringe-field DEA.

Figure 25 shows a comparison of a single sample of an 8% MC panel. It shows good correlation between the two techniques. Unfortunately, the noise in the parallel-plate method masks much of the curve's trend. The parallel-plate method is not as sensitive to the dielectric change occurring at the bond-line as the fringe-field method. Background noise nearly overwhelms the signal.

The correlation between samples should decrease as the number of plys increases. Since the fringe-field sensor measures only one bond-line, while the parallel-plate set-up measures throughout the entire thickness of the panel, the dielectric response should be much different. Figures 26, 27, and 28 indicate the influence of bond-line position for the two methods with the difference illustrated by the trend of the normalized loss factor.

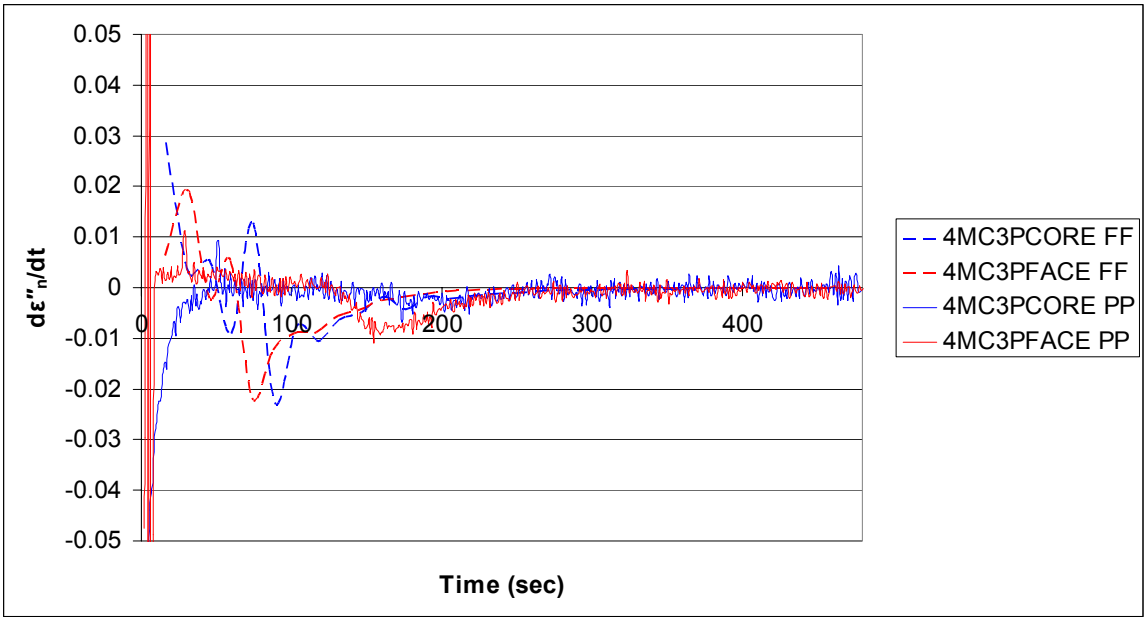

Figure 26 Normalized time derivative of the loss factor at 200 Hz using parallel-plate and fringe-field DEA on the 3ply samples.

The data from the 3ply fringe-field and parallel-plate DEA (Figure 26) correlate fairly well within their own groups in terms of the approach towards a zero slope, and there is correlation with the parallel-plate and fringe-field curves as the curves approach zero. This is expected because, though there are two bond-lines in the sample, they are an equal distance from the hot-press platens. The two bond-lines received heat at the same rate and there should have been no difference between the two bond-lines. Consequently, the parallel-plate DEA should not have experienced overlapping signals from two different cure events.

The response of the resin is again masked by the noise in the parallel-plate data.

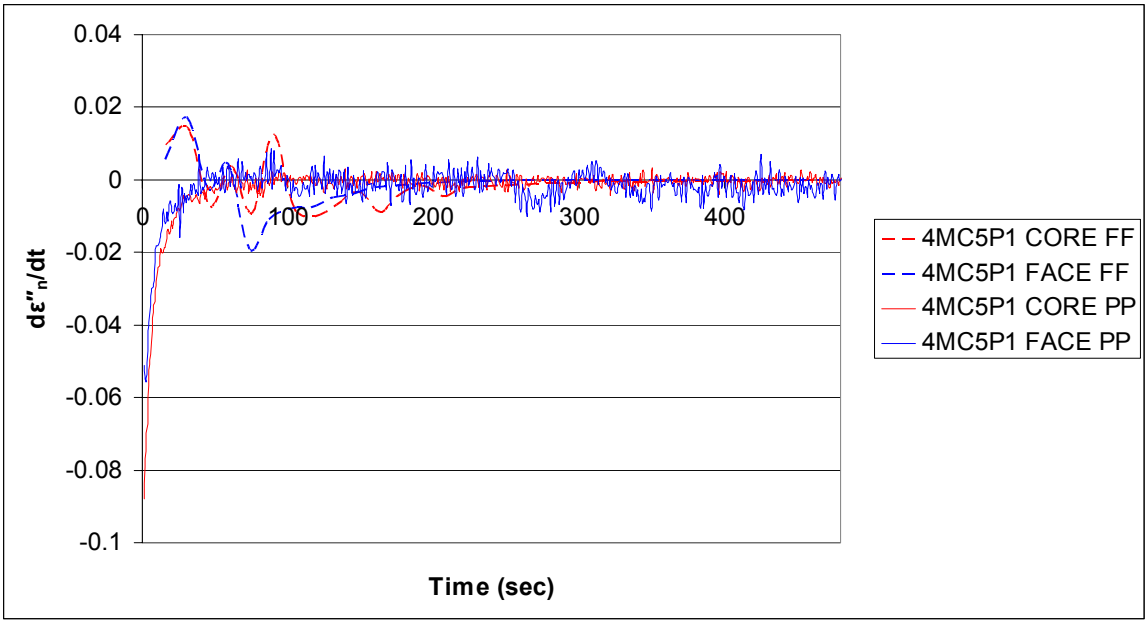

Figure 27 Normalized time derivative of the loss factor at 200 Hz using parallel-plate and fringe-field DEA

Figures 26 and 27 show the results of the multiple bond-line analysis for the 5ply samples. The fringe-field sensor detects the end of cure in the first position, but the middle bond-line was still curing when the hot-press cycle was ended. The parallel-plate method collects dielectric data from all bond-lines, broadening any dielectric events that occur, and completely masking some specific cure events.

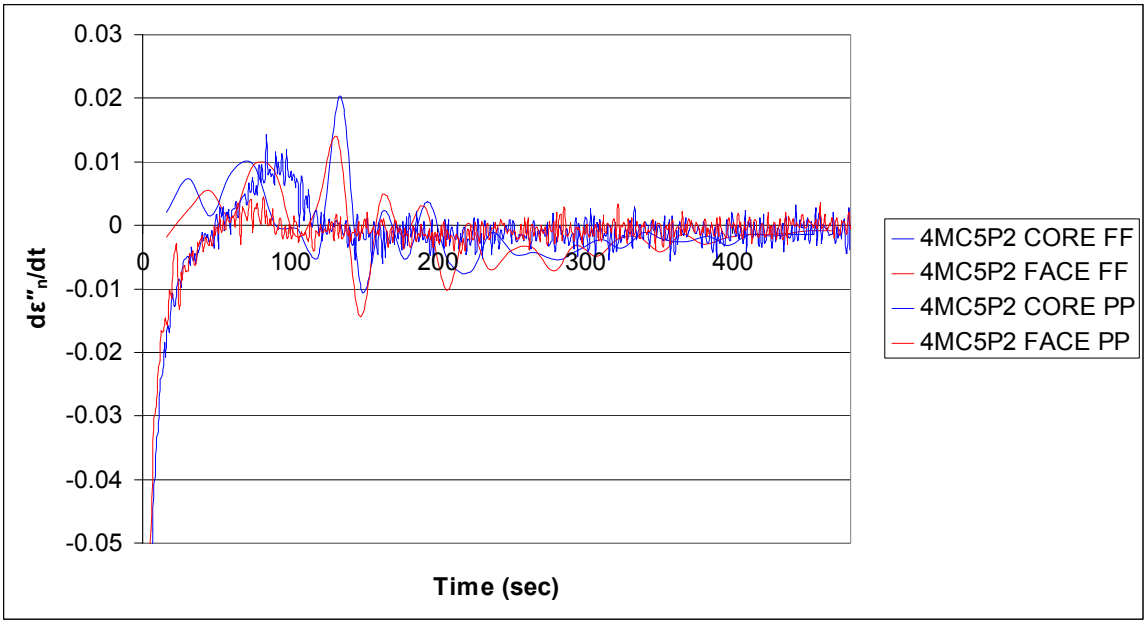

Figure 28 Normalized time derivative of the loss factor at 200 Hz using parallel-plate and fringe-field DEA.

The parallel-plate examples match the overall shape of the fringe-field curves, but they are much more muted as they are measuring the bond-lines in positions 1, 3 and 4, in addition to position 2. It is difficult to determine if they have any points in the cure profile that match without the cure proceeding to completion. This data does suggest that the final cure points could correlate. Additionally, there is some cure masked by the nature of the normalized curve. Because the final cure is not realized, the minimum of the proportional loss factor in the parallel-plate values is larger than it would be with absolute, calibrated loss factor; this contributes to the overall flatness of the curve and exacerbates the uncertainty due to the noisy data.

4.3 Summary of Results

The results of the parallel-plate rheometry portion of this experiment found the two resins were very similar in their degree of cure rates as a function of temperature rise. The core

resin does cure more rapidly in the initial portion of its degree of cure curve, but the two plots eventually cross twice. Though the two resins have differences in their formulations, there was little difference in their overall cure rates. A statistically significant difference in temperature at the final cure point was detected, though the practical difference between the two temperatures was not great.

The results from the DEA portion of this experiment show agreement with the rheometry portion in that there was little difference found between the two resins. There was no statistically significant effect detected when the resins were compared. However, through the variation in the data some clear points in the resin cure profile were observed. Many factors seem that they would be statistically significant with a larger sample size, such as differences in the resins when compared using fringe-field DEA (see Figure 16 and Table 10).

The most important development of this project was demonstrating that the parallel-plate and fringe-field dielectric results were comparable in a single bond-line application. When the normalized loss factor time derivative was examined for the 2ply and 3ply samples, the curves matched up well as the values approached zero, indicating complete cure. However, there was substantial lack of sensitivity in the parallel-plate method.

5. Conclusions and Recommendations

5.1 Conclusions

This research was able to characterize the cure rate by parallel-plate rheometry of the two phenol formaldehyde resins and found little difference in the overall cure rate, which was consistent with the DEA results.

The research does show that both fringe-field and parallel-plate dielectric spectroscopy can characterize the macro trends in phenol-formaldehyde resin cure in a laminated wood composite and even detect specific points in the process, such as final cure.

It was shown that the fringe-field and parallel-plate methods appear to show agreement when the normalized loss factor is examined. The curves of the normalized loss factor approach zero at the same point, indicating complete cure is observed at the same time regardless of the method used. The methods were found not to correlate when thicker samples were compared.

5.2 Recommendations

Because of the expense of the dielectric sensors, the number of replications was sacrificed in order to test more treatments. In hindsight, fewer treatments should have been used. The multiple resin comparison should have been eliminated; that alone would

have doubled the samples sizes without sacrificing any dielectric analysis objectives. Carrying the cure to completion of dielectric activity would also have allowed for a better degree of cure comparison. This was particularly true for the 5ply samples that cured to mechanical integrity, but lacked comparison points in the loss factor profile. Finally, I would recommend that temperature profiles of the bond-line of interest be included in future research, this would help in determining why certain noise occurs in the fringe-field analysis in addition to explaining some differences in cure profiles that may exist between different moisture content groups. Eliminating some of the frequency scans of the DEA would help increase the rate of data collection in the fringe-field method and therefore help compare the two methods. Concentrating the scans to frequencies identified in this research would match the data more closely to the parallel-plate data collection rate.

6. References

1. Zheng, J. (2002): Studies of PF Resole/Isocyanate Hybrid Adhesives, PhD dissertation, Virginia Polytechnic Institute and State University, Blacksburg, Virginia. 198pp.

2. Gillham, J. (1997). The TBA torsion pendulum: a technique for characterizing the cure and properties of thermosetting systems. *Polymer International*, 44(3), 262-276.

3. Ross-Murphy, S. (1994). Rheological characterization of polymer gels and networks. *Polymer Gels and Networks*, 2(3-4). 229-237.

4. Halley, P. & MacKay, M. (1996). Chemorheology of thermosets - an overview. *Polymer Engineering and Science*, 36(5). 593-609.

5. Cook, R. W. & Tod, D. A. (1993). A study of the cure of adhesives using dynamic mechanical analysis. *International Journal of Adhesion and Adhesives,* 13(3). 157-162.

6. Peng W. & Riedl B. (1995). Thermosetting Resins. *Journal of Chemical Education*, 72(7). 587-592.

7. Chambon, F., Petrovic, Z., McKnight., & Henning Winter, H. (1986). Rheology of model polyurethanes at the gel point. *Macromolecules*, 19: 2149-2157

8. Chambon, F. & Winter, H. H. (1987). Linear viscoelasticity at the gel point of a crosslinking PDMS with imbalanced stoichiometry. *Journal of Rheology*, 31(8). 683-697.

9. Kranbuehl, D. E. (1997). Dielectric Monitoring of Polymerization and Cure. In J. P. Runt and J.J. Fitzgerald (Eds.), *Dielectric Spectroscopy of Polymeric Materials*. (pp. 303-328). Washington DC: American Chemical Society.

10. Mijovic, J., Kenny, J., Maffezzoli, A., Trivisana, A., Bellucci, F., & Nicolais, L. (1993). The Principles of Dielectric Measurements for *in situ* Monitoring of Composite Processing. *Composites Science and Technology*, 49(3). 277-290.

11. McGettrick, B. P., Jagdish, K., Vij. & McArdle C. (1994). Dielectric spectroscopy of anaerobic adhesive cure. *International Journal of Adhesion and Adhesives*, 14(4). 211-236.

12. Hedvig, P. (1977). Chapter 1 in *Dielectric Spectroscopy of Polymers*. New York: John Wiley & Sons

13. Kranbuehl, D., Delos, S., Hoff, M., Haverty, P., Freeman, W., Hoffman, R., & Godfrey, J. (1989). Use of the frequency dependence of the impendence to monitor viscosity during cure. *Polymer Engineering and Science,* 29(5). 285-289.

14. Kamke, F. A., Sernek, M., Scott, B., & Frazier, C. E.. (2004). *Modeling cure of a phenol-formaldehyde adhesive.* In: Proc. Eighth European Panel Products Symposium, Llandudno, Wales, Oct. 13 – 14, 2004. BioComposites Centre, UWB, Bangor, UK, p.3.23 – 3.34.

15. Ungarish, M., Joseph, R., Vittoser, J., Zur, E., & Kenig, S. (1991). Dielectric cure monitoring and optimization of film adhesives. *International Journal of Adhesion and Adhesives*, 11(2): 87-91.

16. Li, Y., Cordovez, M., &.Karbhari, M. V. (2002). Dielectric and mechanical characterization of processing and moisture uptake effects in E-glass/epoxy composites. *Composites: Part B Engineering,* 34(4). 383-390.

17. Wang, J, Laborie, M and Wolcott, M 2004. Washington State University, Pullman, Washington. Personal communication of the characteristics of the face and core resins.

18. Sall, J. (2001). *JUMPIN* [Computer Program] Cary, NC: SAS Institute.

7. Appendix

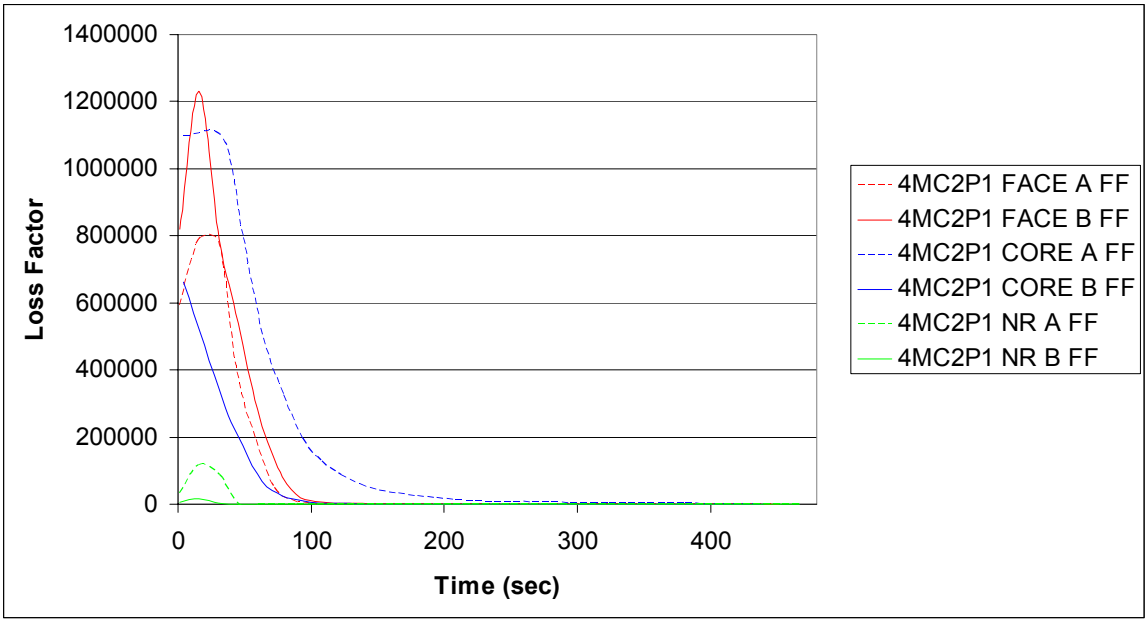

Figure A-1: Fringe-field Loss Factor vs. Time of individual 4MC2P Samples at 200 Hz.

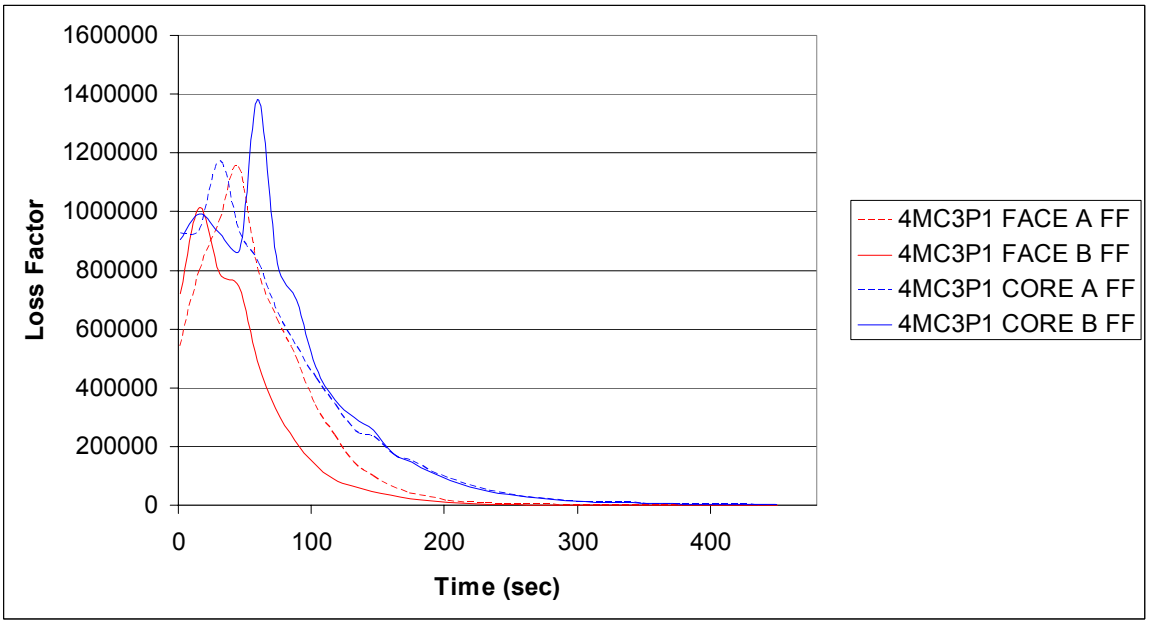

Figure A-2: Fringe-field Loss Factor vs. Time of individual 4MC3P Samples at 200 Hz.

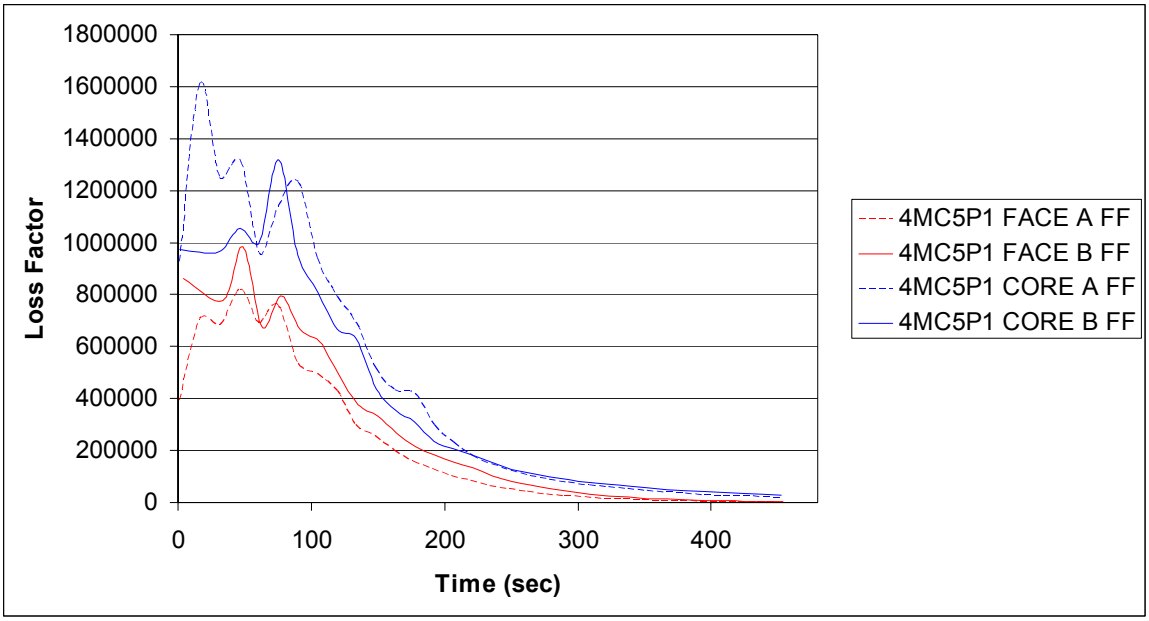

Figure A-3: Fringe-field Loss Factor vs. Time of individual 4MC5P1 Samples at 200 Hz.

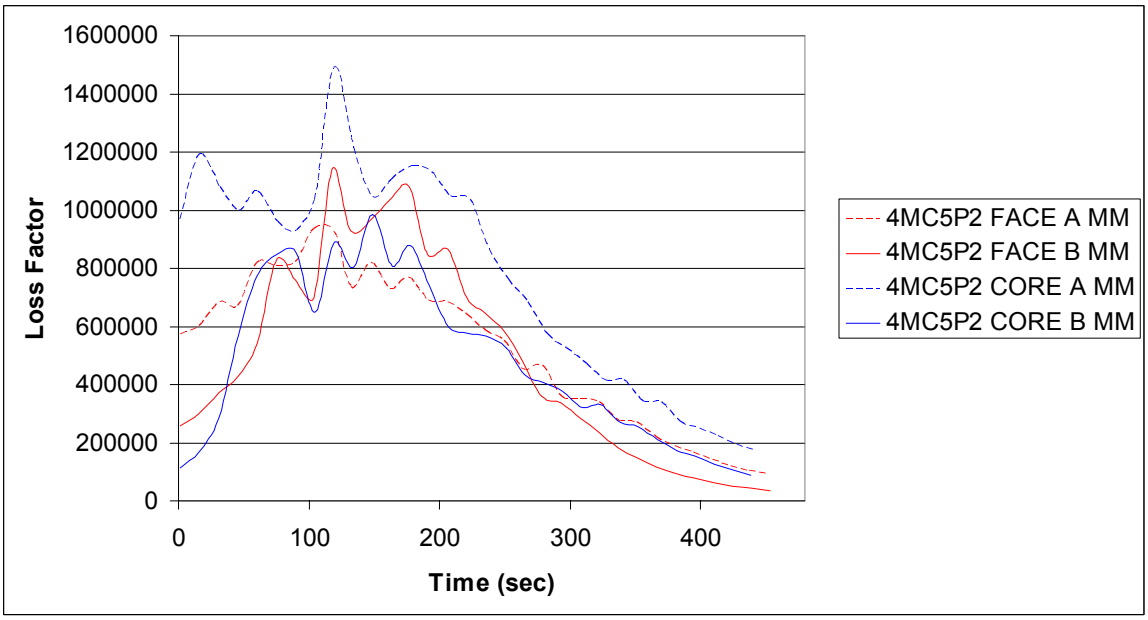

Figure A-4: Fringe-field Loss Factor vs. Time of individual 4MC5P2 Samples at 200 Hz.

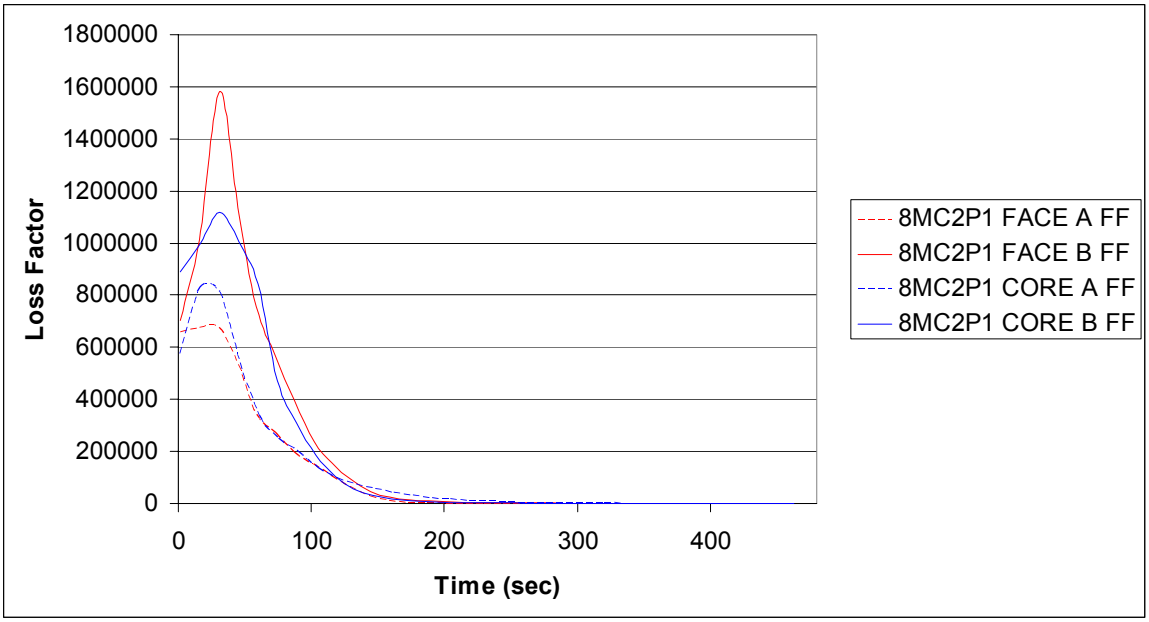

Figure A-5: Fringe-field Loss Factor vs. Time of individual 8MC2P Samples at 200 Hz.

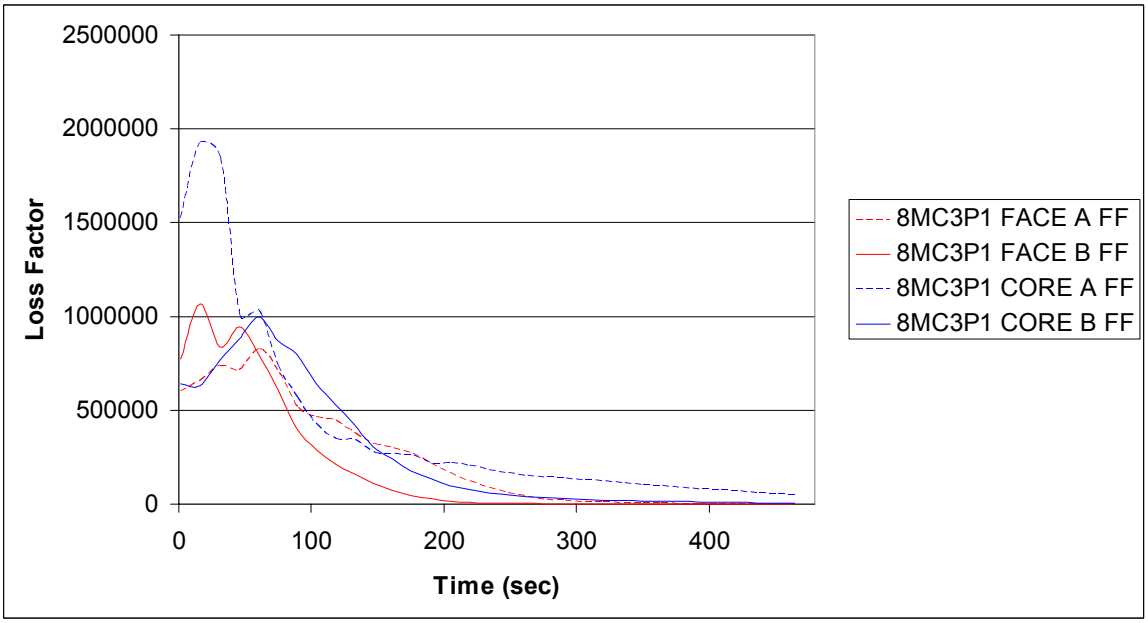

Figure A-6: Fringe-field Loss Factor vs. Time of individual 8MC3P Samples at 200 Hz.

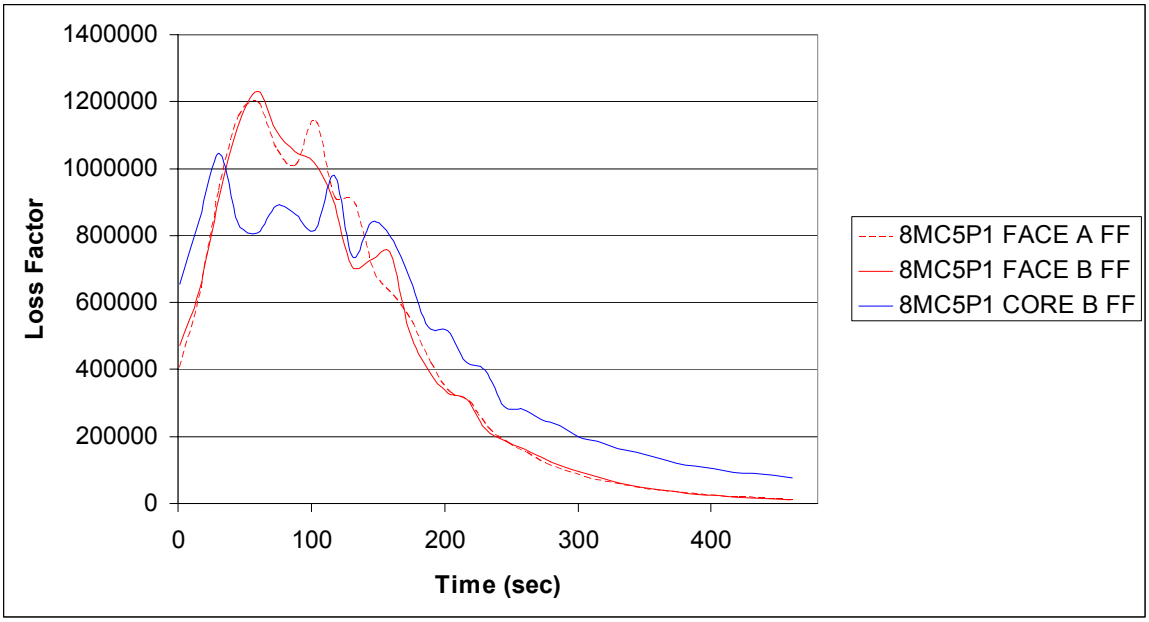

Figure A-7: Fringe-field Loss Factor vs. Time of individual 8MC5P1 Samples at 200 Hz.

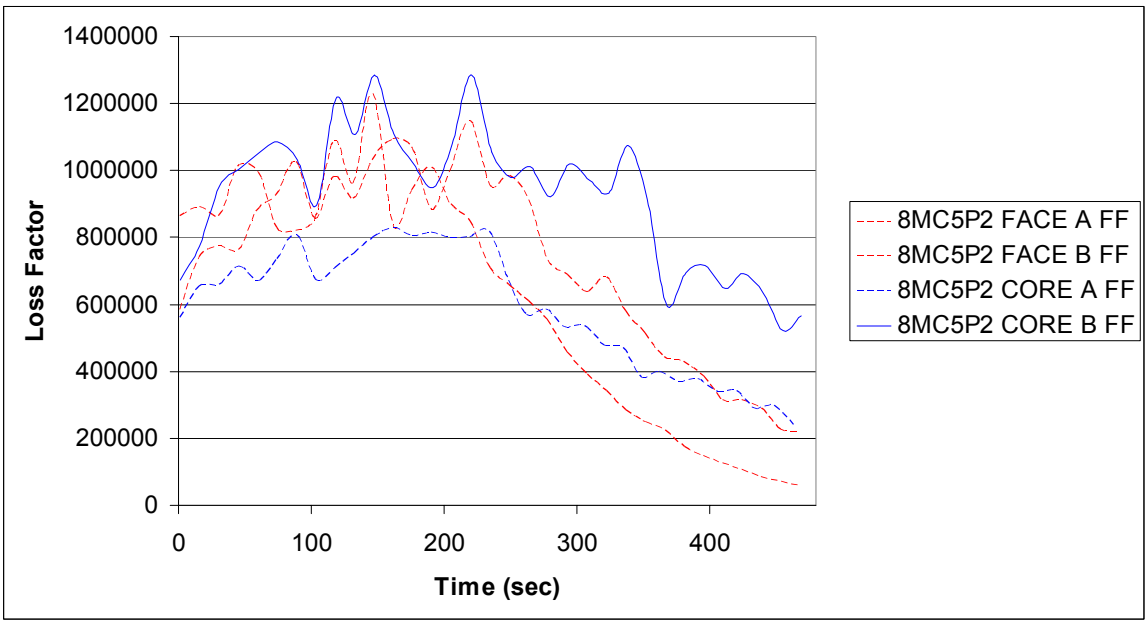

Figure A-8: Fringe-field Loss Factor vs. Time of individual 8MC5P2 Samples at 200 Hz.

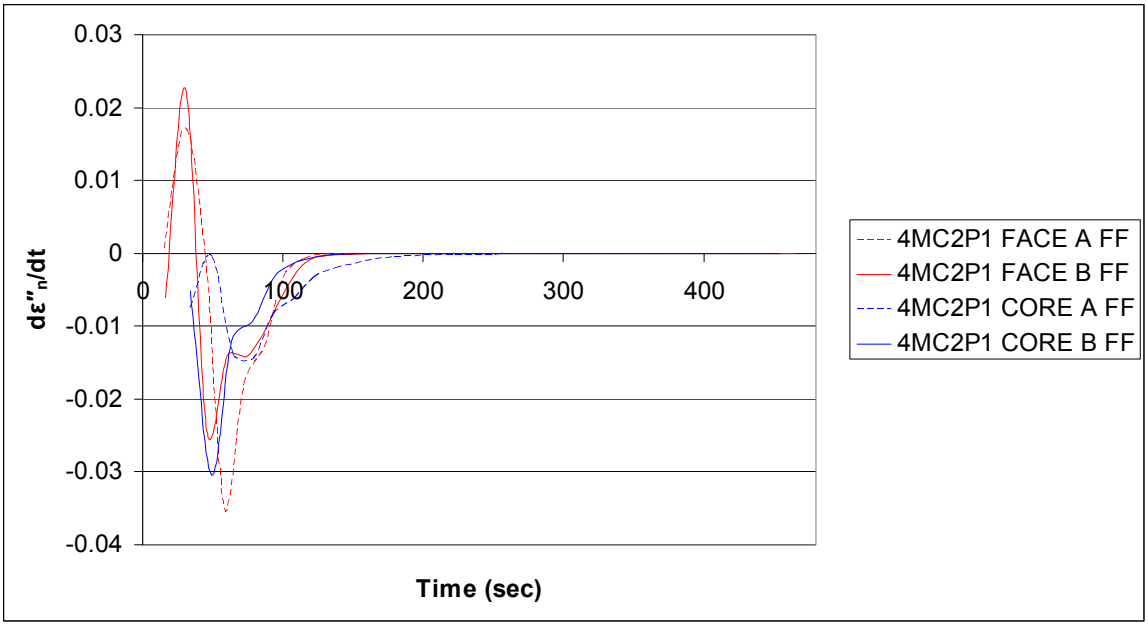

Figure A-9: Normalized time derivative of the loss factor of individual 4MC2P samples at 200 Hz by fringe-field DEA.

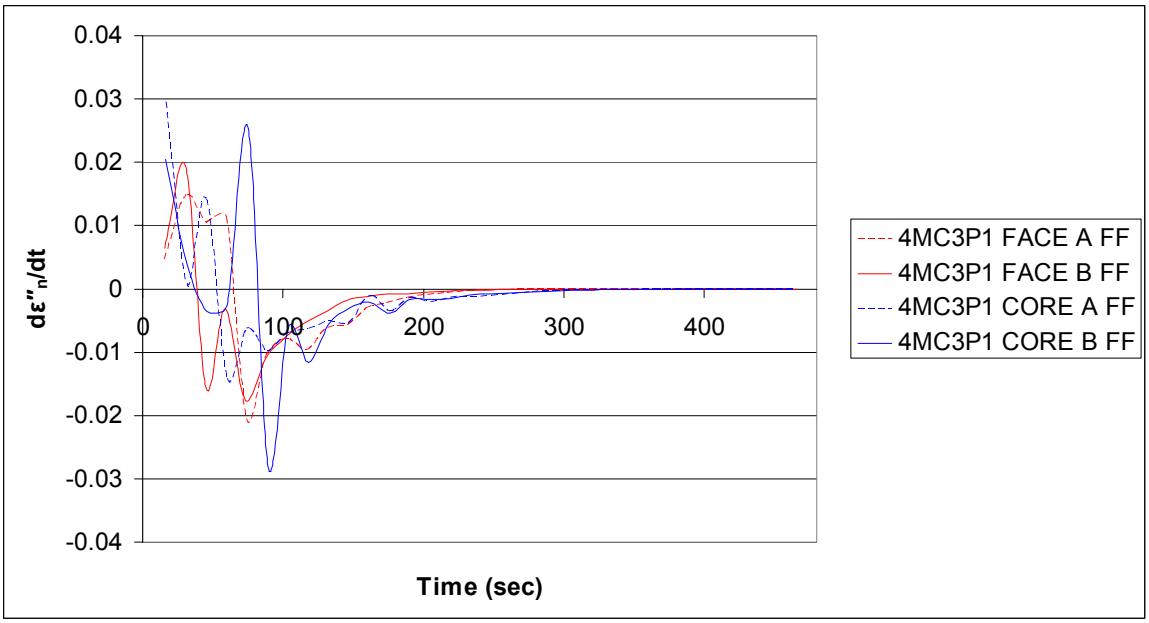

Figure A-10: Normalized time derivative of the loss factor of individual 8MC3P samples at 200 Hz by fringe-field DEA.

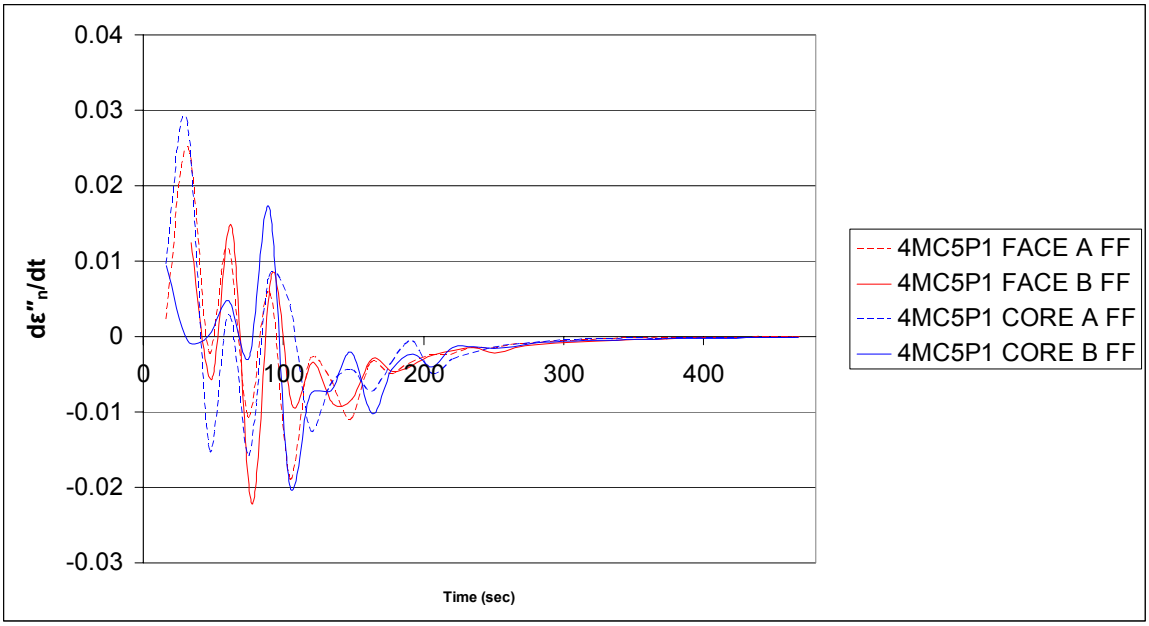

Figure A-11: Normalized time derivative of the loss factor of individual 8MC5P1 samples at 200 Hz by fringe-field DEA.

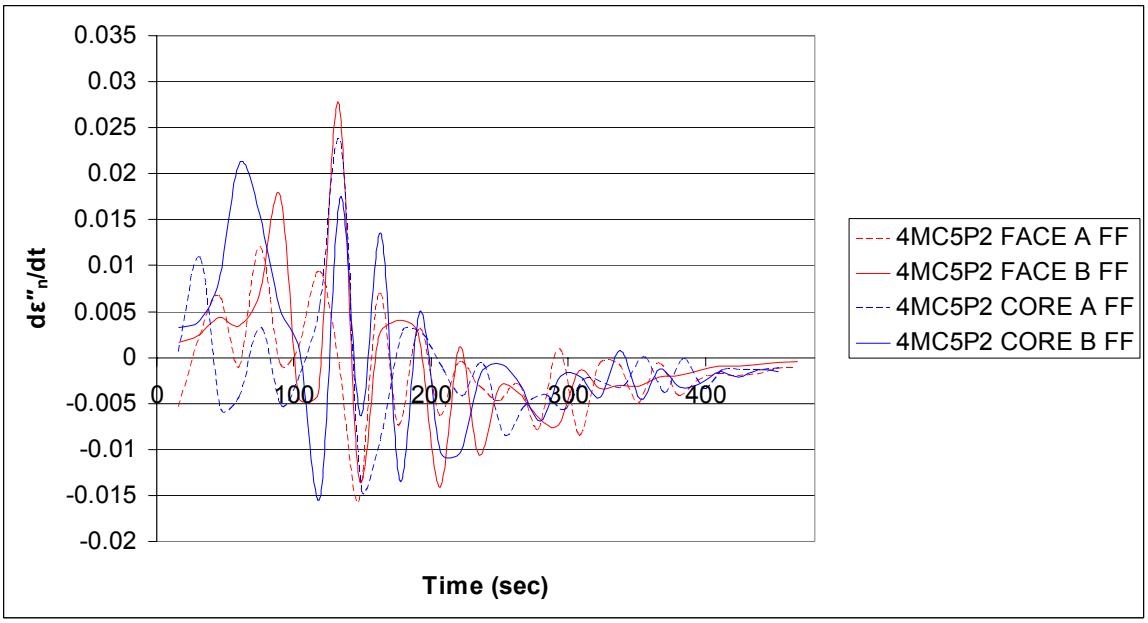

Figure A-12: Normalized time derivative of the loss factor of individual 8MC5P2 samples at 200 Hz by fringe-field DEA.

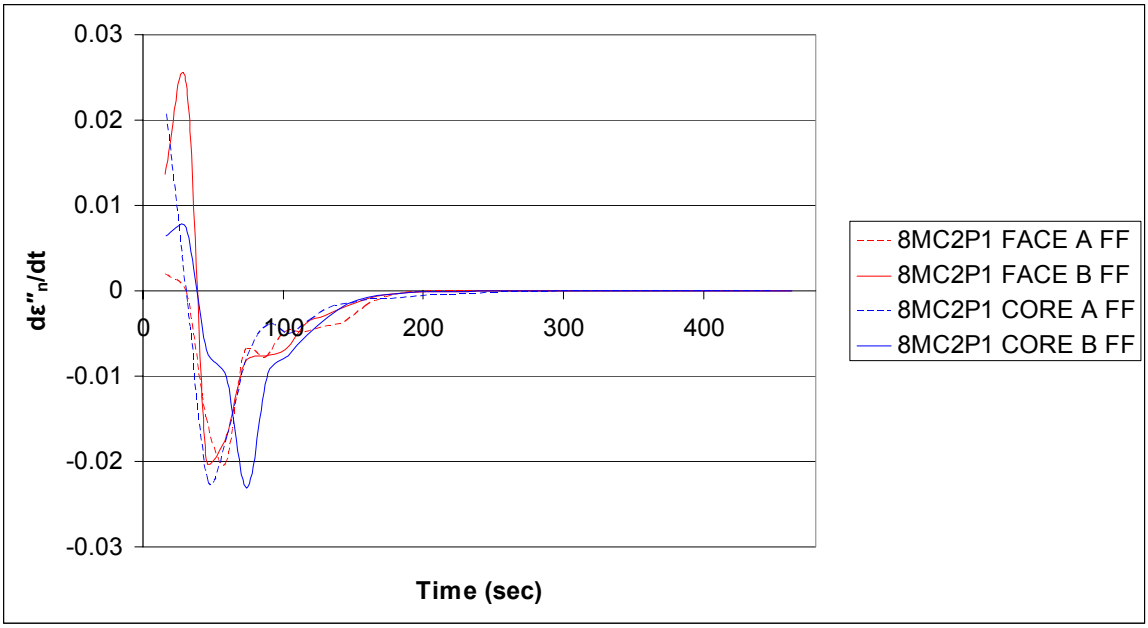

Figure A-13: Normalized time derivative of the loss factor of individual 8MC2P samples at 200 Hz by fringe-field DEA.

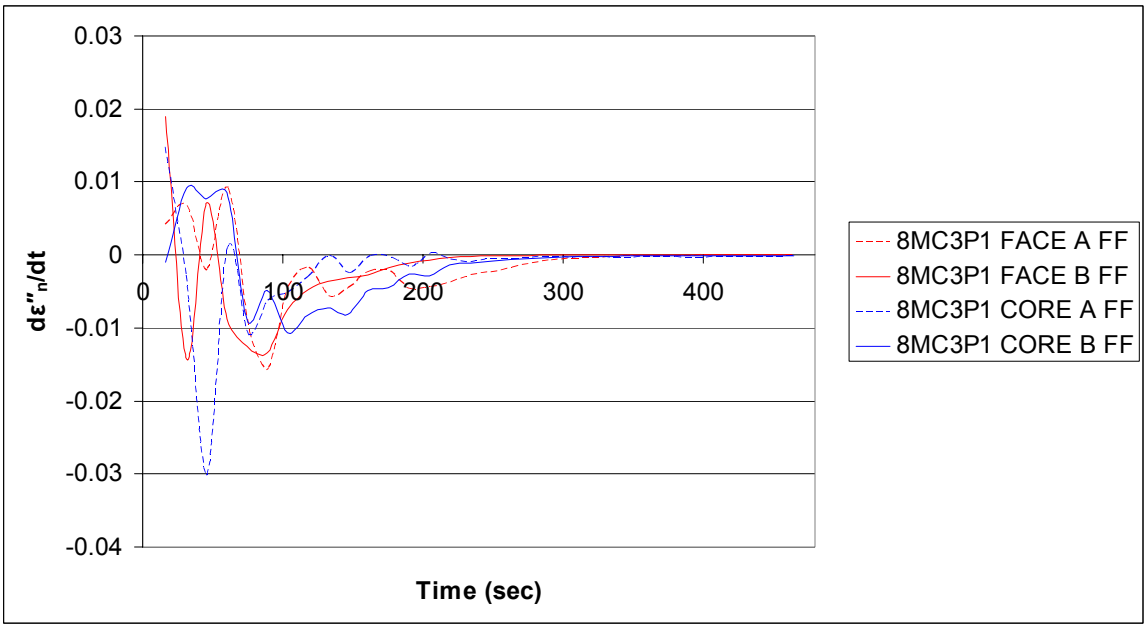

Figure A-14: Normalized time derivative of the loss factor of individual 8MC3P samples at 200 Hz by fringe-field DEA.

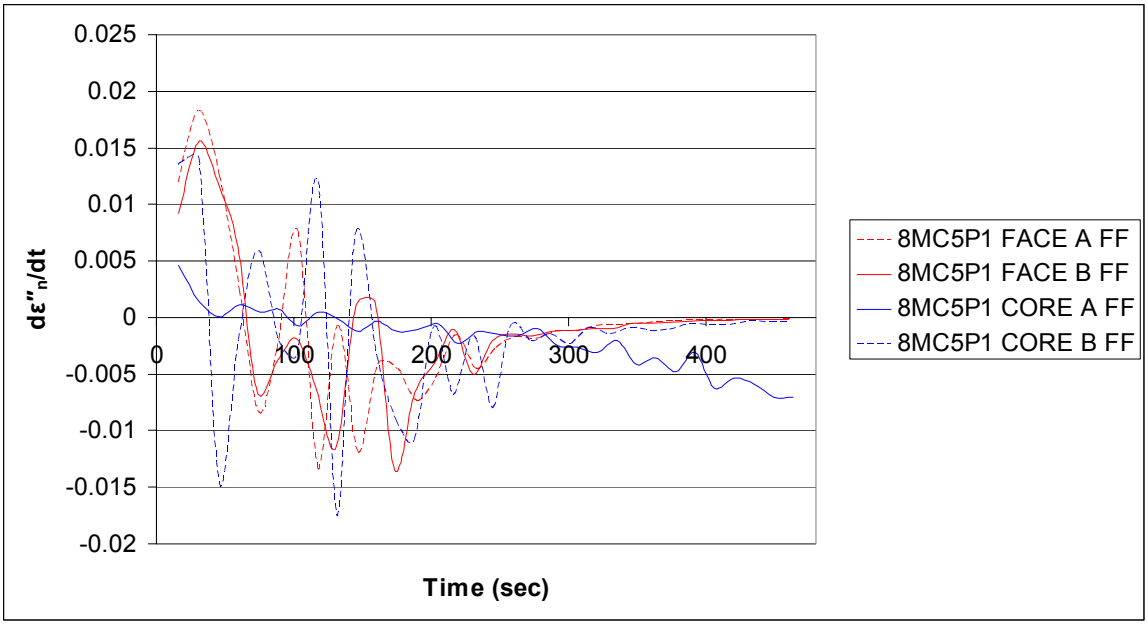

Figure A-15: Normalized time derivative of the loss factor of individual 8MC5P1 samples at 200 Hz by fringe-filed DEA.

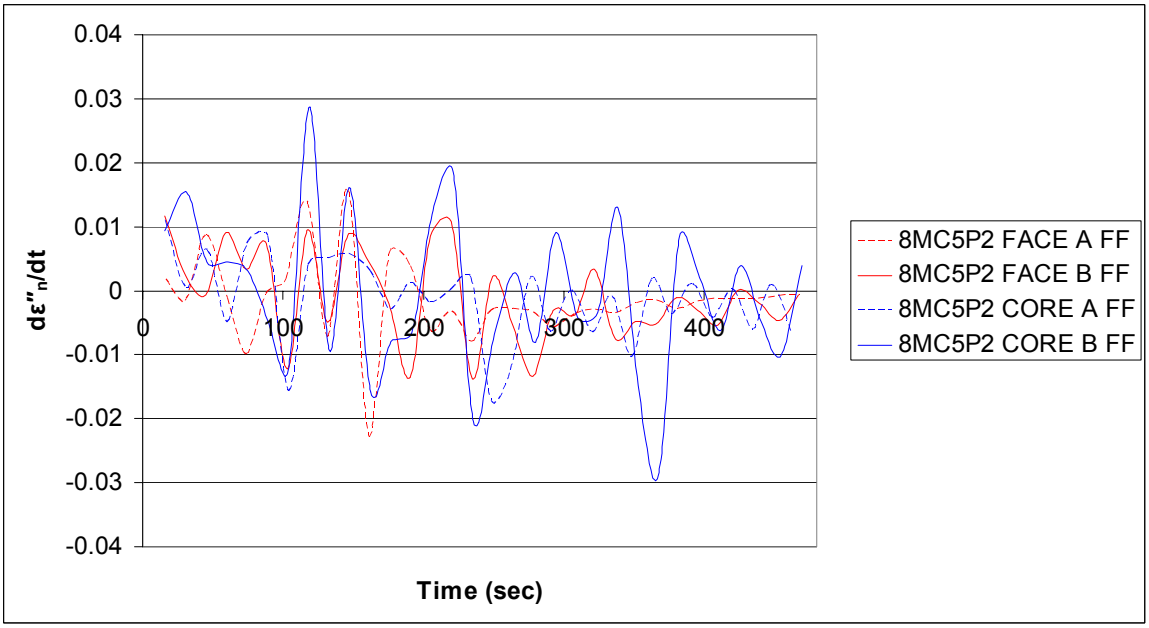

Figure A-16: Normalized time derivative of the loss factor of individual 8MC5P2 samples at 200 Hz by fringe-field DEA.

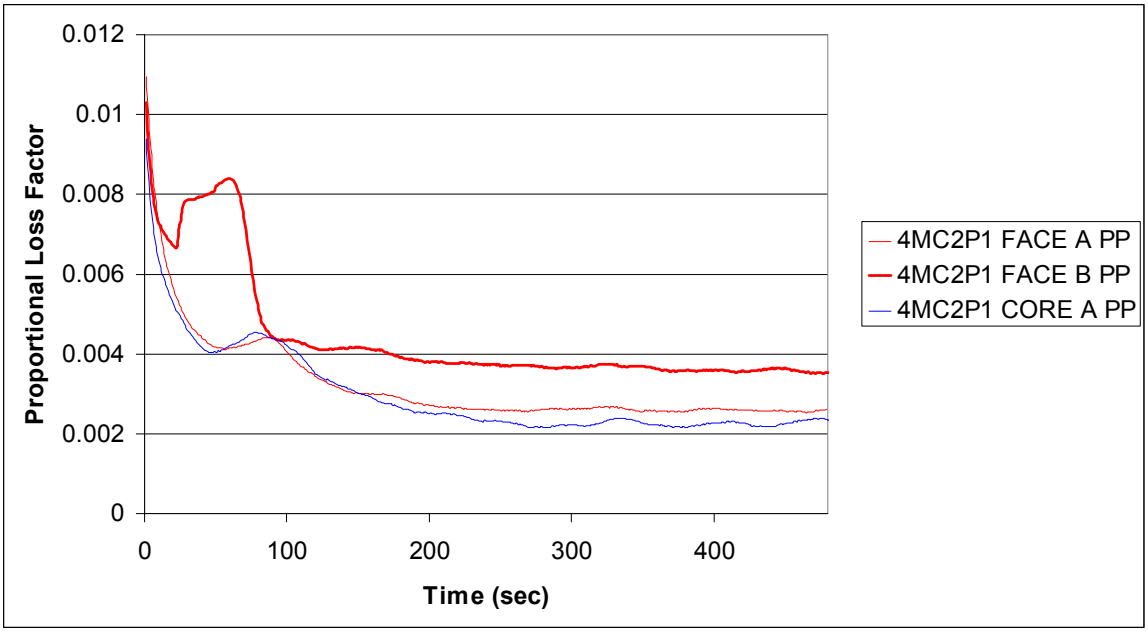

Figure A-17: Proportional loss factor vs. time of individual 4MC2P samples at 200 Hz by parallel-plate DEA.

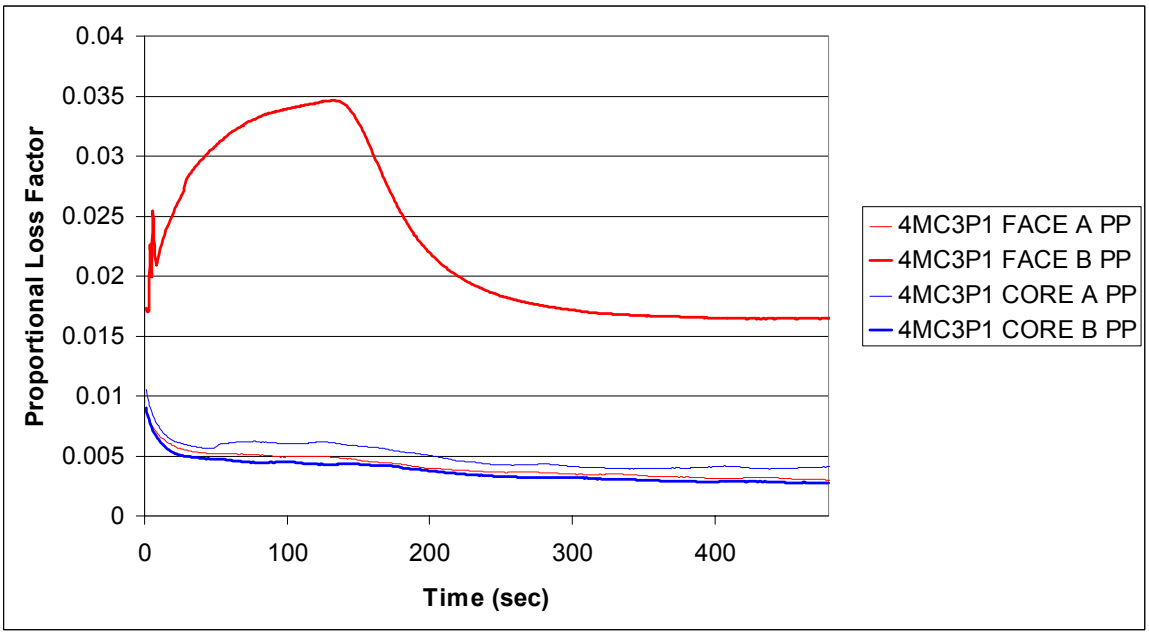

Figure A-18: Proportional loss factor vs. time of individual 4MC3P samples at 200 Hz by parallel-plate DEA.

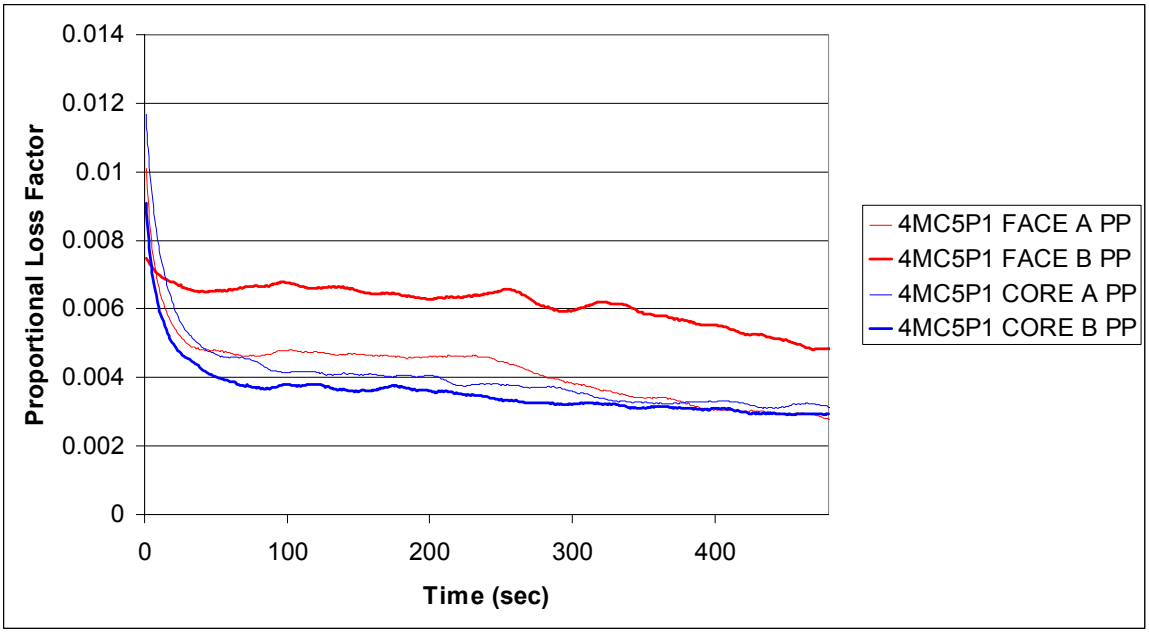

Figure A-19: Proportional loss factor vs. time of individual 4MC5P1 samples at 200 Hz by parallel-plate DEA.

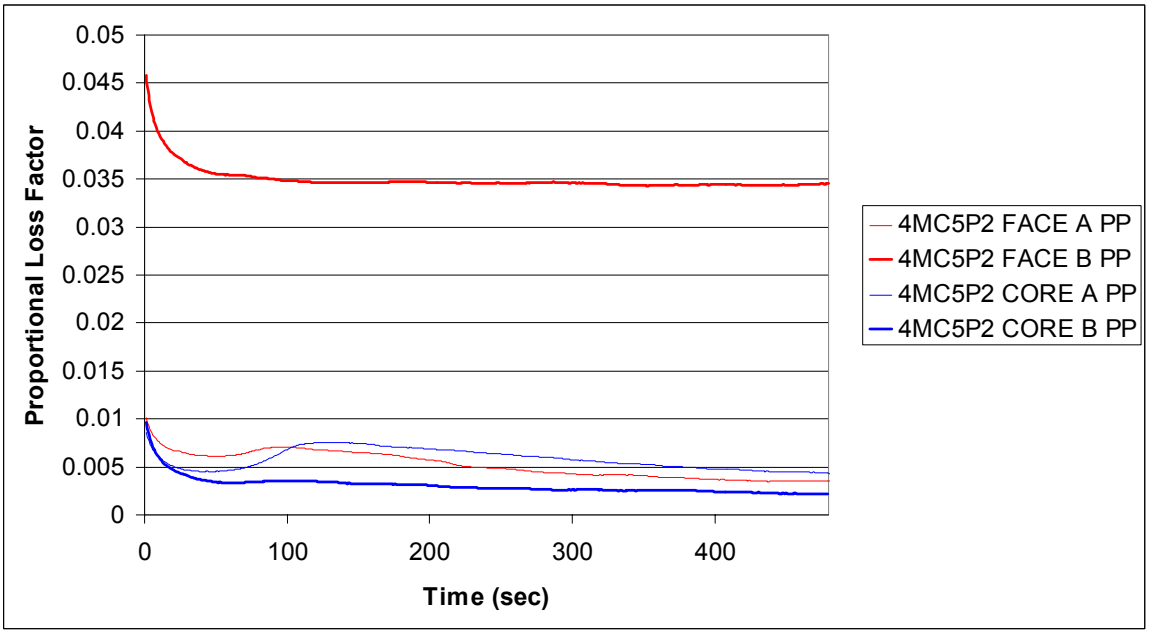

Figure A-20: Proportional loss factor vs. time of individual 4MC5P2 samples at 200 Hz by parallel-plate DEA.

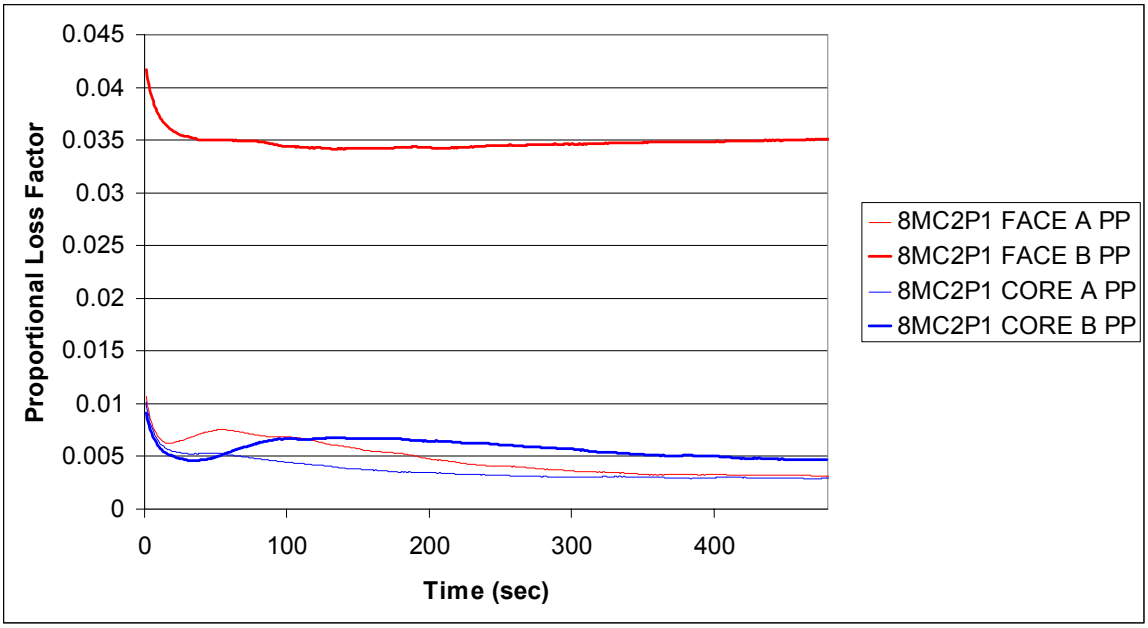

Figure A-21: Proportional loss factor vs. time of individual 8MC2P samples at 200 Hz by parallel-plate DEA.

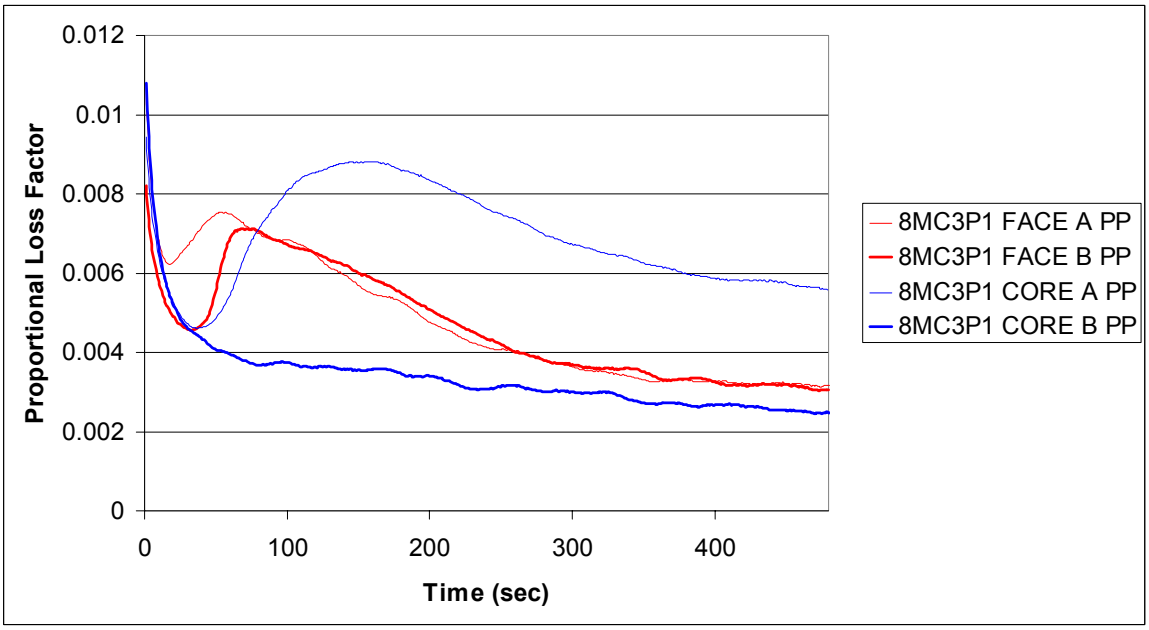

Figure A-22: Proportional loss factor vs. time of individual 8MC3P samples at 200 Hz by parallel-plate DEA.

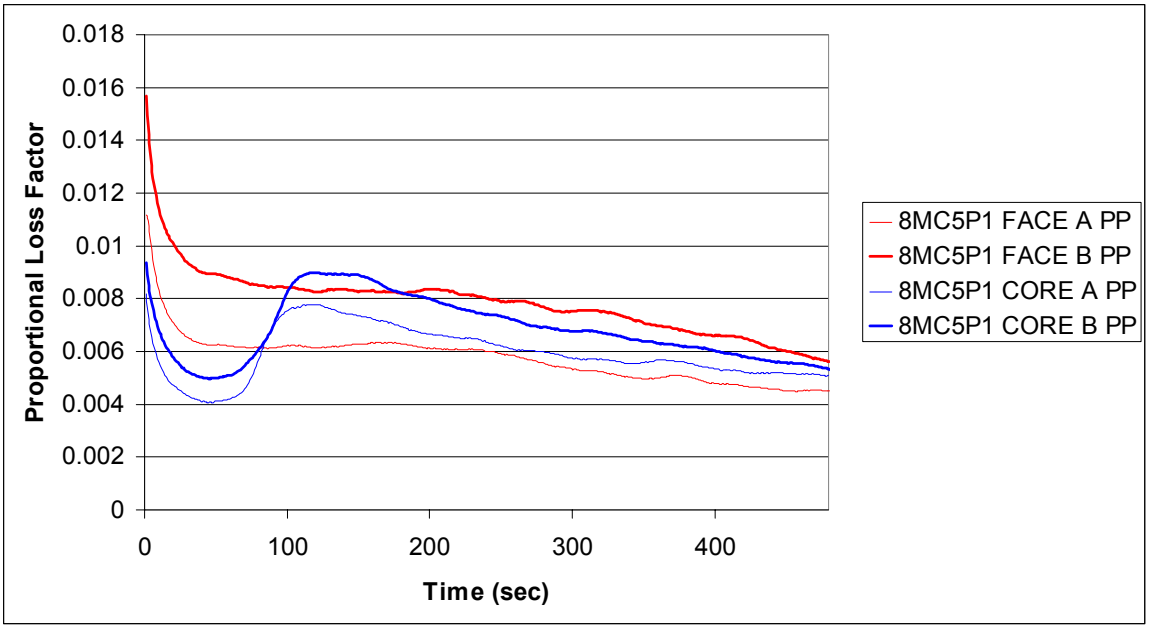

Figure A-23: Proportional loss factor vs. time of individual 8MC5P1 samples at 200 Hz by parallel-plate DEA.

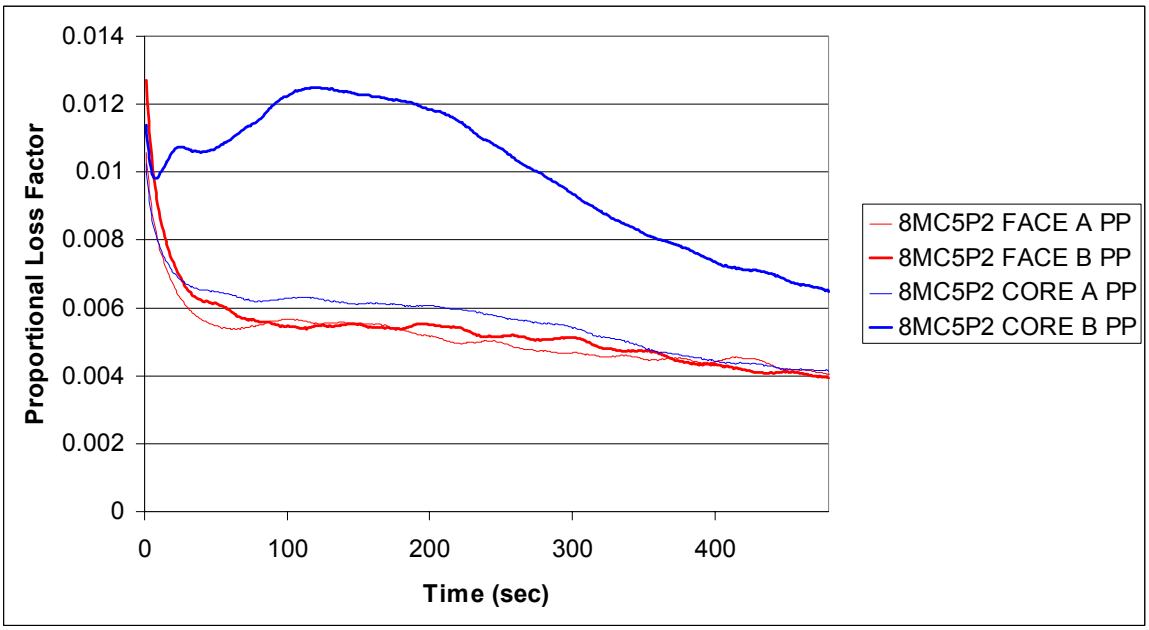

Figure A-24: Proportional loss factor vs. time of individual 8MC5P2 samples at 200 Hz by parallel-plate DEA.

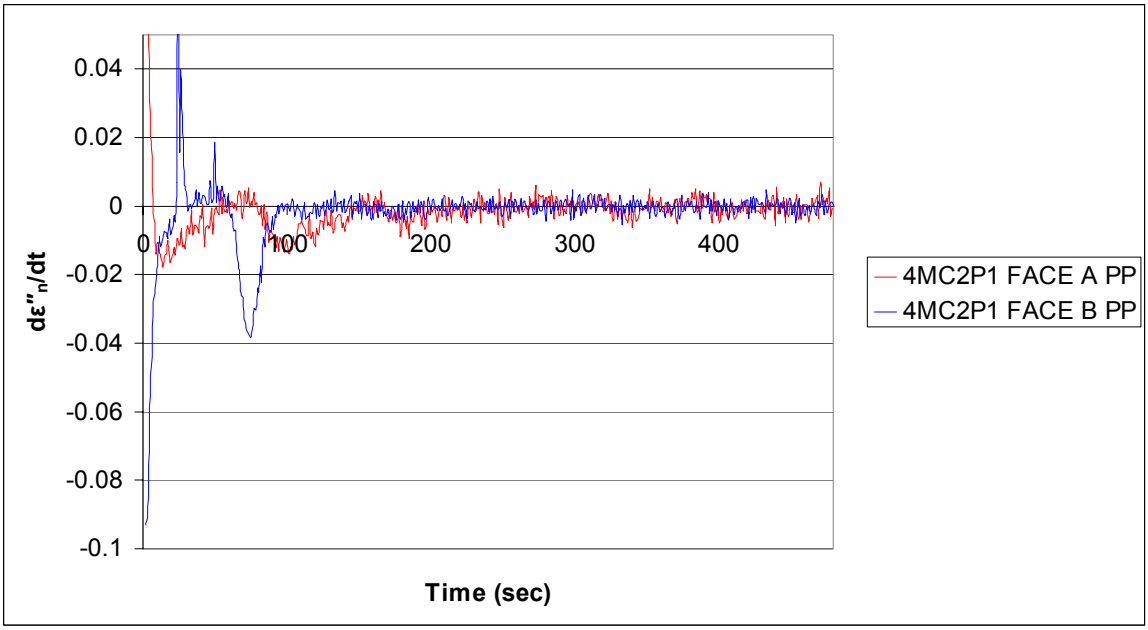

Figure A-25: Normalized time derivative of the loss factor of individual 4MC2P samples at 200 Hz by parallel-plate DEA.

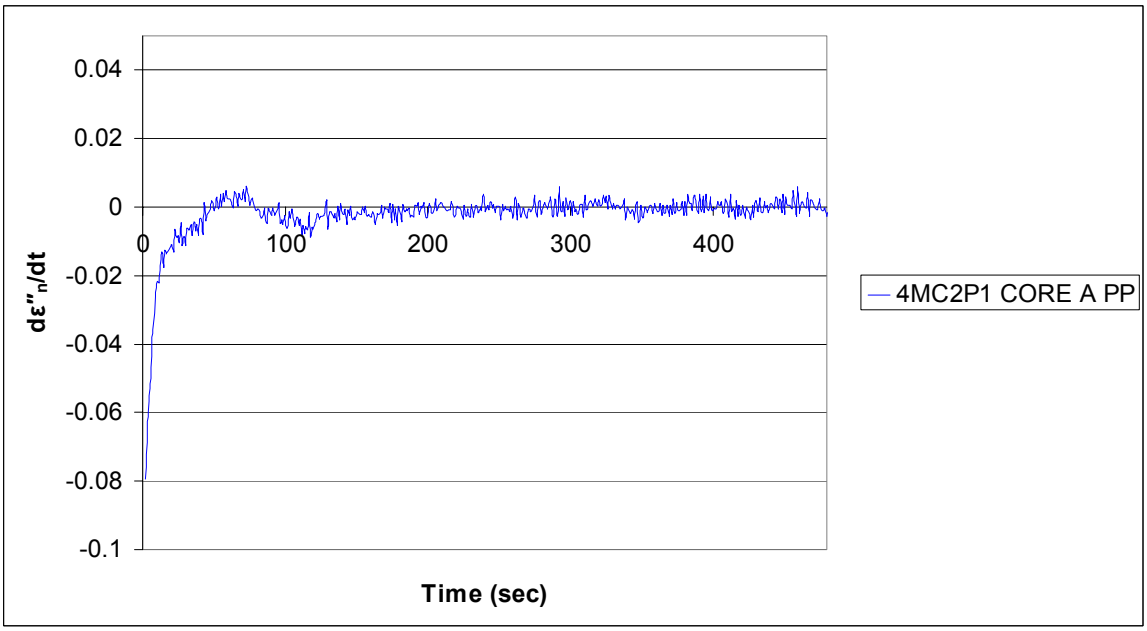

Figure A-26: Normalized time derivative of the loss factor of individual 4MC2P samples at 200 Hz by parallel-plate DEA.

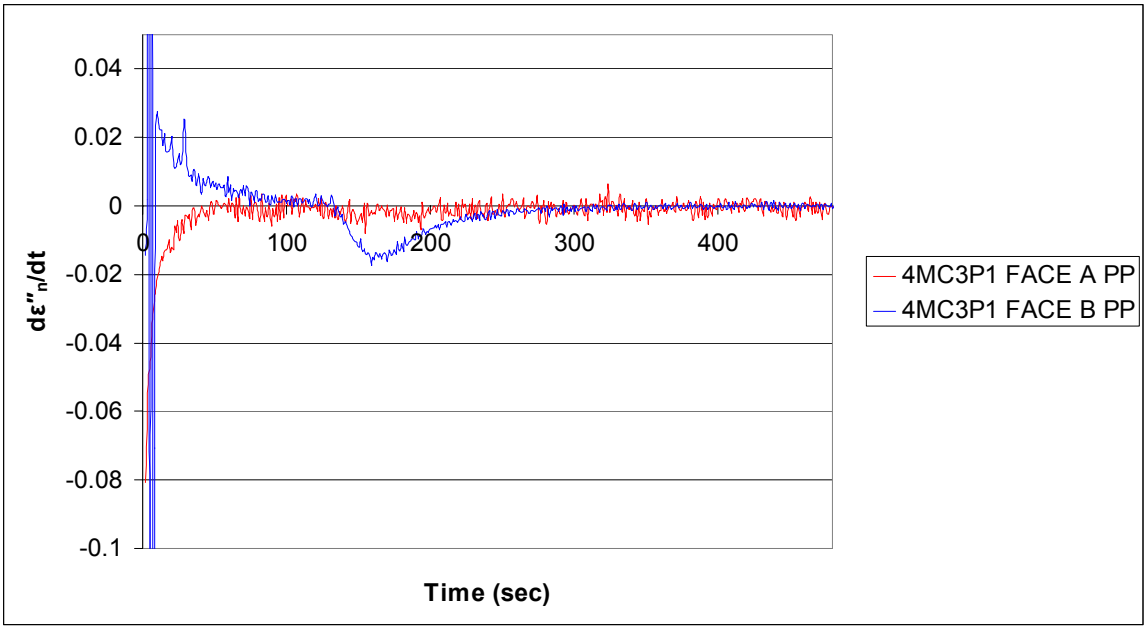

Figure A-27: Normalized time derivative of the loss factor of individual 4MC3P samples at 200 Hz by parallel-plate DEA.

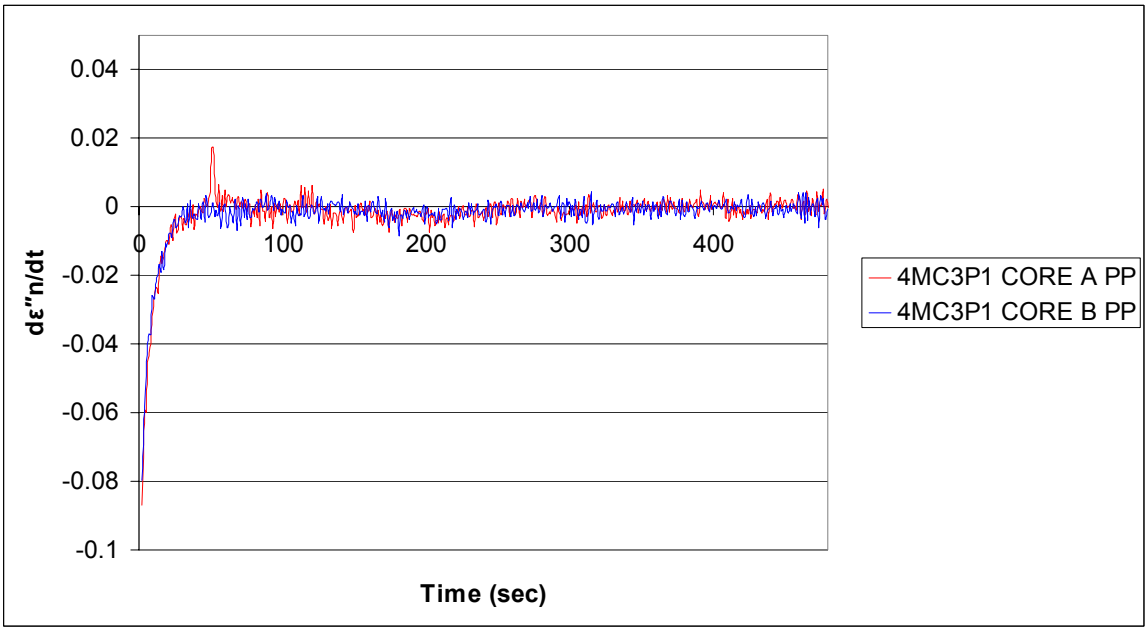

Figure A-28: Normalized time derivative of the loss factor of individual 4MC3P samples at 200 Hz by parallel-plate DEA.

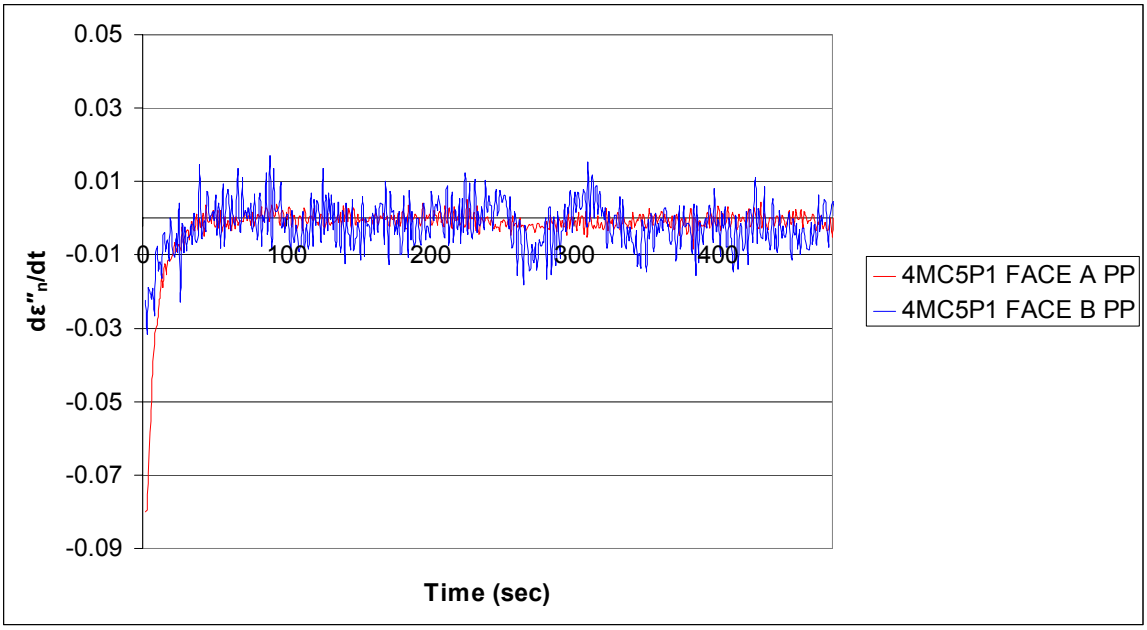

Figure A-29: Normalized time derivative of the loss factor of individual 4MC5P1 samples at 200 Hz by parallel-plate DEA.

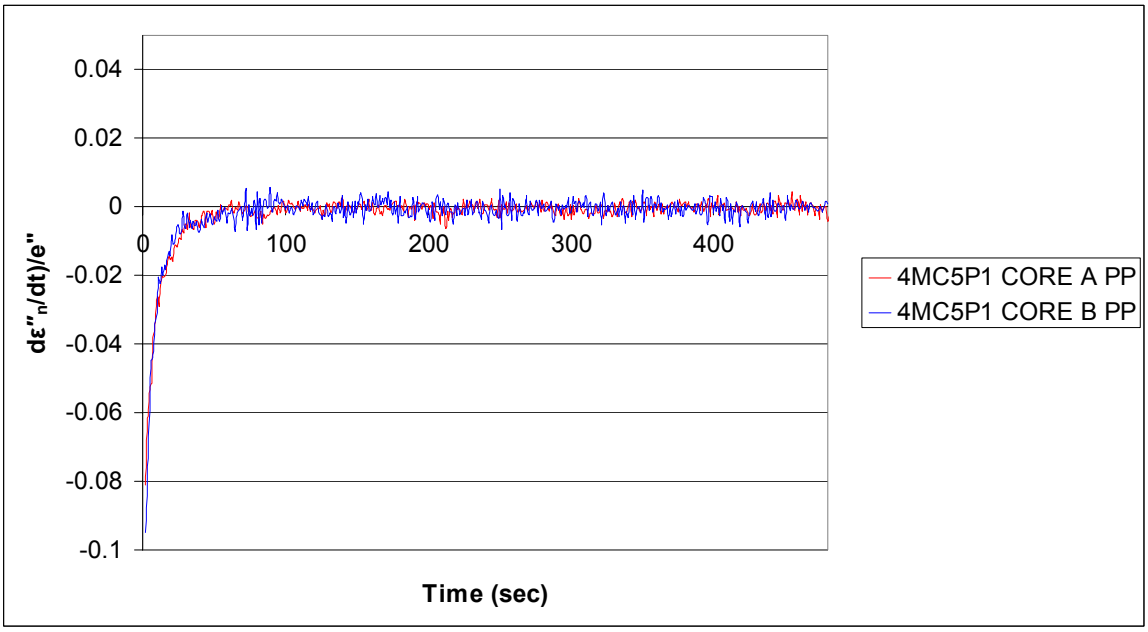

Figure A-30: Normalized time derivative of the loss facotr of individual 4MC5P1 samples at 200 Hz by parallel-plate DEA.

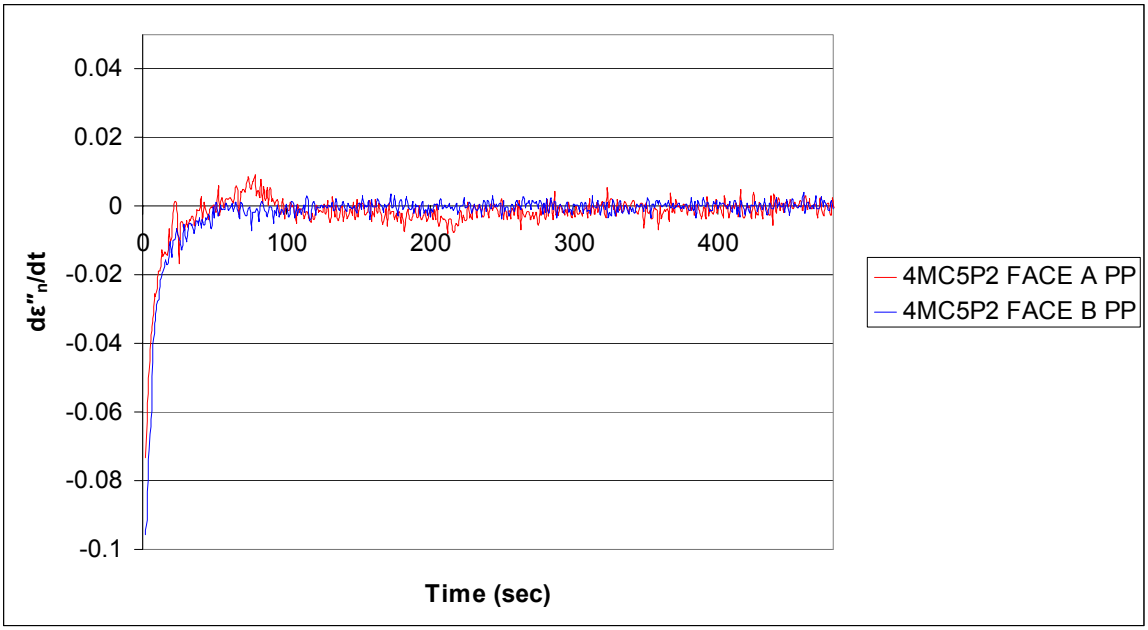

Figure A-31: Normalized time derivative of the loss factor of individual 4MC5P2 samples at 200 Hz by parallel-plate DEA.

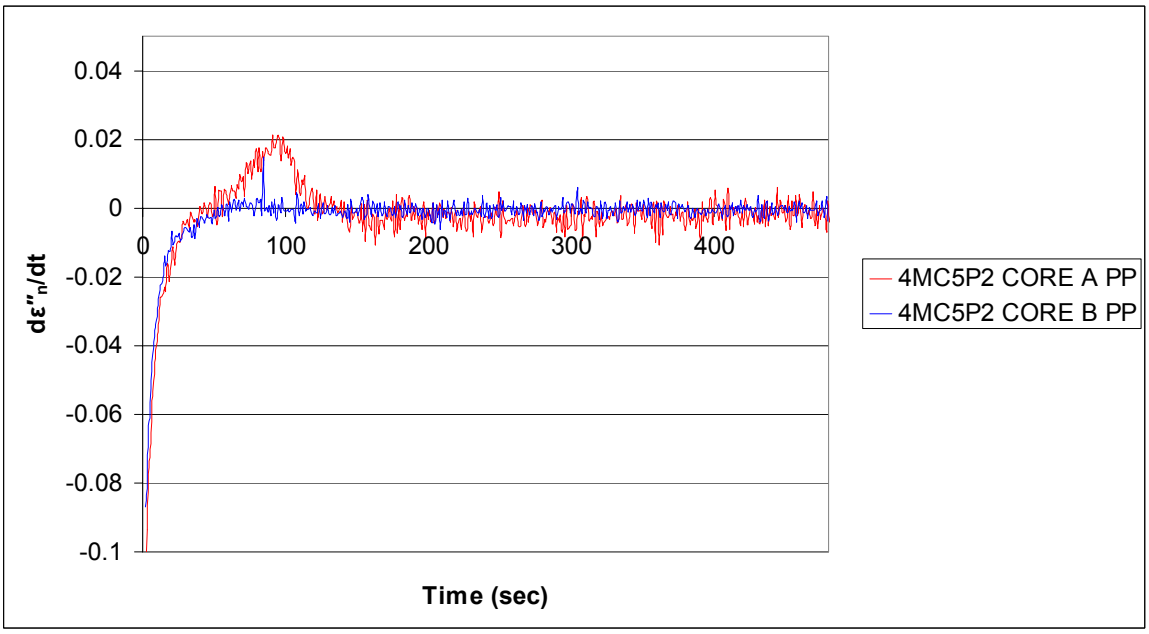

Figure A-32: Normalized time derivative of the loss factor of individual 4MC5P2 samples at 200 Hz by parallel-plate DEA.

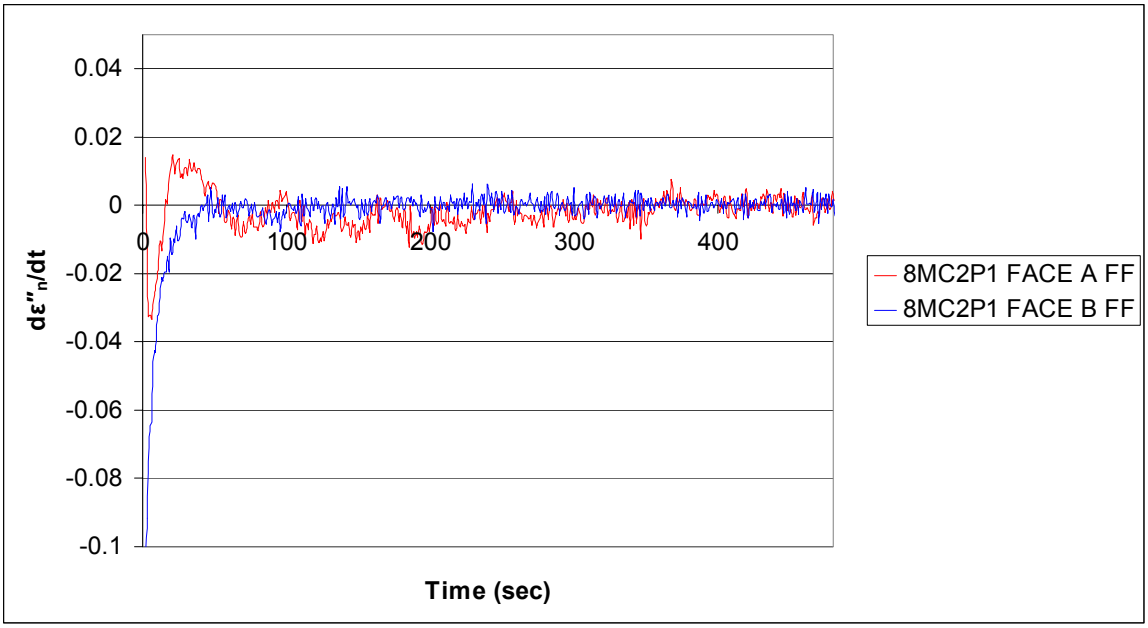

Figure A-33: Normalized time derivative of the loss factor of individual 8MC2P samples at 200 Hz by fringe-field DEA.

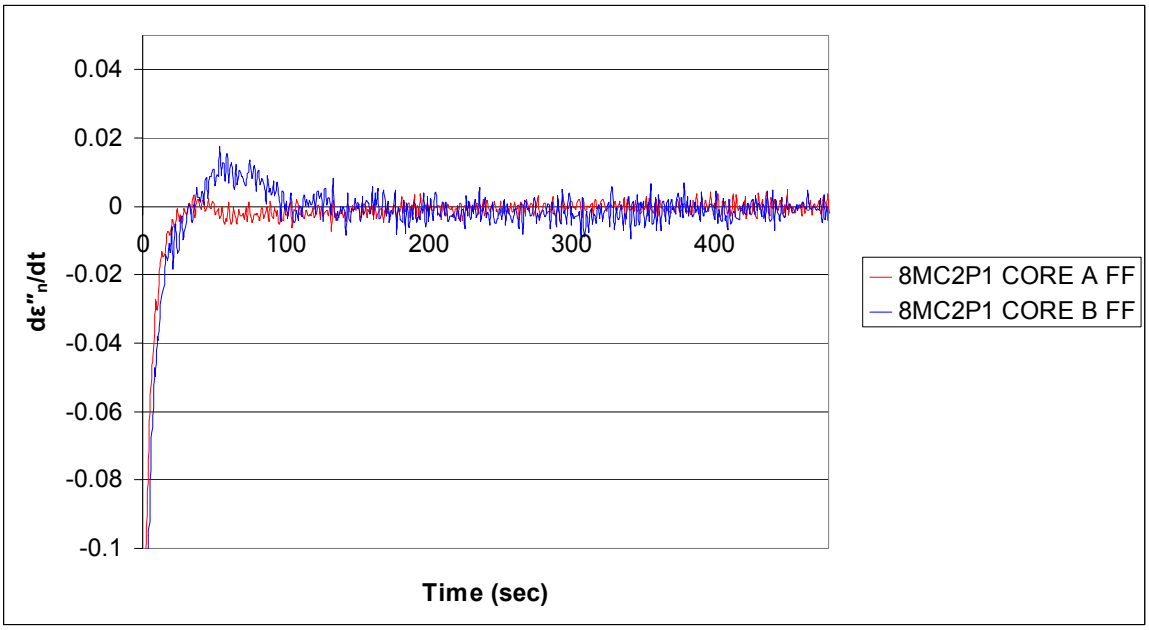

Figure A-34: Normalized time derivative of the loss factor of individual 8MC2P samples at 200 Hz by fringe-field DEA.

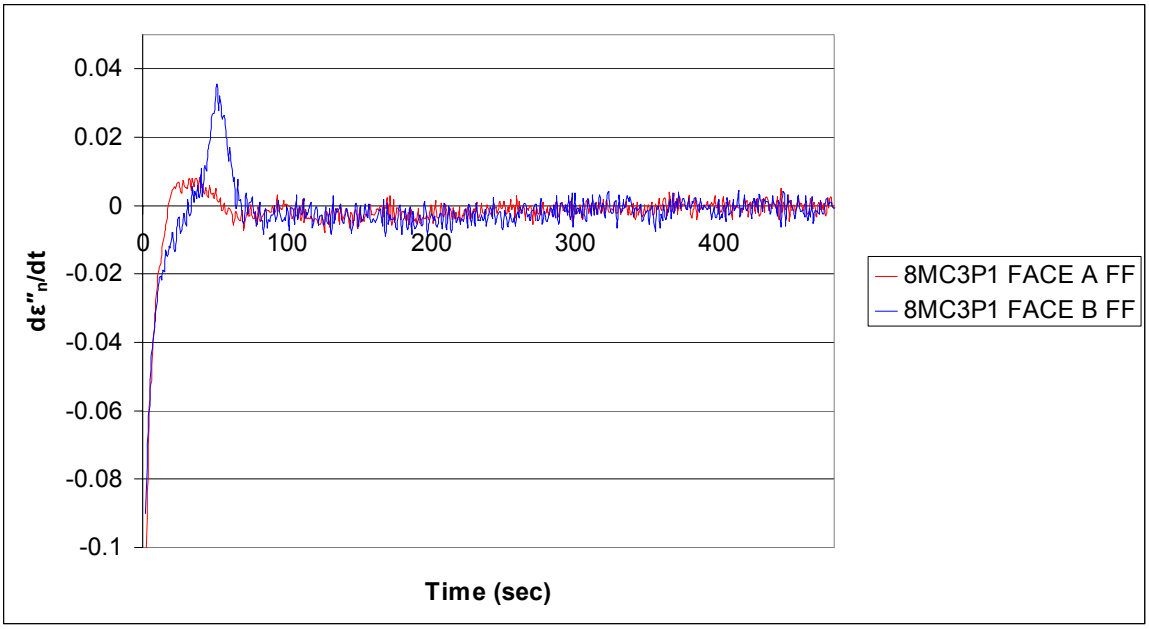

Figure A-35: Normalized time derivative of the loss factor of individual 8MC3P samples at 200 Hz by fringe-field DEA.

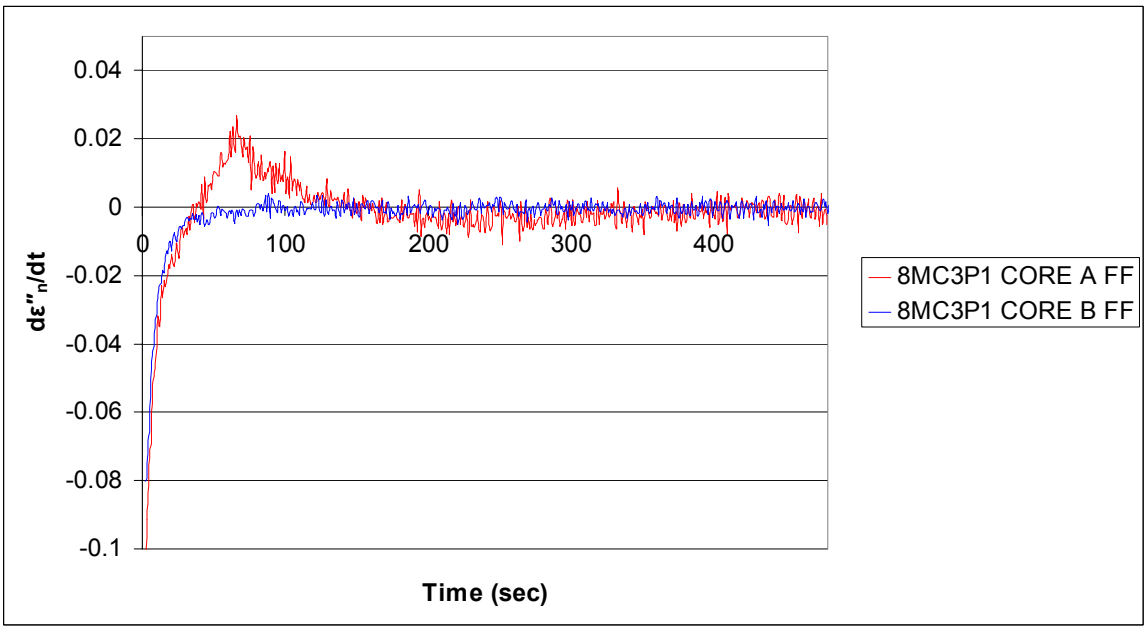

Figure A-36: Normalized time derivative of the loss factor of individual 8MC3P samples at 200 Hz by fringe-field DEA.

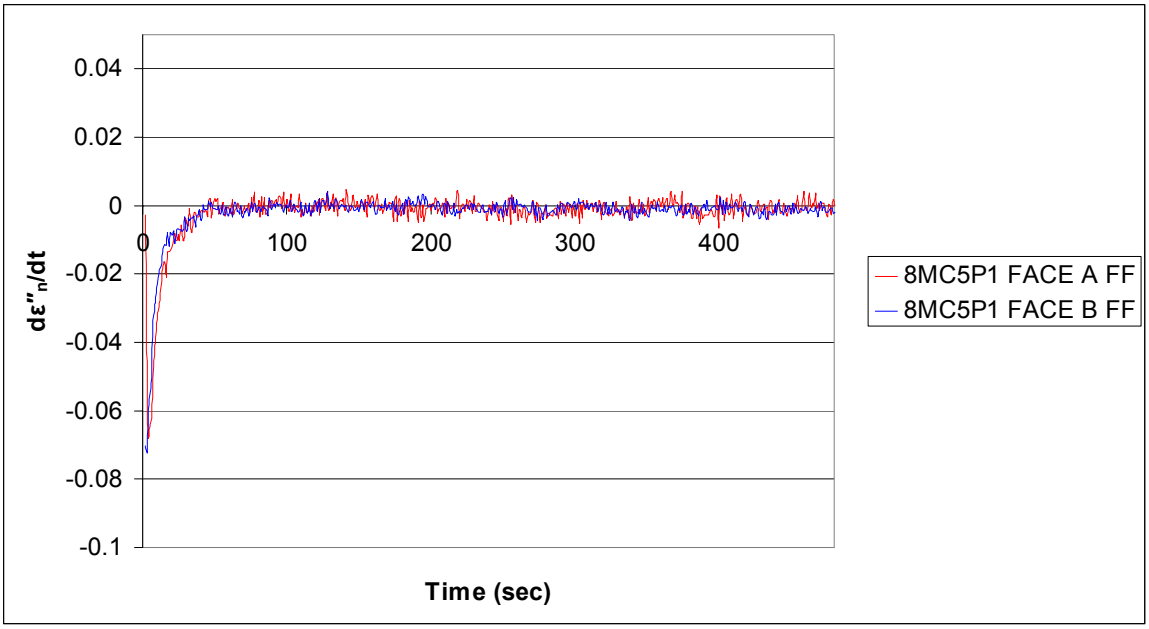

Figure A-37: Normalized time derivative of the loss factor of individual 8MC5P1 samples at 200 Hz by fringe-field DEA.

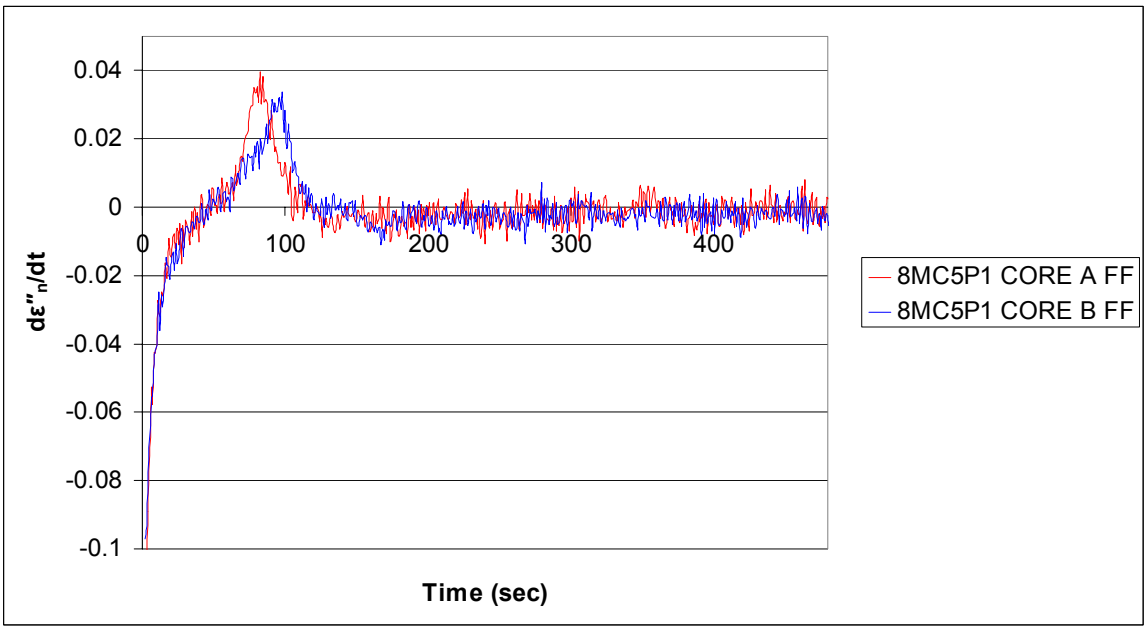

Figure A-38: Normalized time derivative of the loss factor of individual 8MC5P1 samples at 200 Hz by fringe-field DEA.

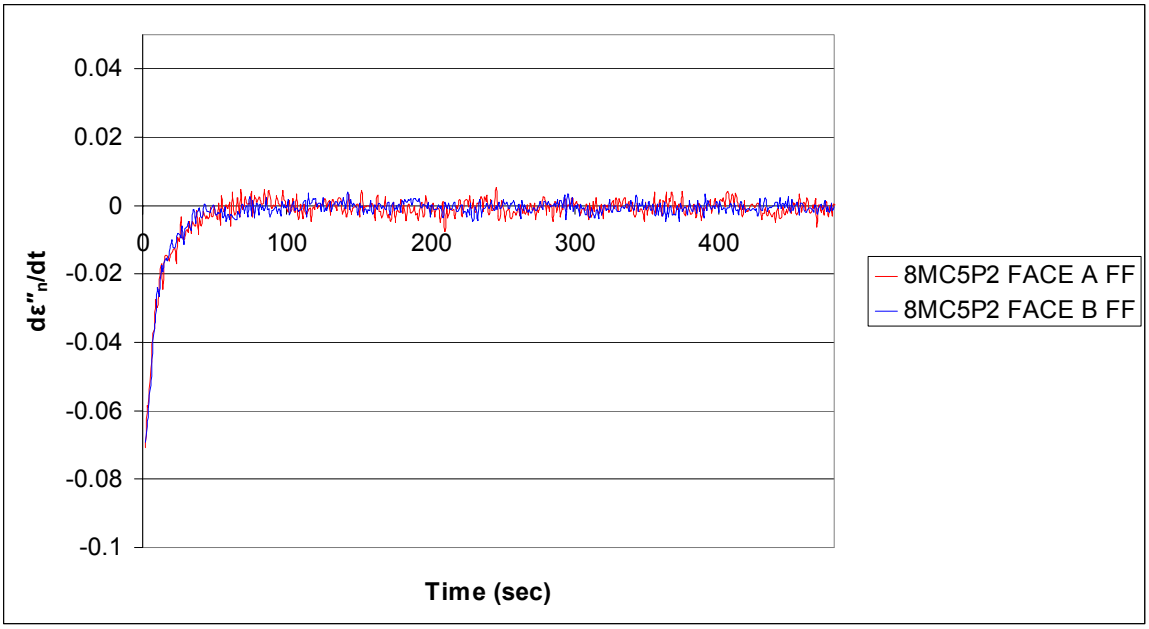

Figure A-39: Normalized time derivative of the loss factor of individual 8MC5P2 samples at 200 Hz by fringe-field DEA.

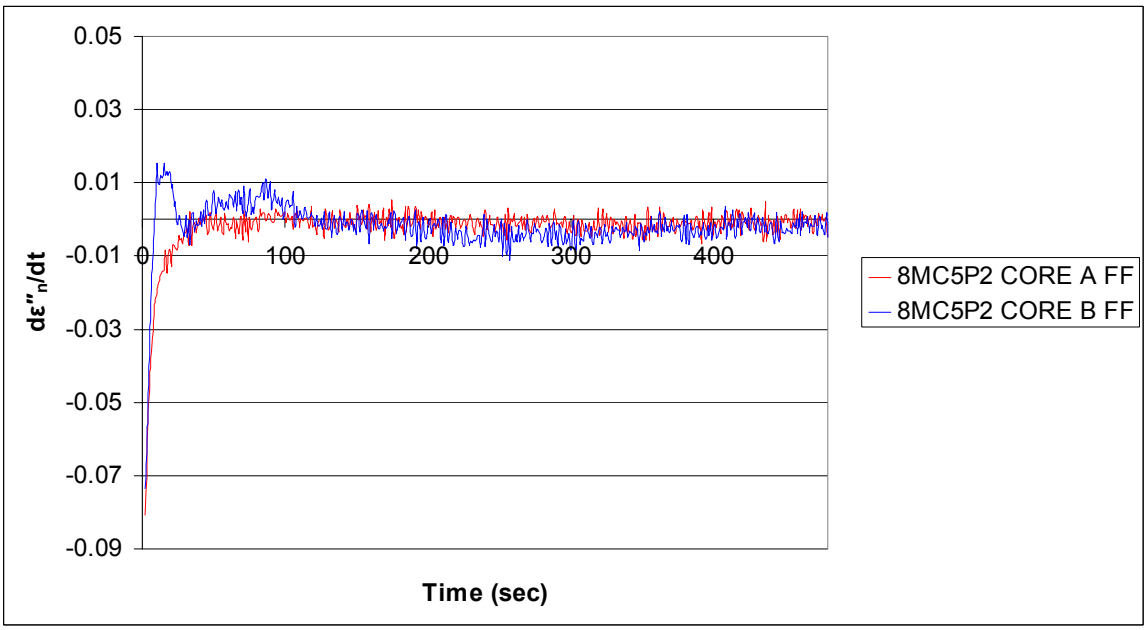

Figure A-40: Normalized time derivative of the loss factor of individual 8MC5P2 samples at 200 Hz by fringe-field DEA.

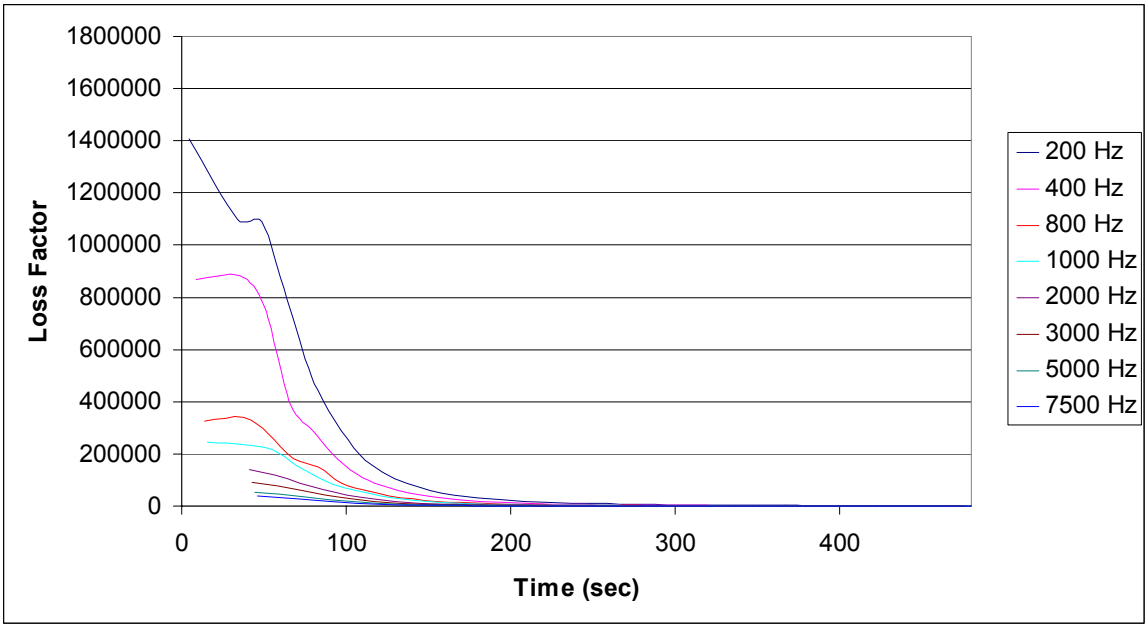

Figure A-41: Loss factor vs. time of 4MC2P1 CORE A samples at multiple frequencies using the fringe-field technique.

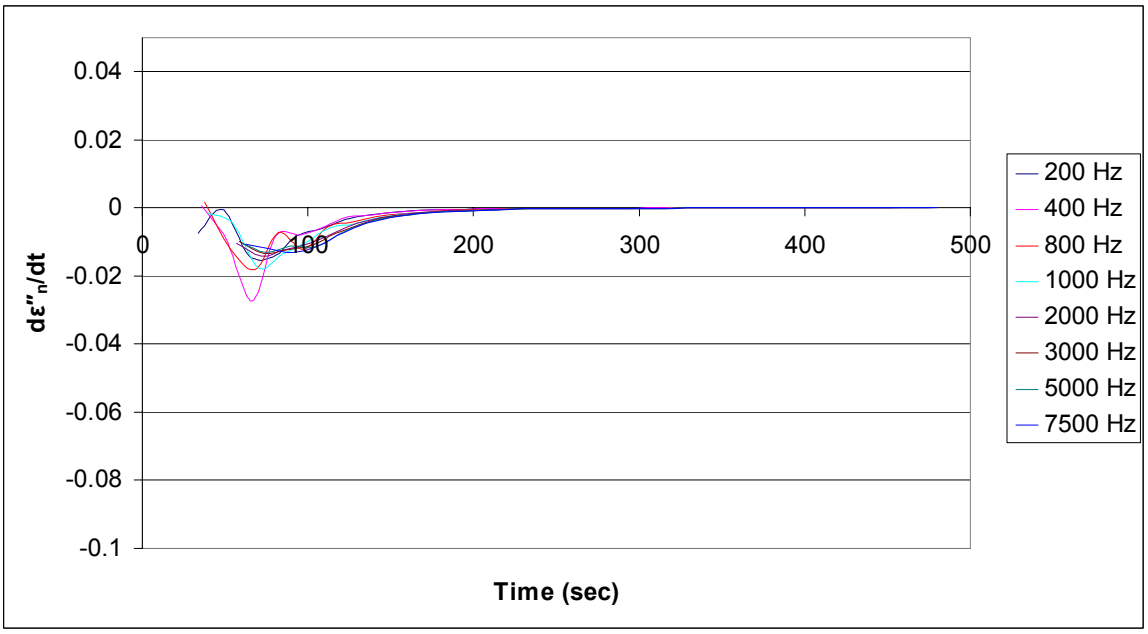

Figure A-42: Normalized time derivative of the loss factor of 4MC2P1 CORE A samples at multiple frequencies using the fringe-field technique.

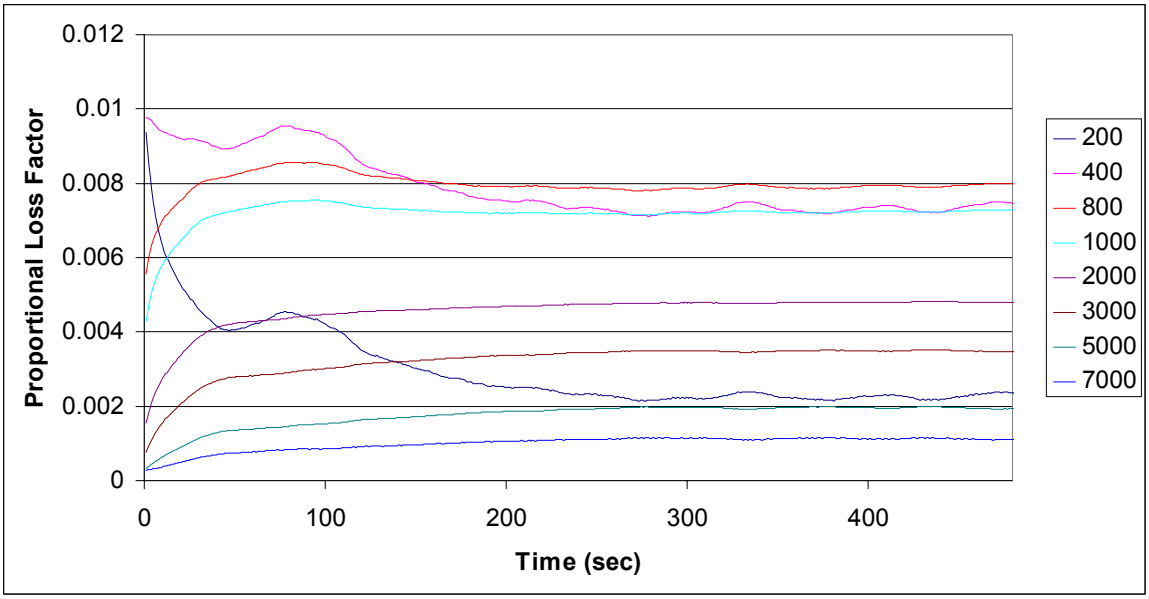

Figure A-43: Proportional Loss Factor vs. time of 4MC2P1 CORE A samples at multiple frequencies using the parallel-plate method.

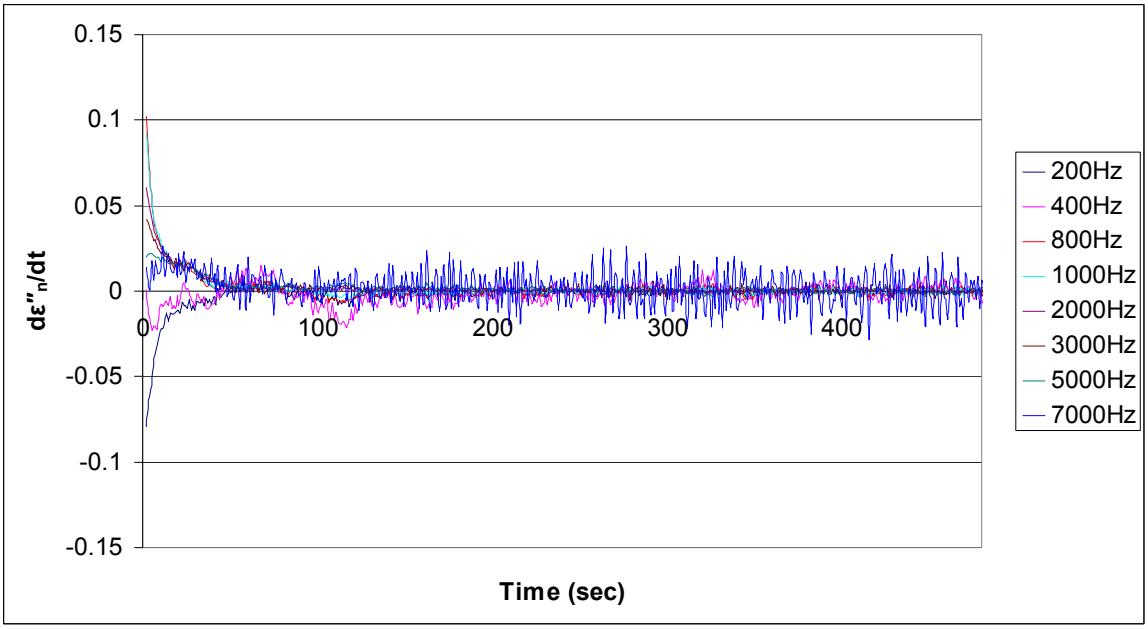

Figure A-44: Normalized time derivative of the loss factor of 4MC2P1 CORE A samples at multiple frequencies using the parallel-plate method.

Table A-1: Moisture content per panel (including water in the resin) and actual resin spread per bond-line (including water weight).

Sample	Actual MC	Resin Spread per ply (g/m^2)
4MC2P1NRA	4.0	0.00
4MC2P1NRB	4.0	0.00
8MC2P1NRA	8.0	0.00
8MC2P1NRB	8.0	0.00
4MC2P1R CORE A	4.7	341.44
4MC2P1R CORE B	4.7	328.05
4MC3P1R CORE A	4.7	272.13
4MC3P1R CORE B	4.7	258.06
4MC5P1R CORE A	4.7	229.23
4MC5P1R CORE B	4.7	209.78
4MC5P2R CORE A	4.7	226.82
4MC5P2R CORE B	4.7	196.29
8MC2P1R CORE A	8.0	310.09
8MC2P1R CORE B	8.0	334.84
8MC3P1R CORE A	8.0	259.18
8MC3P1R CORE B	8.0	250.98
8MC5P1R CORE A	8.0	210.99
8MC5P1R CORE B	8.0	224.02
8MC5P2R CORE A	8.0	205.81
8MC5P2R CORE B	8.0	215.75
4MC2P1R FACE A	4.7	322.34
4MC2P1R FACE B	4.7	348.23
4MC3P1R FACE A	4.7	258.42
4MC3P1R FACE B	4.7	277.39
4MC5P1R FACE A	4.7	220.64
4MC5P1R FACE B	4.7	210.68
4MC5P2R FACE A	4.7	186.59
4MC5P2R FACE B	4.7	213.86
8MC2P1R FACE A	8.0	360.38
8MC2P1R FACE B	8.0	357.00
8MC3P1R FACE A	8.0	264.63
8MC3P1R FACE B	8.0	264.78
8MC5P1R FACE A	8.0	221.90
8MC5P1R FACE B	8.0	231.78
8MC5P2R FACE A	8.0	219.92
8MC5P2R FACE B	8.0	222.73